THE EFFECTS OF THE PUNCHING PROCESS UPON THE MAGNETIC PROPERTIES OF STEEL LAMINATIONS

Thesis submitted for the Degree of M.Sc. in the University of Aston in Birmingham

L. A. Walters

October, 1972

CONTENTS

SYNOPSIS

The punching process used to stamp out iron laminations causes a deterioration in the magnetic properties of the lamination material. This investigation is concerned with an experimental examination of the deterioration and finding the magnitude of the change in material properties due to punching. The punching effect is considered in terms of the ratio of total surface area of the lamination to the punched area, the material thickness and the punching tool clearance.

Annular laminations of various sizes are punched out of sheet material and their magnetic properties measured under static and dynamic conditions. The material is then annealed and the tests repeated. A particular feature of the investigation is the equipment used for the dynamic tests. This consists of an electronic hysteresigraph, which maintains the rate of change of flux density constant for each hysteresis loop, used in conjunction with a specially designed test rig and an on-line digital computer.

A metallurgical analysis of the material is made so as to obtain the optimum temperature for annealing and also to assist in determining the extent of the plastic deformation. The deformation of the punched edge is also examined in terms of its micro-hardness and the Kerr optical method is used to investigate the reduction in permeability in the region of the punched edge.

ACKNOWLEDGEMENTS

The author acknowledges with thanks the opportunity given to him by the Senate of the University of Aston in Birmingham to work for this degree. Thanks are also due to Professor E. J. Davies for the use of the facilities of the Electrical Engineering Department in general and for the interest he has taken in the work.

The author is also indebted to Joseph Lucas Limited for permitting part of their research programme to be used for a full-time external research degree.

Gratitude is expressed to Mr. B. James and Mr. M. A. Thompson for all the help and encouragement they gave throughout the project and for the important contribution made by Mr. Thompson in designing and building a modified form of the Mazzetti and Soardo electronic hysteresigraph.

The author is also very grateful to Mr. J. P. Merriman for designing the test rig, and for the many hours spent assisting with the dynamic tests. Thanks are also due to the author's wife for drawing the curves.

Grateful thanks are also due to the Wolfson Centre at Cardiff University for all the assistance they have given with Kerr Magneto-Optic Effect test method. Acknowledgement is also extended to the Production Engineering Research Association for freely allowing a summary to be made of their Report No. 93.

GLOSSARY OF METALLURGICAL TERMS

Annealing:

A heat treatment process applied to metal which has been subjected to strain, the object of which is to revert the physical and mechanical properties to their most stable low energy state.

Deformed region:

The region of the material where strain has distorted the crystal structure and effected a change in the properties of the metal.

Dislocation:

An imperfection within the crystal structure caused by the displacement of two adjacent planes of atoms.

Lattice structure:

The symmetrical spacial arrangement of the atoms within a crystal.

Microstructure:

The structure of a metal, revealed after polishing and etching, at magnifications greater than 10.

Nucleation:

The process by which certain lattice regions become favoured sites for the development and growth of new crystal structures within a deformed material.

Plane slip:

The relative movement of two adjacent regions of a metal lattice.

Plastic deformation:

The permanent distortion of a metal produced by straining the material beyond its elastic limit.

Polygonization:

The application of thermal energy to reduce the dislocation density within a deformed lattice. This is achieved by partial elimination of dislocations resulting in their orderly re-arrangement within the lattice.

Strain free material:

A material having no distortion and minimum internal energy.

Wall-shifting process:

The physical aspect of magnetization which involves the movement of domain boundaries.

Work hardening:

The process in which the hardness of a metal is increased by permanent deformation.

The Effect of Punching on the Domain Wall Mobility

All ferromagnetic material consists of a large number of small regions, each spontaneously magnetized to saturation. These regions are known as domains and there are one or several domains to each ferromagnetic crystal. In a demagnetized material, the direction of magnetization of the individual domains are randomly distributed in various directions. When an external magnetic field is applied to the material, the first thing that happens is that the domains which are magnetized in a direction close to the direction of the excitation field, grow at the expense of those which are magnetized away from the field direction. Increasing the excitation causes more of the domains to align themselves in a direction near to that of the applied field. This process continues until all the domains are orientated in the one direction. At still higher field strengths the direction of magnetization rotates towards the direction of the applied field.

There are certain preferred directions within a ferromagnetic crystal structure in which domains magnetization vectors can be located. Each domain is separated from the other by boundary walls, which are known as Bloch walls. Bulk magnetization involves a wall-shifting process in which energy is expended in changing the direction of the domain vectors. This irreversible change of direction is achieved by a series of discrete jumps across successive domains boundaries.

The plastic deformation, which occurs in the punched edges of steel laminations, distort the crystall structure and so produce dislocations. These dislocations cause a hindrance to the wall-shifting process and so extra energy is required to orientate the domain. The consequence of this is a reduction in permeability of the material.

The dislocations in the material can be removed by thermally activating the material at an elevated temperature by a process known as annealing. This is achieved because the application of heat relieves the strain energy of the lattice structure.

SECTION 1

Introduction

The laminations used in electrical machines are usually of low carbon (less than 1%) silicon steel of thickness between 0.035 cm. and 0.076 cm. The material is supplied in strip form and a punching process is used to produce the laminations.

For several decades it has been realised by machine manufacturers that the punching process can have a detrimental effect on the magnetic properties of the material. In some cases the magnitude of the deterioration caused by the punching can be such that the manufacturer's magnetization and iron loss curves are no longer accurate. This means that it becomes impossible for the designer to predict accurately the performance of the machine using these curves.

The advent of the digital computer has enabled more accurate and reliable methods to be used in the design of electrical machines. This major step forward, in analytical techniques, has emphasized the fact that no matter how sophisticated the design programme may be, its accuracy is very dependant on the input data. This is especially so as far as the magnetic characteristics and specific iron losses of the punched lamination material are concerned.

The main aims of this project are as follows:-

1. To investigate the deterioration, due to the punching process, of the magnetic properties of lamination material. This will enable the steel manufacturers' curves, for magnetization and specific iron loss, to be modified. This information is required to be expressed in such a form that it can easily and directly be translated into corresponding new curves by the machine designer after having determined the geometry and

size of the laminations.

2. To investigate the physical and magnetic properties of the lamination material in the regions where punching operations cause plastic deformation. The possibility of establishing a correlation between the change in physical and magnetic properties will be examined.

SECTION 2

LITERATURE SURVEY

2.1. Introduction

The survey of the relevant literature published to date has been categorised into two sections. The first section relates to the investigation of the punching effect on magnetic lamination material. There are only three papers 1,2,3 in this section and they do not attempt to obtain a relationship between the manufacturers' magnetic characteristic curves and the curves obtained after punching.

The second section 4 to 11 relates to the physical analysis of the deformation process and to papers concerned with the study of iron loss in magnetic material. The survey shows that the process of plastic deformation in metals is reasonably understood and that there is a considerable amount of information concerning recent studies of iron losses in magnetic materials.

One of the main aims of the present project is to determine the iron losses by measuring the area of the dynamic hysteresis loop. This method is made possible because of the resultant widening of the loop for the same peak values of flux density and magnetizing force, as the rate of cycling around the loop is increased. Since this present project uses the measurement of the loop area for dynamic loss, the papers in the second section have been reviewed with respect to this. In particular, information was sought on the behaviour of the dynamic loop, and how the total energy loss in the loop may be divided up into its static and dynamic components.

This review shows that the hysteresis loss is affected by the punching strain. For this reason, it was thought relevant to seek information on the experimental evidence supporting Steinmetz's equation for hysteresis loss.

2.2. Punching Effect

The first quantitative study of this effect was that undertaken by Cole[1], which was concerned with "The increase in hysteresis loss, decrease in permeability and change in microstructure caused by the punching operation".

In his tests, Cole used a series of rings punched from several grades of steel laminations. For each grade, different lamination thicknesses were used. In all cases the ratio of radial width to mean diameter was maintained at approximately 6. The contribution of Cole is a very useful one in gaining a clearer understanding of punching effect. His main conclusions may be summarised as follows:

1. That the strains produced by the punching operation alters the microstructure of the steel considerably for a short distance from the punched edge. The author shows that on 0.036 cms. thick laminations, the microstructure was badly altered upto 0.005 to 0.007 cms. back from the punched edge.
2. That where the microstructure is affected by strain there is an increase in hysteresis loss.
3. That the relative increase in hysteresis loss and reduction in permeability caused by punching strains reduces with increasing flux density.
4. That for the range of thickness studied, increased hysteresis losses produced by punching strains are approximately a linear function of the lamination thickness.

5. That for the range studied, the influence of thickness on punching strains was much less than that of the radial width of the specimen.
6. That annealing will relieve the effect of punching strains.

Cole's work does not however attempt to obtain a relationship between the manufacturers' magnetic characteristic curves and the curves obtained after punching.

Almost 40 years after Cole's work was published, a study of the effect of punching was undertaken by Seeger[2]. The results of this investigation clearly show that Seeger's aims were very similar to those of Cole's.

Using various grades of lamination material and different inter-laminar insulation, Seeger carried out tests on the following forms of laminations:

a) Various sizes of lamination strip, the strip being cut by a guillotine process.
b) Laminations in ring form, with outside diameter 20 cms and inside diameter 12 cms.

The main conclusions of Seeger's work can be summarised as follows:-

1. That plastic deformation in lamination material causes an additional hindrance to the wall-shifting processes in regions under strain. The consequence of this is increased hysteresis loss.
2. That eddy-current losses are not measurably influenced by plastic deformation in the material.
3. That the increase in hysteresis loss, caused by deformation, is not dependant upon the relationship between the direction of punching and the rolling direction of the material.

4. That removing of the burr edges from the laminations by grinding causes a further deterioration in the magnetic properties of the material.
5. That using a machining operation to obtain the final dimensions of a lamination stack can result in high additional eddy-current losses by shorting out the individual laminations. This practice is widely used on machines having small air gaps where it is necessary to remove inaccuracies in the punching and stacking.
6. That generally, there is no very stringent requirement for the inter-laminar insulation, since the potential gradient between the laminations is usually very small.
7. That the effect of plastic deformation on the B/H characteristics is most pronounced at the lower values of flux density. The effects in the region of high saturation are very slight, which is in agreement with Cole's findings.
8. That the degree of deterioration of the magnetic properties, caused by the plastic deformation, is very dependant upon the ratio of punched area to total surface area of the laminations.

The results of Seeger's work shows that several important factors were considered by him, which Cole did not take into account. In particular he notes that the ratio of punched area to total surface area is an influencing factor. Like Cole, however, he does not attempt to relate the curves of the punched material to those of manufacturers'.

In a paper which is concerned with means of obtaining more economic machine design, Oberretl[3] considers the effect of punching in narrow parallel teeth, taking as an example a small induction motor. By annealing the punched laminations, in a

nitrogen atmosphere at 800°C, the iron circuit m.m.f. was reduced by about 20%. The author emphasizes the fact that with such machines it is of particular importance to ensure that the punching tools are in first class condition.

2.3. Deformation and Losses

Whenever a punching operation is used on a metal, there is always a zone of deformation along the punched edges of the material. This deformation zone is a result of plastic strain caused by the punching operation.

Some of the salient characteristics of the deformation are given in a Production Engineering Research Association Report[4]. It is a very comprehensive metallographical study of the effect of punching. Some of the relevant conclusions are:

1. That the width of the severely deformed zone is greatly affected by the shape of the punching tool used.
2. That cracks, when present, are seen to be confined to the edge of the severely deformed region.
3. That cracks are initiated in advance of the punch, and propagate back towards the punched edge, where they are opened up by frictional forces between the punch and the work material.
4. That a region of work-hardening is always found associated with the region of shear.
5. That the region of work-hardening extends considerably beyond the area indicated by chemical etching agents.
6. That distinct differences between soft or annealed material and previously work-hardened material can be detected in the work-hardening arising during punching.

7. That in annealed or soft material only, the total width of the work-hardened zone varies with the material thickness and to a smaller extent with the punch/die clearance.

It will be realized from these observations that the work-hardened zones, which are always present around the punched edges of the laminations, are a result of the punching strains.

Risch[5] discusses how the area of the dynamic hysteresis loop is a measure of the static hysteresis loss and the eddy current loss. He explains how, for each value of flux density in the dynamic loop, there are three distinct values of field strength (see Fig. 1), these being:

1. The field strength H_h, given by the hysteresis loop under static condition. This is the actual field strength prevailing in the material.
2. The field strength H_d, attributable to the dynamic loss which Risch says is equivalent to the eddy current loss.
3. The field strength H_t, produced by the magnetizing current and equal to the sum of H_h and H_d.

It can be seen from Fig. 1 that if H_d is plotted against the flux density axis the dynamic loop is obtained, which for a time varying sinusoidal flux distribution is in the form of a vertical ellipse.

Any consideration of the dynamic loop must take into account the fact that the magnetization of a ferromagnetic material involves movement of the domain structure, the result being that, except for very slow rates of flux density change, the instantaneous value of the magetiziing force will always be in advance of its corresponding value of flux density.

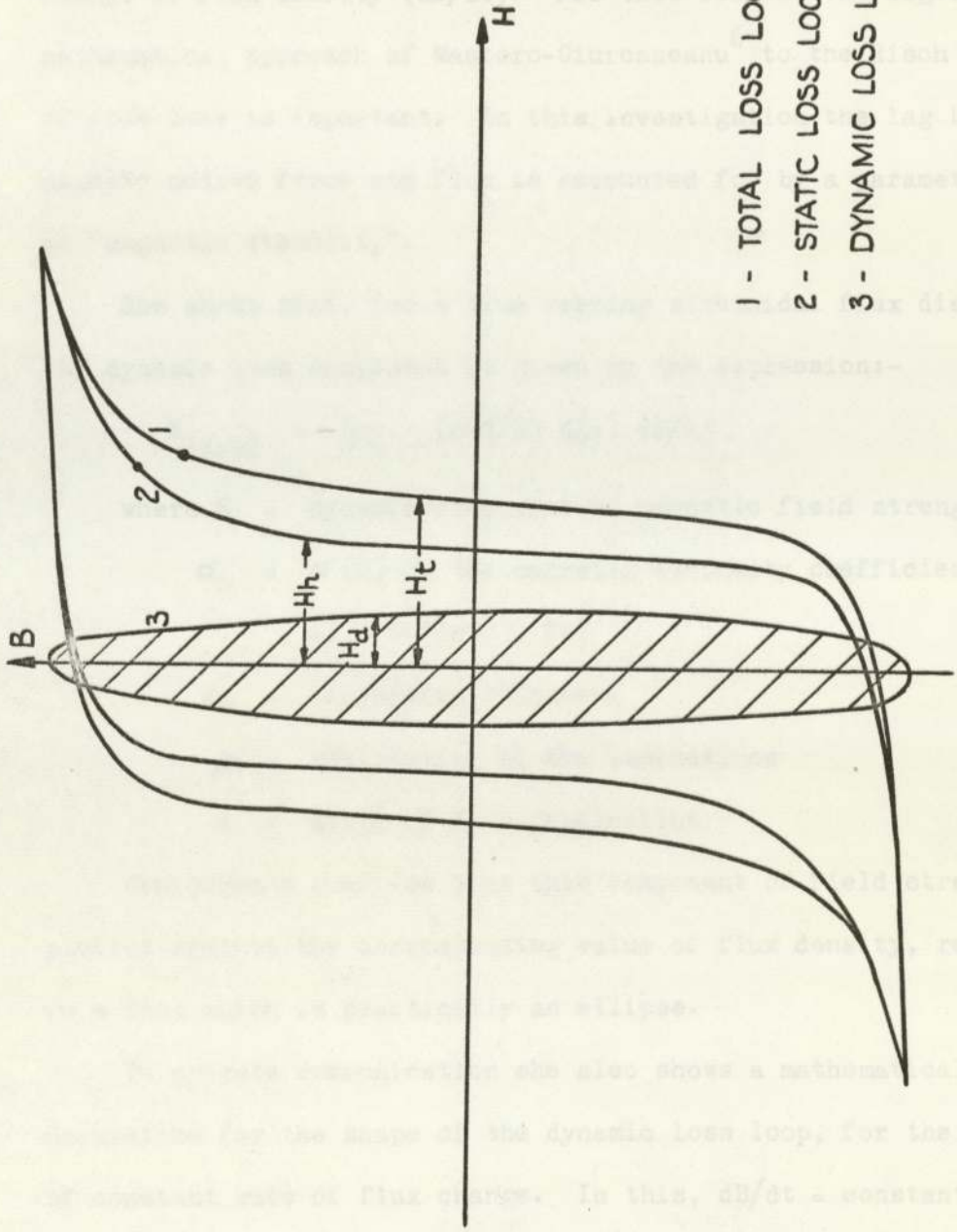

FIG. 1. LOOPS IN THE RISCH MAGNETIZATION DIAGRAM.

The important difference between Risch's work and the present work is that Risch considers time varying sinusoidal flux density distribution, whereas the present work uses a constant rate of change of flux density (dB/dt). For this reason, the rigorous mathematical approach of Mastero-Giurcaneanu[6] to the Risch concept of iron loss is important. In this investigation the lag between magneto motive force and flux is accounted for by a parameter known as "magnetic viscosity".

She shows that, for a time varying sinusoidal flux distribution, the dynamic loss component is given by the expression:-

$$H_{(d,t)} = (\sigma_0 - (a-d/2)\, d/\rho)\, dB/dt \qquad (2.1)$$

where H = dynamic component of magnetic field strength

σ_0 = $\sigma(0)$ is the magnetic viscosity coefficient at = 0 (or d = 2a)

2a = lamination thickness

ρ = resistivity of the laminations

d = depth of flux penetration

Giurcaneanu confirms that this component of field strength, plotted against the corresponding value of flux density, results in a loop which is practically an ellipse.

In private communication she also shows a mathematical derivation for the shape of the dynamic loss loop, for the condition of constant rate of flux change. In this, dB/dt = constant = b and so (2.1) now becomes:-

$$H\,(d,t) = b(\sigma_0 - (a-d/2)\, d/\rho \qquad (2.2)$$

at the surface of the laminations $H_{(0,t)} = b.\sigma_0$

This results in a dynamic loss loop having a flat top and bottom, which is shown in Fig. 2. Whilst agreeing with Risch that the area of the difference loop represents the dynamic loss,

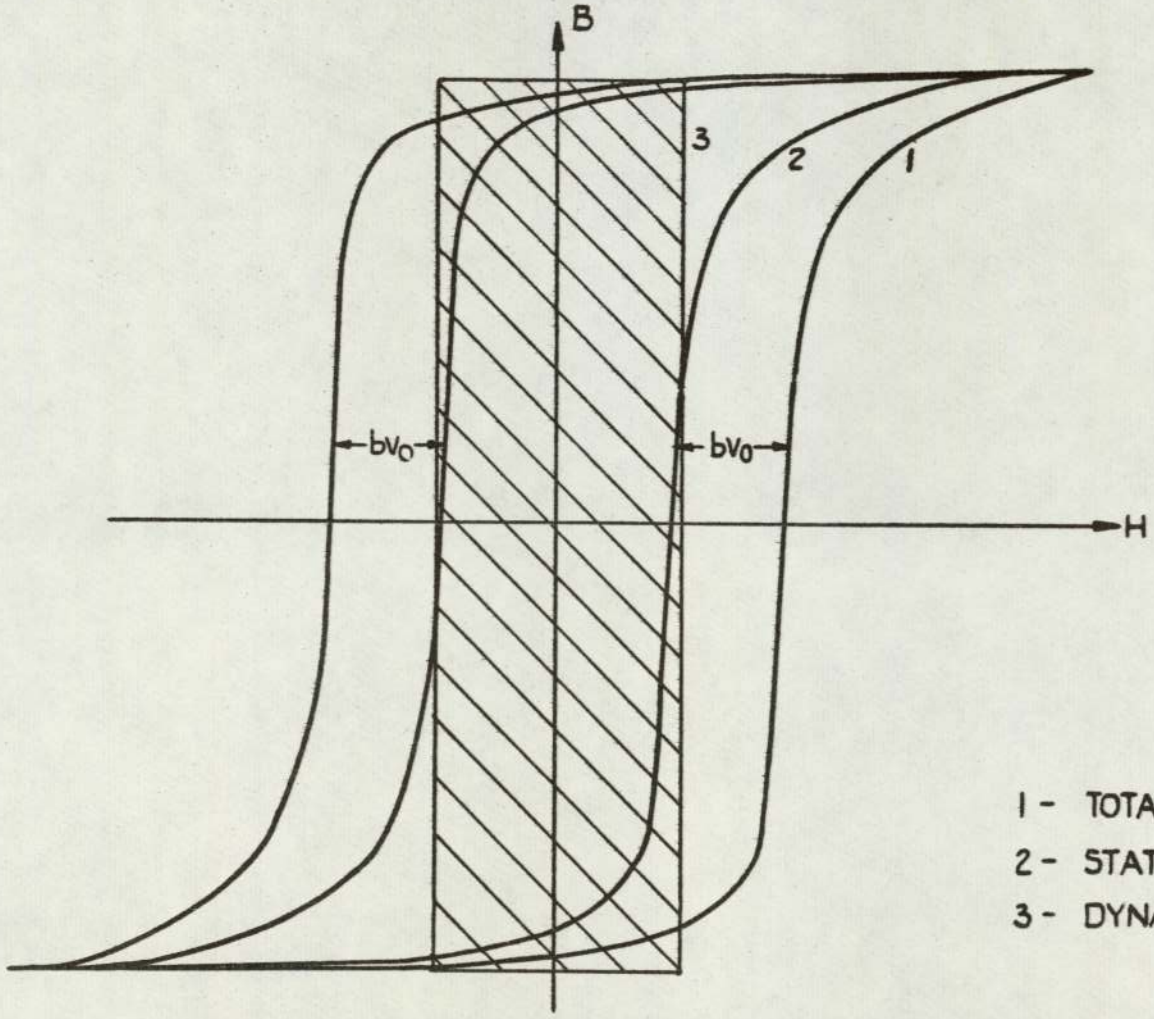

FIG. 2. LOOPS IN THE MAGNETIZATION DIAGRAM FOR CONSTANT dB/dt.

Giurcaneanu does not consider that this is completely eddy-current loss.

Steinmetz[7] made an attempt to eliminate the need to determine the hysteresis loop area in the calculation of this loss, by introducing the following empirical law which is based on experimental results:

$$W = N. B_{max}^{x}.f \quad \text{Watts} \qquad (2.3)$$

where

N = the hysteresis coefficient

B_{max} = the maximum value of magnetic flux density, T

f = frequency, Hz

The exponent x was found to be sensibly constant, being approximately 1.6 for most grades of ferromagnetic material, and N depends on the grade of magnetic material and is very much influenced by the anisotropy of the material. Generally, this coefficient is within the range of 30 - 55.

Steinmetz's equation gives reasonable results for flux densities up to 1.0 T. From 1910 onwards, workers began to realize that if this method was to be used for flux densities above 1.0 T, then the value of the exponent would have to be changed. Webb[8], who made a summary of the findings of other investigators, confirmed that when using an exponent of 1.6, the hysteresis loss corresponds to Steinmetz's equation up to a density of 1.0 T. The exponent may rise above 2.5 for flux densities between 1.0 and 1.6 T and may fall to less than 1.6 for flux densities beyond 1.6 T.

A dimensional analysis for obtaining a relationship between the total iron loss at any frequency and the measured hysteresis loss was obtained by Richardson and Falkowski[9]. In this work the principal loss variables were arranged into four dimensional

ratios and from these several empirical equations were obtained, each equation giving the relationship between the losses over a given flux density range. Over a range of frequencies from 30 to 300 Hz, these equations seem to reflect accurately the magnitude of the iron loss. Test and calculated losses are in good agreement.

In a review of ferromagnetic material, which places an emphasis on iron and its alloys with silicon, Littman[10] discusses several factors which are relevant to the present investigation. These factors are summarised as follows:

Iron has a low resistivity and it is fortuitous that large increases in resistivity are obtained when iron is alloyed with silicon. Most alloy elements increase the electrical resistivity of iron.

Silicon content in commercial materials usually represents a compromise between the benefits of improved resistivity and lower hysteresis loss and the detrimental effects of lower saturation and decreased ductility. It should also be mentioned that the presence of silicon stabilises the material structure.

The presence of carbon can be very harmful to the permeability at low inductions and can also cause an increase in hysteresis loss. It is therefore always advantageous to reduce the carbon content of the material as far as is commercially practicable.

Thinner laminations tend to have higher hysteresis loss, probably because of higher magnetostatic energy associated with grains having favourable directions not parallel to the sheet surface. The effects of thickness on hysteresis and eddy-current losses are opposed, therefore the total core loss measured as a function of thickness, passes through a minimum point depending on grain orientation and other factors such as grain size,

stress and the composition and texture of the material.

In another review of ferromagnetic material, Randall and Scholefield[11] consider the nature of the hysteresis loop in detail. The authors state that coercivity is mainly dependant on internal strain, and that remanence is mainly dependant on structural and domain orientation. The greater the degree of preferred grain orientation, the higher the remanence. This therefore means that the narrowest hysteresis loops are achieved when the internal strain is reduced to a minimum, and that virtually rectangular loops are achieved when a high degree of structural and domain orientation is present.

When a magnetic material is subjected to internal strain, increased energy is required to move a domain boundary. Not only does the internal strain increase the area of the hysteresis loop, but it will also result in a reduction in permeability. The grain structure in a deformed material tends to rotate into a common orientation. This preferred orientation develops gradually with increasing deformation.

SECTION 3

THE SCOPE OF THIS INVESTIGATION

3.1. The Choice of Material

The grade chosen was Ferrosil 216, which is equivalent to Losil 22, because of its extensive use in the manufacture of electrical machines and since it appears to be a typical cold reduced non-oriented silicon steel. The three material thicknesses used were 0.036 cms., 0.051 cms. and 0.064 cms. The material was manufactured by the British Steel Corporation and its chemical composition is given in Section 7.2.

Having established the punching effect for this grade it is hoped that there will be an opportunity to extend the investigation to other grades of magnetic materials used in the manufacture of electrical machines.

3.2. Form of Test Laminations

In this investigation the lamination parameters were as follows:

1. The ratio of punch area to total surface area (see Section 3.3).
2. Lamination thickness.
3. Punching tool clearance (punch/die clearance).

It might be thought in the first instant that the best approach would be to use actual machine laminations in the test programme. The disadvantages of this are that the geometry of machine laminations are such that within the laminations there is a range of flux densities, e.g. high densities in narrow parallel teeth. It would be difficult to obtain a relationship between a given magnetization force and a corresponding flux density in the lamination material and establish a relationship between the degree of deterioration and the magnetic properties.

Therefore it was decided to use a ring form of lamination circumferentially magnetized which has the following advantages:

a) The sectional area is the same all the way around the stack and although the flux density will vary with radius of the section, the density at the mean magnetic radius will be the same throughout the length of the mean magnetic path. It would be extremely difficult to achieve such an even distribution of flux with any other geometry of the lamination.

b) This geometry was considered the best for controlling the ratio of punch area to total surface area.

c) It becomes a simple matter to increase the tool clearance employing a circular punching tool.

In electrical machines, the direction of flux is often such that it has to cross the boundary of the punched section of the lamination at right angles. In this investigation however, it is realized that the direction of the flux is confined to a direction which is parallel to the lamination boundary. Nevertheless, the evidence of Cole[1] and Seeger[2] shows that the present work should provide much useful information.

3.3. Selection of Laminations

The area which undergoes alteration in microstructure, due to the punching operation, is a function of the length of material surface which comes into contact with the punching tool.

In the ring lamination shown below, a punching operation is used for both the inside and outside diameters. Therefore the surface area affected by punching strain (punch area) is:

$$\pi\ (D_1 + D_2)\quad .\delta w \qquad (3.1)$$

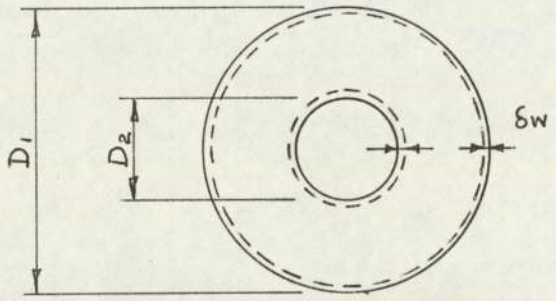

$$\text{Total surface area} = \pi/4(D_1^2 - D_2^2) \qquad (3.2)$$

Since the ratio of punch area to total surface area is considered a criterion for assessing the influence of punching strains, dividing (3.1) by (3.2) provides a means for investigating the influence of the punching strains on the total area:

$$\frac{\pi (D_1 + D_2).\ \delta w}{\pi/4\ (D_1^2 - D_2^2)} = \frac{4.\ \delta w}{(D_1 - D_2)} \qquad (3.3)$$

The numerator, 4. δw, in (3.3) can be taken as constant and the influence of punching strains can be assessed by:

$$\frac{1}{(D_1 - D_2)} \qquad (3.4)$$

Equation (3.4) is termed the punching factor.

Five sizes of lamination were chosen so as to give equal increments of the punching factor over the required range (see Fig. 3). The tooling arrangement was planned in such a way that only 5 tool sets were required to produce the 10 punching operations.

Cole uses ring width as a criterion for selecting ring size. This method of selection differs considerably from that of using a punching factor in that Cole takes no account of this factor.

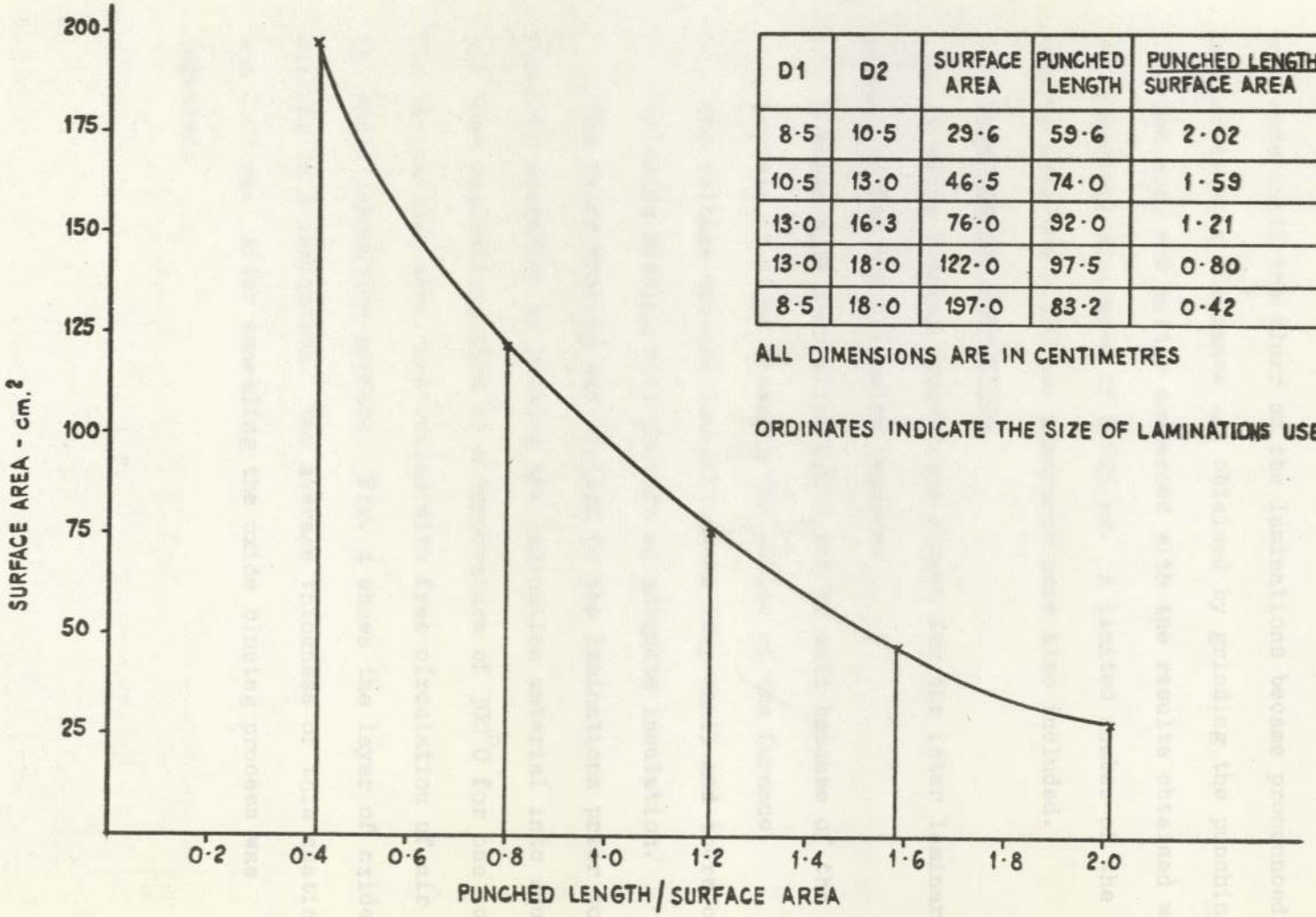

D1	D2	SURFACE AREA	PUNCHED LENGTH	PUNCHED LENGTH / SURFACE AREA
8·5	10·5	29·6	59·6	2·02
10·5	13·0	46·5	74·0	1·59
13·0	16·3	76·0	92·0	1·21
13·0	18·0	122·0	97·5	0·80
8·5	18·0	197·0	83·2	0·42

ALL DIMENSIONS ARE IN CENTIMETRES

ORDINATES INDICATE THE SIZE OF LAMINATIONS USED.

FIG.3. LAMINATION SURFACE AREA AGAINST RATIO OF PUNCHED LENGTH TO SURFACE AREA

3.4. Tool Clearances

Starting with a minimum diametral clearance, between the punch and die, of 0.025 mm., incremental increases in the clearance were made until the blurr on the laminations became pronounced. Each successive clearance was obtained by grinding the punching tools.

The work was mainly concerned with the results obtained with the diametral clearance of 0.025 mm. A limited number of the results from the 0.050 mm. clearance were also included.

3.5. Interlaminar Insulation

An oxide blueing process was chosen for the inter laminar insulation for the following reasons:

1. A resin type insulation could not be used because of the deposit it might leave on the inside of the furnace.
2. The voltage between laminations is very small and therefore an oxide coating will provide an adequate insulation.

The oxide coating was applied to the laminations prior to the punching operation by cutting the lamination material into squares and then maintaining them at a temperature of $300^{\circ}C$ for one hour. The laminations were then cooled with free circulation of air over the whole lamination surface. Fig. 4 shows the layer of oxide coating on a lamination. The average thickness of this coating was 0.01 mm. After annealing the oxide blueing process was repeated.

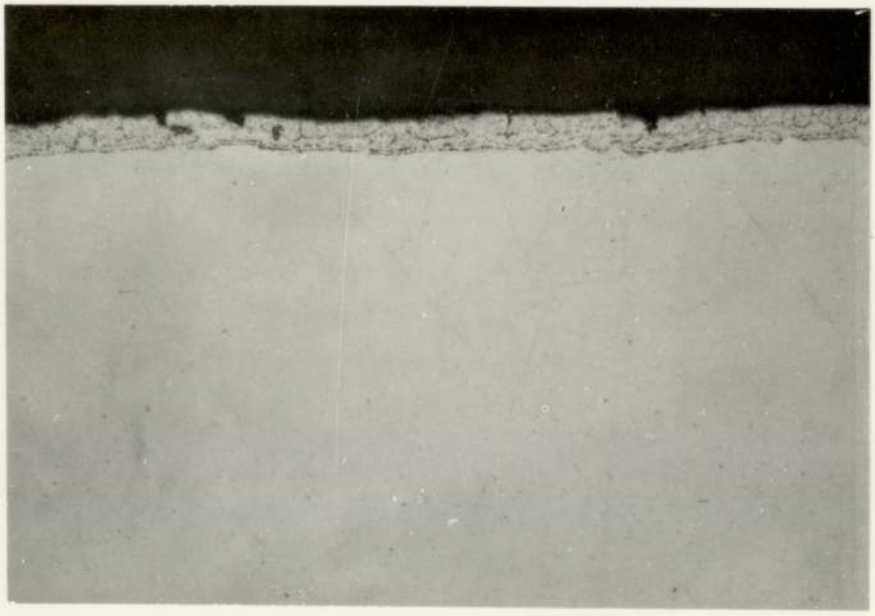

MAGNIFICATION = 500

EXT. DIA. = 18·0 CMS INT. DIA. = 13·0 CMS

0·036 CMS THICKNESS 1 ST CLEARANCE

FIG. 4. OXIDE COATING ON LAMINATION

SECTION 4

TEST EQUIPMENT

4.1. Dynamic Tests

4.1.1. Introduction

Standard methods of dynamic iron loss measurement, such as the Epstein square[12], were not considered suitable for this work because of the following reasons:-

(a) The rate of change of flux density is a variable (sine wave) and therefore the eddy current effect will be a variable during a cycle.

(b) The loss measurement must allow for other circuit losses.

The equipment described below was designed to overcome limitations (a) and (b) described above. The design of the equipment was such as to facilitate easy and rapid means of testing which would require little effort in changing the laminations being tested.

The equipment consisted of three principal components, these being a test rig, an electronic hysteresigraph and an on-line digital computer.

4.1.2. The test rig

Figs. 5 and 6 shows the test rig which consisted of a composite stack of iron laminations (1) in ring form mounted between thick insulating rings (2). The insulating rings were in turn mounted between two thick aluminium alloy plates (3). The lamination stack was correctly spaced by means of location pins, which were removed once the stack has been positioned. Three pneumatic air cylinders (6), which were supported by an aluminium alloy platform and were spaced 120° apart, held and located the top plate. Three steel tubes (4), situated midway between the air cylinders, separated the bottom plate from the platform.

1. LAMINATION STACK
2. TUFNOL INSULATING RINGS
3. ALUMINIUM ALLOY PLATES
4. LOAD CELL
5. PIN AND SOCKET TERMINAL
6. PNEUMATIC AIR CYLINDER
7. EXCITATION COIL
8. POWER AMPLIFIER
9. COMPARATOR
10. P_1 & P_2 CONTROL

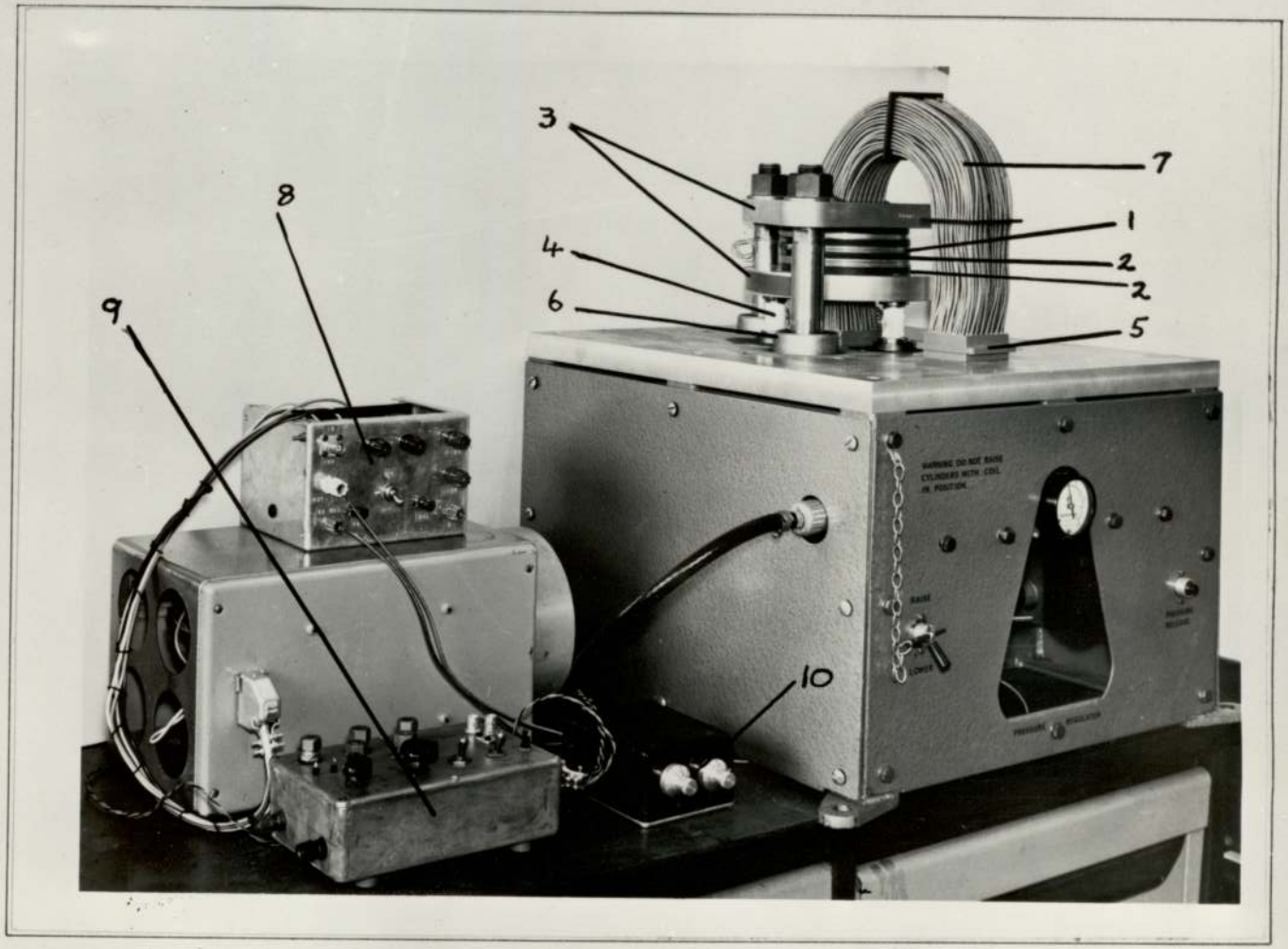

FIG.5. TEST RIG AND ELECTRONIC HYSTERESISGRAPH

1. LAMINATION STACK
2. TUFNOL INSULATING RINGS
3. ALUMINIUM ALLOY PLATES
4. LOAD CELL
5. PIN AND SOCKET TERMINAL
6. PNEUMATIC AIR CYLINDER
7. EXCITATION COIL

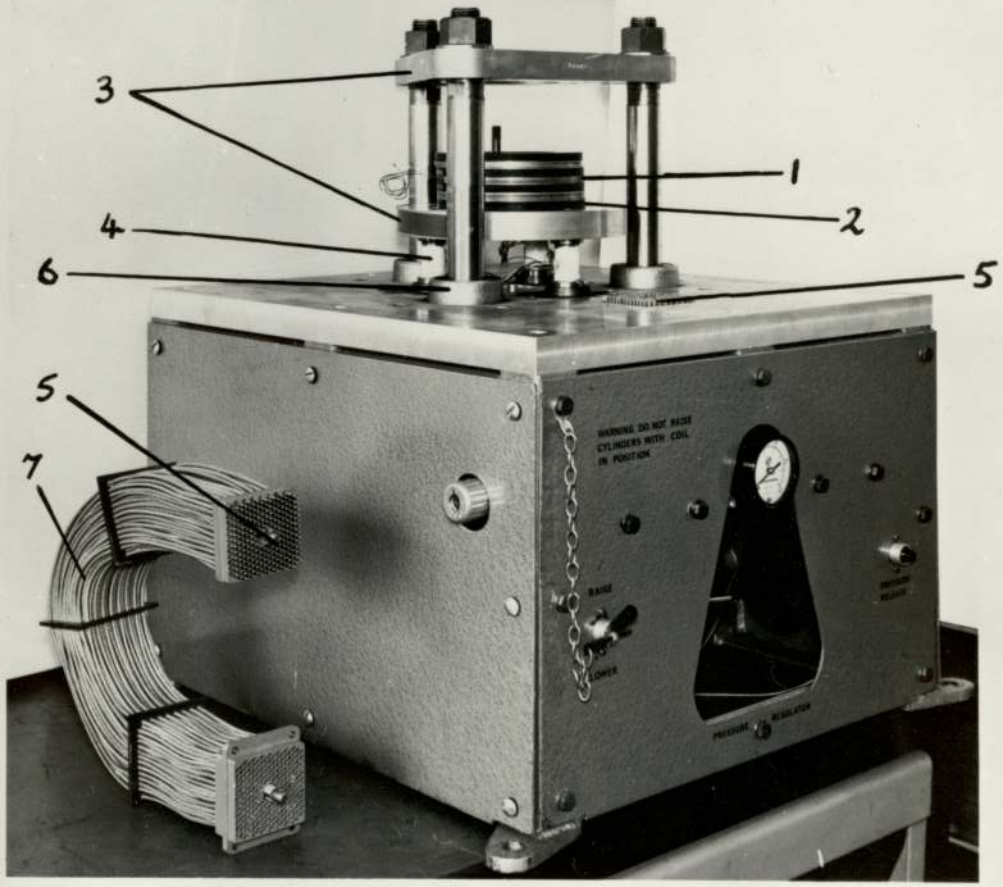

FIG. 6. TEST RIG WITH EXCITATION COIL REMOVED AND THE PNEUMATIC AIR CYLINDERS IN RAISE POSITION

The three tubes (4), on which strain gauges were mounted formed load cells for measuring the pressure directly on the laminations when they were under compression. The load cells were located with respect to the platform by means of steel pillars permanently fitted into the bottom plate and passing through ball bushings in the platform. This was done mainly to minimize frictional forces. The pneumatic air circuit was also fitted with a pressure gauge for measuring pressure where very precise readings were not required.

The schematic arrangement of the pneumatic circuit used in this system is shown in Fig. 7. The three pneumatic air cylinders were used to apply any pressure between 0 and 550 $kN.m^{-2}$ uniformly to the lamination stack. Each of the three cylinders was double acting and were connected together to work in parallel. This method of connection afforded a means of employing one main valve to supply the three cylinders. This main valve was 4-way air operated and the two exhaust ports were fitted with throttle valves. The throttle valves were used to prevent shock on the system when the pressure was released to the atmosphere. The control of the main valve was achieved with ease by means of a lever-operated pilot valve.

The pressure, which could be adjusted as a test variable, was maintained constant by means of a non-return valve which was located on the input side of the main valve. This meant that once the lamination pressure had been set, it was independant of the rest of the air circuit supply.

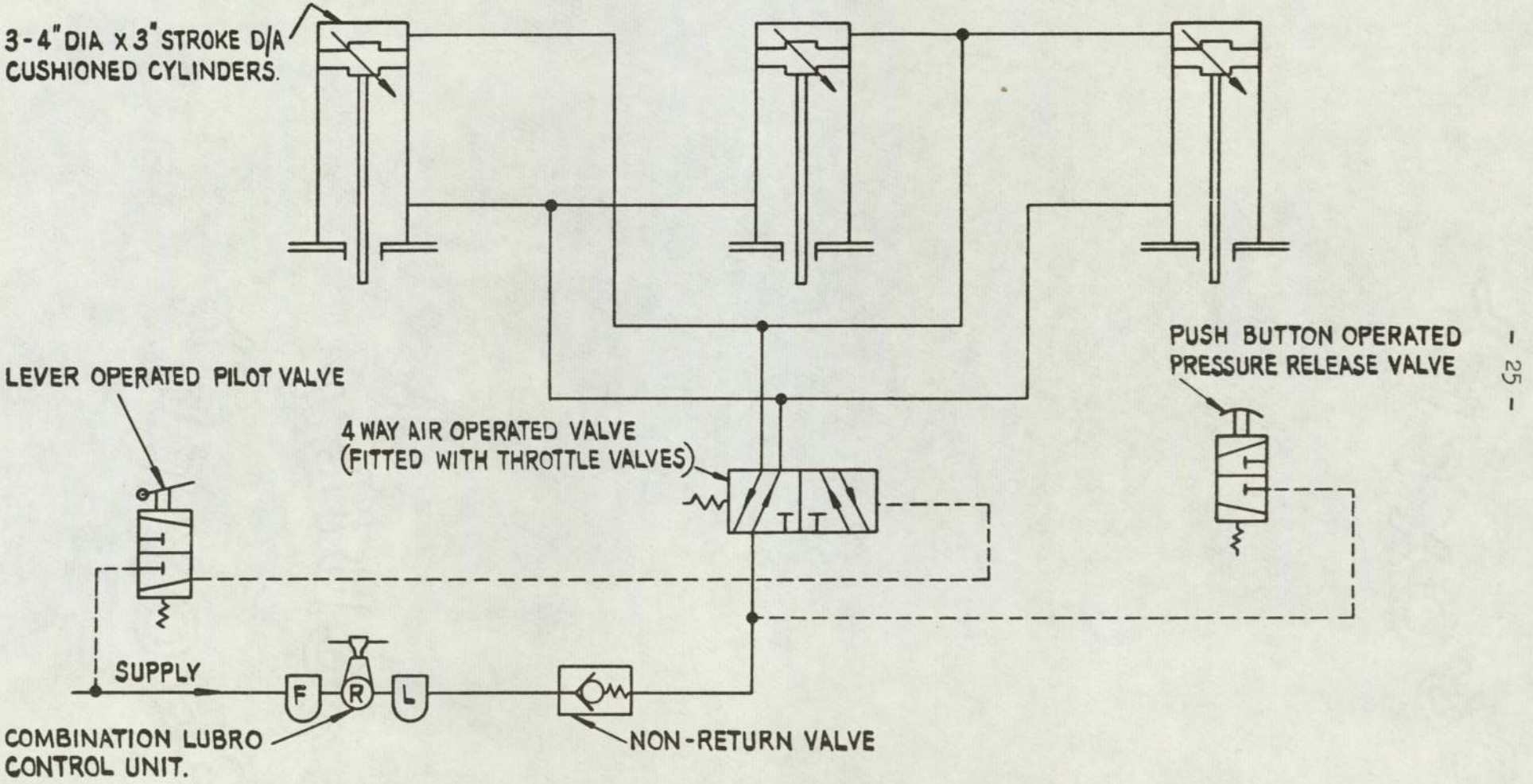

FIG. 7. SCHEMATIC ARRANGEMENT OF PNEUMATIC CIRCUIT USED ON TEST RIG.

The lamination stack was magnetized in a circumferential direction by means of a coil which passed through the centre of the stack. The excitation coil (7) consisted of 212 turns of 40/0.0076 (40/.193 mm.) tinned copper wire, all connected in series and insulated with class F insulation. At the platform the coil entered two plug and socket connectors (5) which provided a convenient means of removing the coil when changing the lamination stack. Ideally the magnetizing coil should be uniformly distributed round the stack. In view of the large number of samples to be tested however, this was not practicable. A search coil for measuring flux was also wound on the lamination stack.

4.1.3. The electronic hysteresigraph

A modified version of the electronic hysteresigraph developed by Mazzetti and Soardo[13] (see Appendix A) was used. The principle of this hysteresigraph was that, for any given hysteresis loop, the rate of change of flux density (dB/dt) was maintained constant around the loop. The magnitude of dB/dt could be varied for different loops.

The block diagram of the circuit is as shown in Fig. 8. The lamination stack had two windings which were interdependant. These were the excitation winding and the search coil winding in which the induced voltage was proportional to dB/dt.

Exciting current was supplied to the excitation winding by the power amplifier which was driven by the comparator. The output of this comparator was the integral of the algebraic sum of the following two voltages.

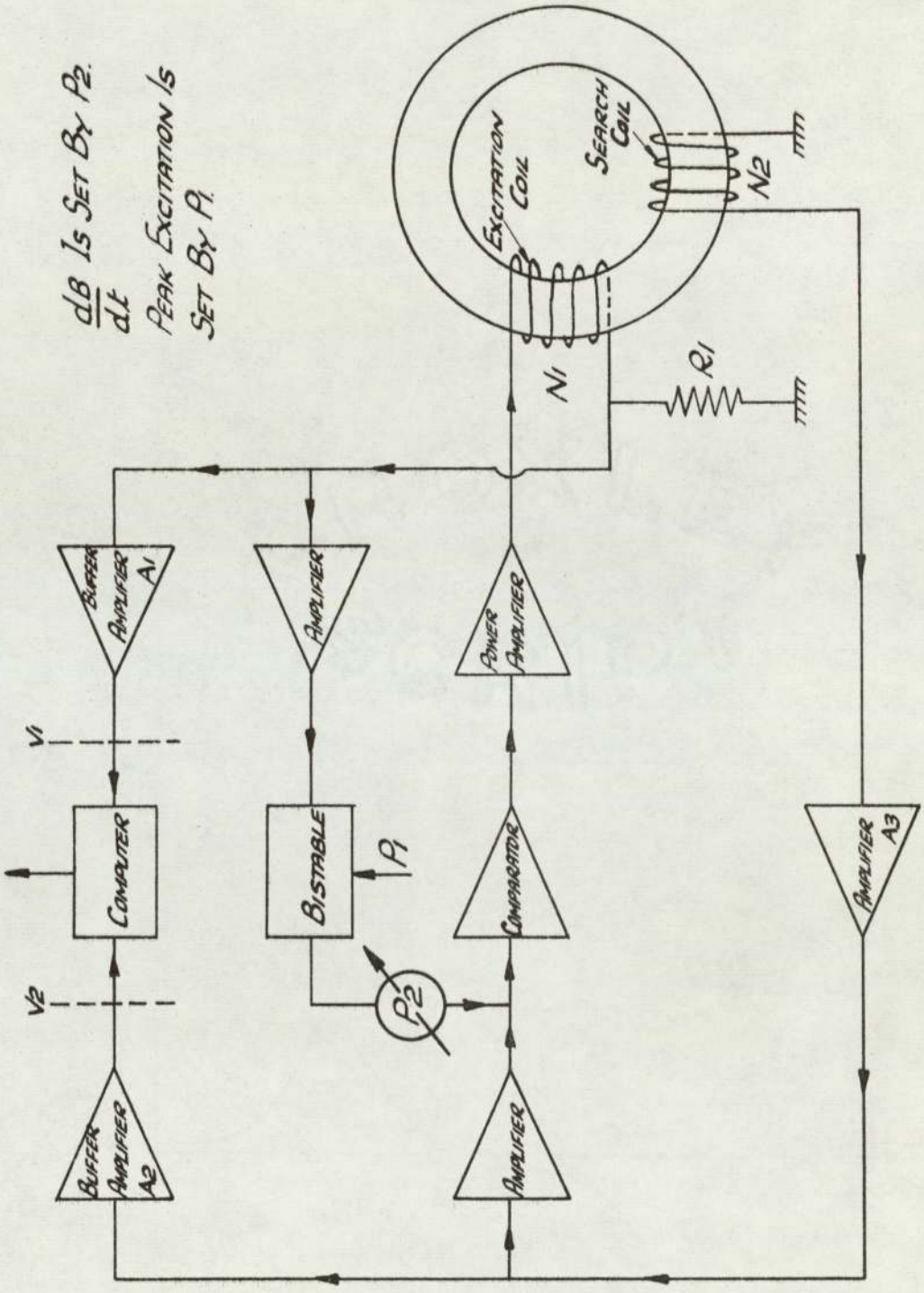

FIG 8. CIRCUIT DIAGRAM FOR DYNAMIC TESTS.

(i) a constant voltage from the bistable circuit. This circuit was a voltage comparator having two stable states, each being excited when its input assumed two fixed values. For a symmetrical hysteresis loop, these two values were equal and opposite.

(ii) a voltage which was proportional to the induced voltage in the search coil.

When the search coil was connected via amplifiers to the comparator, the output voltage of the comparator became:

$$V_1 = K_1 \int V_B \cdot dt + K_2 \int \frac{dB}{dt} \cdot dt$$

$$K_1 \int V_B \cdot dt + K_2 \int dB$$

where K_1 and K_2 = Circuit constants

The addition of the $K_2 \int dB$ term to the V_1 voltage expression had the effect of changing the time duration required to reach the maximum voltage of the bistable. This meant that any change in dB/dt would produce a change in voltage V_1. After amplification through the power amplifier this output would produce the necessary change in excitation current so as to maintain dB/dt constant.

Typical waveforms of flux, dB/dt and excitation current obtained with the Lucas built electronic hysteresigraph are shown in Fig. 9.

4.1.4. The computer

Voltage signals, directly proportional to field strength and search coil voltage were fed into a Digital Equipment PDP9 computer via an analog-to-digital converter. These signals were processed in a computer program which performed the following operations:

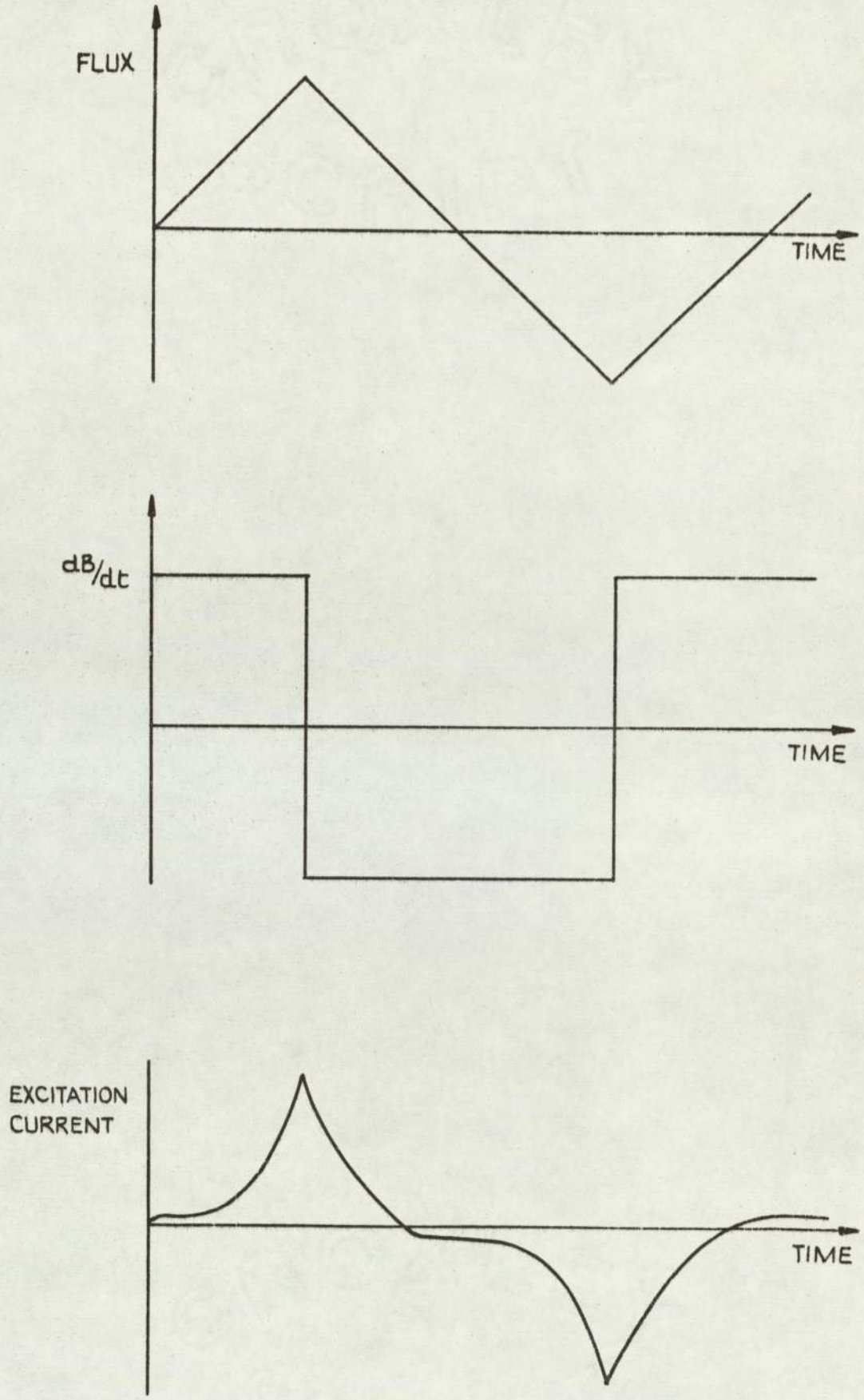

FIG. 9. TYPICAL WAVEFORMS OBTAINED WITH THE LUCAS BUILT ELECTRONIC HYSTERESIGRAPH.

1) Measured the period of the hysteresis loop.

2) Calculated and stored on magnetic tape a given number of field strength (X_H) and flux density (Y_B) co-ordinates. These were taken at regular time intervals throughout the cycle of the hysteresis loop.

3) Printed out, in tabular form, all, or any predetermined sequence, of the X_H and Y_B co-ordinates. For each pair of co-ordinates, the value of the dB/dt between them and the previous sample was also printed out.

4) Calculated the area of the hysteresis loop. This was achieved by integrating the product of the X_H co-ordinate and the $Y_{B2} - Y_{B1}$ co-ordinates. This is shown in Fig. 10. The area of the loop, which was printed out, gave the energy loss in joules per cycle.

5) Printed out the maximum values of X_H and Y_B. This requirement was of particular importance when all the measured loop co-ordinates were not printed out.

6) Printed out the period and frequency of the loop.

7) Calculated and printed out the average dB/dt for the loop. This was based on the time duration between the two peak values of flux density. This calculation provided a check between the average dB/dt and the actual dB/dt's measured between individual samples. (see typical print out in Appendix B).

8) Calculated and printed out the iron loss in watts.

A copy of the program, a flow diagram and a typical print out are shown in Appendix B.

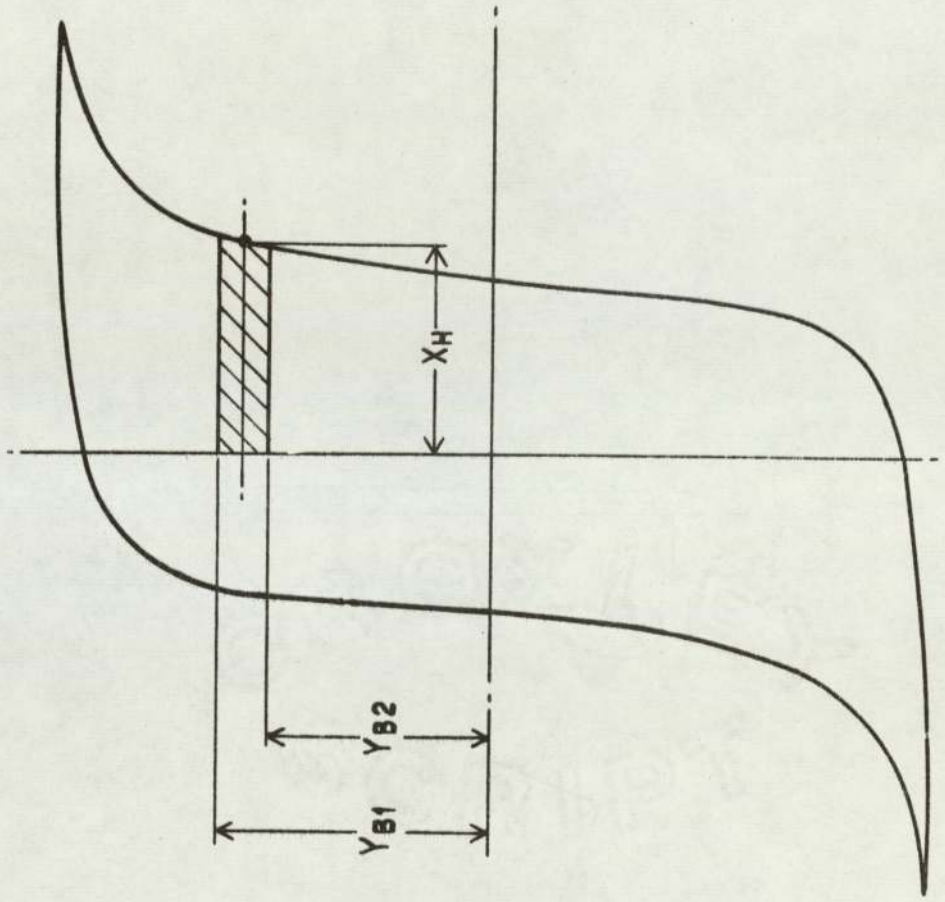

FIG.10. THE PROCESS OF INTEGRATING THE LOOP AREA.

A second program was used to draw hysteresis loops on the X-Y plotter. This program called up the stored data which the first program had deposited on magnetic tape. There was one scale for the flux density and the field strength was plotted on one of five possible scales, depending on the magnitude of the maximum field strength co-ordinate. The dimensions of the lamination stack and the frequency of the loop were printed out on each X-Y plot.

4.1.5. Circuit constants

Referring to Fig. 8, R_1 was a 0.1 ohm. resistance in series with the exciting coil. The voltage drop across this resistance was a direct measurement of the excitation current i_1.

From Fig. 8 it can be seen that potential V_1, with respect to zero, is $A_1 \cdot R_1 \cdot i_1$.

where A_1 = gain of buffer amplifier. This can be set to one of three values depending on the magnitude of i_1 (x 10, x 20 or x 100).

$$i_1 = \frac{V_1}{A_1 \cdot R_1}$$

also $$i_1 = \frac{H \cdot L}{N}$$

where H = magnetic field strength, A/m.

L = mean length of magnetic path, m.

N_1 = No. of turns on excitation coil

$$\therefore \quad H = \frac{N_1 \cdot V_1}{A_1 \cdot R_1 \cdot L}$$

$$C_1 \cdot V \qquad (4.1)$$

where C_1, the m.m.f. constant $= \frac{N_1}{A_1 \cdot R_1 \cdot L}$ (4.2)

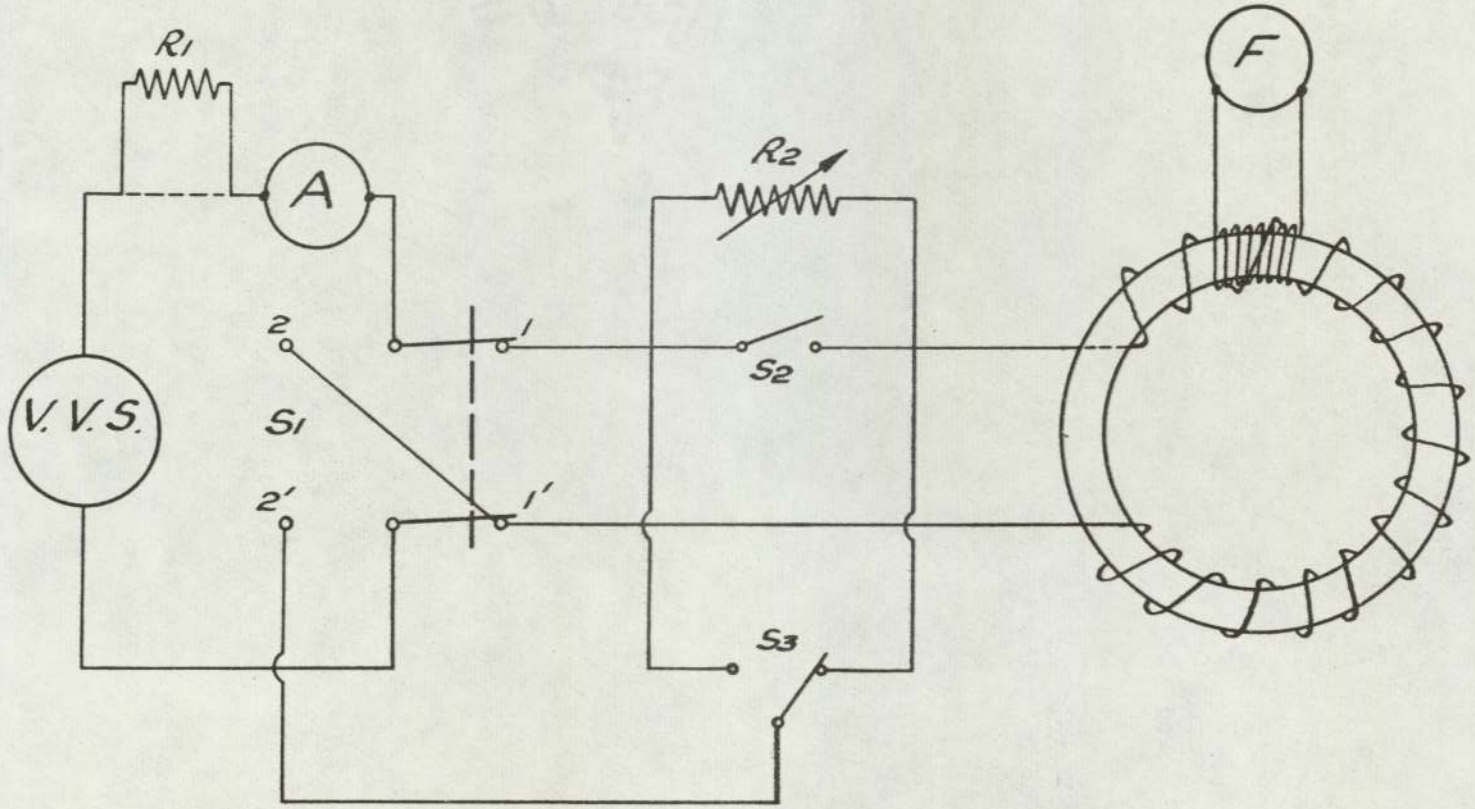

FIG 11. CIRCUIT DIAGRAM FOR STATIC TESTS.

It can also be seen from Fig. 8 that the potential V_2, with respect to zero, is a function of the e.m.f. induced in the search coil.

$$V_2 = A_2 \cdot A_3 \cdot N_2 \cdot d\Phi/dt$$

$$= A_2 \cdot A_3 \cdot N_2 \cdot A \cdot dB/dt \qquad (4.3)$$

where A_2 = gain of buffer amplifier. This can be set to one of three values, depending on the magnitude of dB/dt (x 1, x 10 or x 100).

A_3 = amplifier with constant gain of 10.

N_2 = No. of turns on search coil

A = sectional area of stack, m^2.

Integrating equation 4.3 gives:

$$B = \frac{1}{A_2 \cdot A_3 \cdot N_2 \cdot A} \int_0^T V_2 \cdot dt \text{ (assume at time t=0, B=0)}$$

$$= C_2 \int_0^T V_2 \cdot dt \qquad (4.4)$$

where C_2 = the flux constant $= \frac{1}{A_2 \cdot A_3 \cdot N_2 \cdot A}$ (4.5)

In obtaining the energy loss per cycle the energy loss constant $C_3 = 1$.

It was however, advantageous to express the magnetizing force in terms of kA/m. This meant that C_1 had to be divided by 1000, and so C_3 became 1000.

C_1, C_2 and C_3 formed part of the input data to the computer.

4.2. Static Tests

Magnetization curves and static hysteresis loop tests were obtained using the equipment shown in Fig. 11. The power source was a Farnell TSV 70 variable voltage supply (V.V.S.) which was capable of providing a stabilised voltage output over

the range of 0 to 35 volts with a maximum current of 10 A, or 0 to 70 volts with a maximum current of 5 A. Low values of current were easier to control by having an 11 ohm. resistance, R_1, in series with the power source. A multi-scale ammeter (A) was also in series with the power source. Exciting currents above 2.5 A were obtained with R_1 left out of circuit, as shown by the dotted line.

F was a Norma Fluxmeter, having a high damping D'Arsonual system which moved in the field of an Alnico core permanent magnet. An optical projection arrangement employing a light source, condensing lenses and a cylindrical mirror was used to indicate the deflection of the coil onto a ground glass scale. The meter had 10 scale ranges which extended from 5×10^{-6} to 5×10^{-3} webers-turns per scale division.

The lamination stack approximately 0.62 cms. thick and the whole of the stack was covered with several layers of insulating tape to prevent any of the coil turns shorting to the stacks. The search coil, which consisted of between 20 and 34 turns of 24 gauge wire, depending on the lamination size, was wound on the stack first. Insulating tape was wound over the search coil and the excitation coil of 21 gauge wire was then wound uniformly round the stack circumference. The number of turns ranged from 120, for the smallest lamination size, to 160 for the largest size.

The test methods used are described by Golding[12].

For the magnetization curves, measurements were taken for various values of magnetic field strength from 80 to 3000 A/m.

The magnetic field strength H, is given by $\frac{I.N_1}{L}$ (4.6)

where I = exciting current, A

N_1 = No. of turns on the coil

L = mean length of flux path, m. (Provided the mean diameter to radial thickness is not less than approximately 6:1, this will equal the mean circumference of the stack).

The magnetic flux density is given by $\frac{\theta . Range}{2 . A . N_2}$ (4.7)

where θ = deflection of fluxmeter

Range = fluxmeter scale range, Wb-Turns

A = sectional area of stack, m^2.

N_2 = No. of turns on search coil

The Reversal Method was used for the static hysteresis loop tests and a digital X-Y plotter was employed to draw the loops. The area of the loops were measured by a planimeter.

SECTION 5

PRELIMINARY TESTS

5.1. Leakage Flux

5.1.1. Introduction

Since the excitation coil could not be wound uniformly round the lamination stack (see Section 4.1.2), it was necessary to obtain data of the leakage flux to ascertain whether the flux density distribution is reasonably uniform around the stack.

5.1.2. Leakage flux measurements

In a paper, which is concerned with flux distribution around an annular iron ring, Hammond[14] derived the following equation for obtaining the leakage flux in an infinitely long hollow iron cylinder magnetized as shown in Fig. 12.

$$\frac{\Phi A}{\Phi B} = \frac{\mu \log \frac{a}{b} - 2 \log \left(1-\frac{c}{b}\right) - 2 \log \left(1-\frac{a}{d}\right)}{\mu \log \frac{a}{b} - 2 \log \left(1+\frac{c}{b}\right) - 2 \log \left(1+\frac{a}{d}\right)} \qquad (5.1)$$

where μ = relative permeability

a, b, c, d = dimensions shown in Fig. 12

In the test rig used in this work, the centre line of the magnetization coil was coaxial with the lamination stack, therefore c in equation (5.1) was 0.

Table 1 shows the values of leakage flux, obtained using equation (5.1), for the 5 lamination sizes.

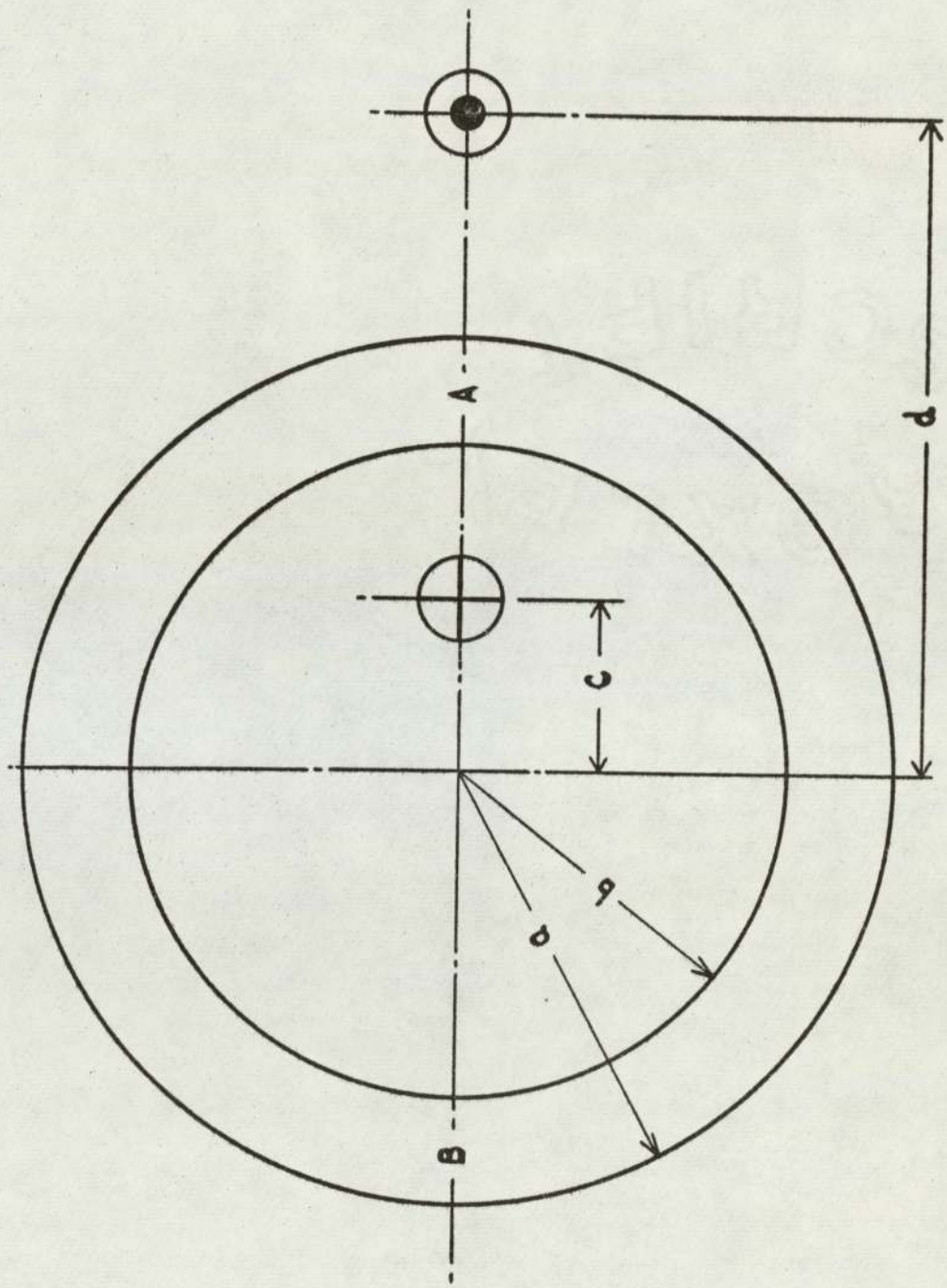

FIG.12. PARAMETERS RELATING TO HAMMOND'S LEAKAGE FLUX EQUATION

TABLE 1

THE CALCULATION OF LEAKAGE FLUX

USING HAMMOND'S EQUATION

Relative Permeability	Leakage flux, %				
	A	B	C	D	E
250	2.46	3.06	3.74	2.95	1.29
500	1.24	1.55	1.89	1.49	0.65
750	0.83	1.03	1.27	1.00	0.43
1000	0.62	0.78	0.95	0.75	0.33
1500	0.41	0.52	0.64	0.50	0.22
2000	0.31	0.39	0.48	0.38	0.16
2500	0.25	0.31	0.38	0.30	0.13
3000	0.21	0.26	0.32	0.25	0.11
3500	0.18	0.22	0.27	0.21	0.09
4000	0.16	0.19	0.24	0.19	0.08

A = 10.5 cm. External Diameter 8.5 cm. Internal Diameter

B = 13.0 " " " 10.5 " " "

C = 16.3 " " " 13.0 " " "

D = 18.0 " " " 13.0 " " "

E = 18.0 " " " 8.5 " " "

A series of tests were arranged to measure the distribution of flux around a lamination stack, whilst it was in position in the test rig. The stack was divided into 3 equal axial sections, each 0.634 cm. high, and insulated from each other by means of Tufnol rings 1.6 cm. thick. Around the centre stack were wound a number

of 10 turn search coils as shown in Fig. 13. The exciting current was progressively increased and at each current level flux measurements were taken on each of the search coils.

The two outer laminations stacks were then removed from the rig and the whole series of tests repeated.

The results of the two tests are shown in Fig. 14. From these results the following two observations could be made.

a) The results obtained with the three stacks in position were lower than the results obtained with the one stack only.

b) Even with the three stacks in position the flux leakage was appreciably higher than the results obtained by using Hammond's equation.

The reason for this discrepancy was that Hammond's calculation is for an iron ring of infinite length with a two dimensional magnetic field. The lamination stack used in this investigation had a small ratio of length to diameter. Therefore the field distribution in the stack could not be considered to be two dimensional. By using the two outer stacks as magnetic end shields the flux distribution in the centre stack became such that the flux leakage, in the plane parallel to the axis of the ring, was reduced.

Tests were also taken on the equipment using only the one search coil which is connected to the hysteresigraph. In these tests the search coil was placed at various positions, relative to the excitation coil, and the output data from the computer was checked for a number of excitation levels. These tests confirm that the order of magnitude of leakage flux was acceptable.

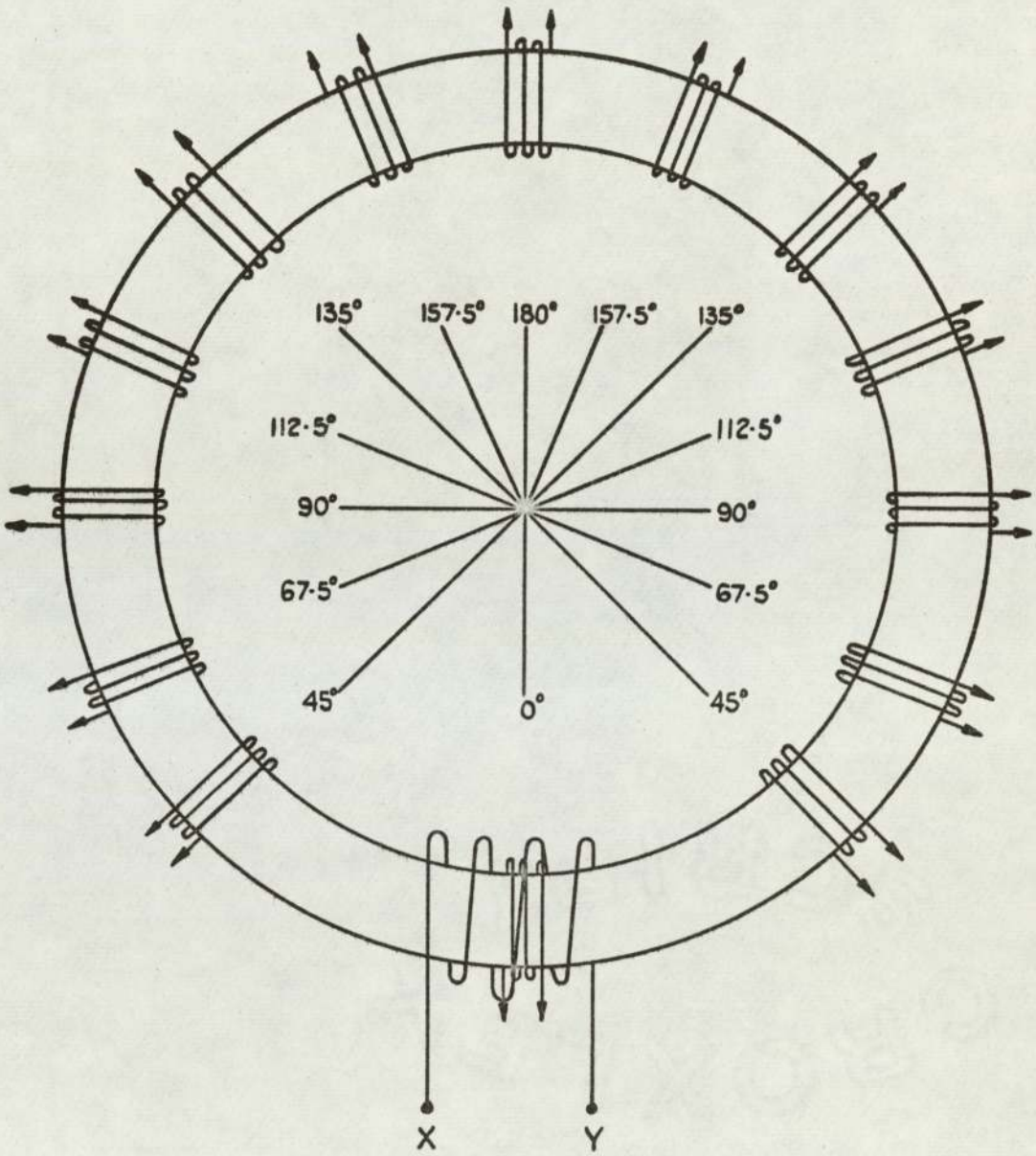

FIG.13. ARRANGEMENT OF SEARCH COILS FOR LEAKAGE TESTS.

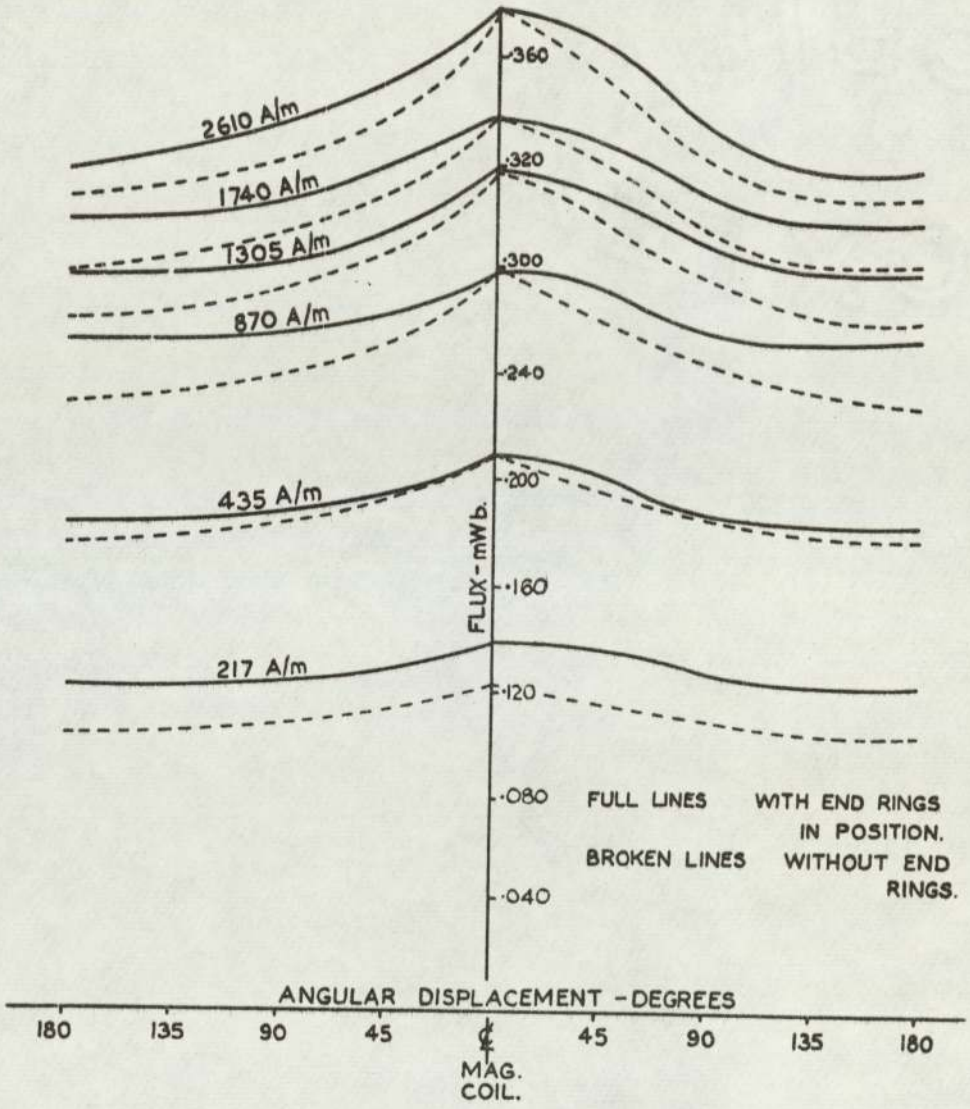

FIG.14. FLUX DISTRIBUTION MEASUREMENTS SEARCH COILS CONNECTED DIRECTLY TO FLUXMETER

It was decided to adopt a standard practice of placing the search coil at a position 90^{o} from the centre line of the excitation coil. This corresponds to the minimum deviation of flux from the average value in the stack. The results show that the leakage fluxes could be neglected for all practical purposes.

5.2. Effect of Pressure

In designing the test rig, it was considered necessary to have the pressure on the lamination stack as a controllable variable. Walker, Rogers and Jackson[15] in a paper on "Pressing and clamping of laminated cores", emphasize that even the most carefully prepared surfaces contain "hills" and "valleys" which are large compared to the molecular dimensions of the material. This implies that the compressive force between the laminations acts on a series of small contact areas, rather than on the total surface area.

The main aim of the present tests was to ensure that over a range of lamination pressure, which extends beyond typical values for electrical machines, the compressive forces at the points of contact do not puncture the oxide layer and reduce the inter-laminar resistance.

A series of tests were taken on a lamination stack over a range of pressure of 0 to 840 kN/m^2. From these test results (Fig. 15) it can be seen that the iron loss was substantially independant of the pressure.

Increasing the clearance between the punch and the die will produce blurrs on the laminations and so the degree of compression on the laminations may become more important.

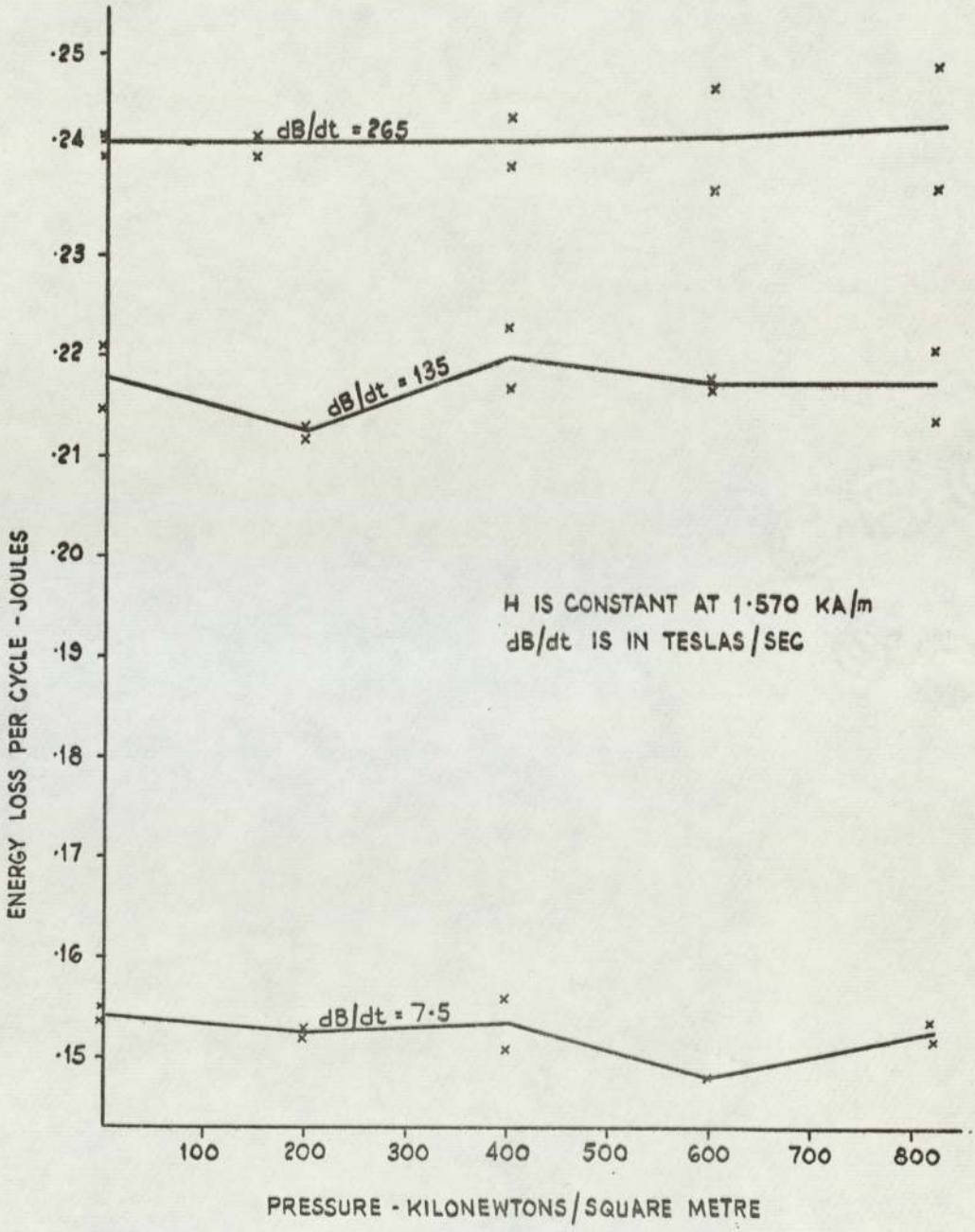

FIG.15. LOSS PER CYCLE AGAINST LAMINATION STACK PRESSURE.

SECTION 6

METHOD OF ANALYSIS

6.1. Introduction

The magnetic characteristics of the samples were measured under static and dynamic conditions. The areas of deformation were then carefully examined and after a full metallurgical study, the correct annealing temperature for the material was obtained (see Section 6.5). After annealing, the magnetic properties were again measured. From the results of these tests, the effects of punching upon the properties of the material was ascertained.

6.2. Dynamic Tests

Published works in recent years 2,5,6, state that the hysteresis loop, measured under dynamic conditions, is a direct measurement of the total iron loss .

For each of the lamination stacks tested, dynamic loss measurements were taken over a range of maximum H. For each maximum value of H, the rate of change of flux density (dB/dt) was varied. At each test point the following were obtained from the computer print out, (see Appendix B).

a) Maximum value of H.

b) Maximum value of flux density.

c) Period and frequency of the hysteresis loop.

d) Energy loss.

e) Power loss.

f) Average value of dB/dt for hysteresis loop.

From the above results, a family of curves of total energy loss in the iron against the rate of change of flux density (dB/dt) was plotted (Fig. 16).

Since the iron was magnetized at a constant dB/dt, it was considered suitable to use a fixed arbitrary value of dB/dt for comparing the total iron losses of the test samples. A dB/dt of 100 Teslas/sec. was chosen for this purpose and using the data obtained from the energy loss, - dB/dt curves, curves of total energy loss at 100 dB/dt against magnetic field strength were plotted for each test (Fig. 17).

In these tests the maximum exciting current was limited by the current rating of the power amplifier. Although this amplifier was force cooled, 5 amp peak excitation was the thermal limit of the device. Exciting current was also limited by the increasing impedance of the excitation coil at higher frequencies.

Magnetization curves may be plotted from the maximum co-ordinates of the loops obtained in these tests. Because these curves relate to the dynamic state of the material, and therefore eddy currents are present which oppose flux change, they may differ slightly from the static magnetization curves.

6.3. Static Tests

The object of these tests were as follows:

a) To obtain magnetization curves under static conditions. These provide a direct comparison with the curves provided by the steel manufacturers. Another advantage of these curves was that it was possible to vary the exciting current over a much wider range than in the dynamic tests, so that the effect of punching on the magnetization curve could be examined well into the region of magnetic saturation.

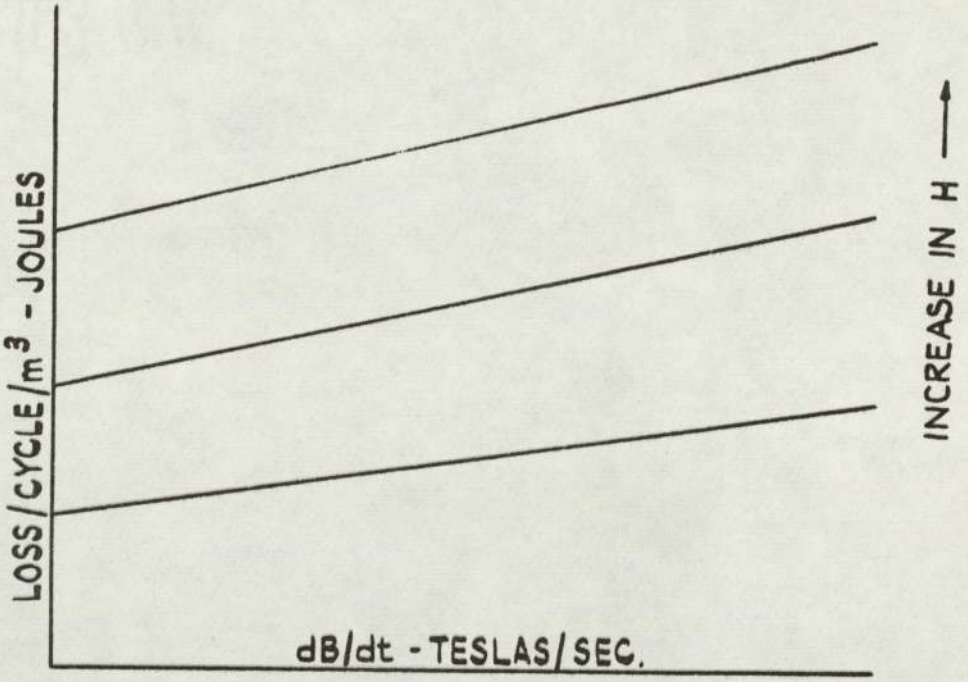

FIG. 16. VARIATION OF ENERGY LOSS WITH RATE OF CHANGE OF FLUX DENSITY.

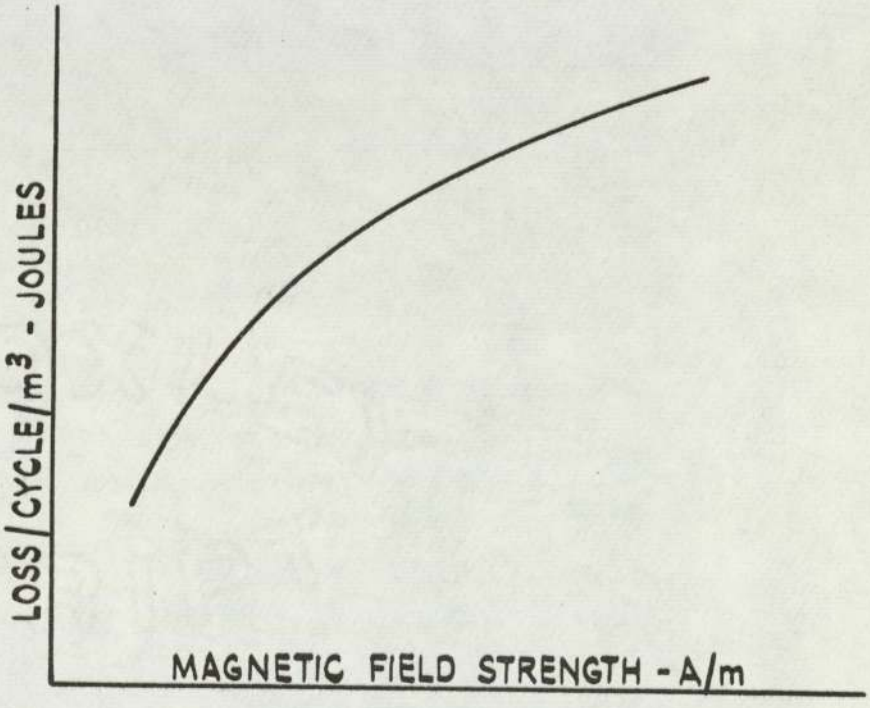

FIG. 17. VARIATION OF TOTAL IRON LOSS AT 100 dB/dt WITH MAGNETIC FIELD STRENGTH.

b) To use the static hysteresis loss results to provide information to verify that the total energy loss - dB/dt relationship, for a given field strength, is a straight line. Had a straight line law not held, then these tests would have provided information regarding the anomaly factor of the material.

c) To compare the static loss results, taken before and after annealing. This provides a means of examining the effect of the punching strains upon this loss and also the confirmation of the results of previous workers[1] and [2].

d) To provide a means of comparing the ratio of static to dynamic loss which was achieved by plotting the static loss to a base of H and comparing the results with the dynamic loss previously measured (see Fig. 17).

6.4. The Annealing Process

6.4.1. Introduction

Whenever plastic deformation occurs in a metal, there are changes in its physical and magnetic properties. Restoration of these properties, so as to give a strain-free material, can be achieved by annealing in a controlled atmosphere, at the correct temperature. This temperature is established by considering the three constituent processes of annealing, these being recovery, recrystallization and grain growth. Although these processes may sometimes overlap, they are clearly distinguished from each other and it is important that each one be considered separately. Smallman[16] is one of the many well known authors who deals in detail with these three processes which are summarized as follows.

6.4.2. Recovery

Deformation in a metal, such as electrical sheet steel, causes the lattice structure of the crystal to become distorted and so the free energy level of the composite atoms is increased. This free energy can be reduced to its original level by thermally activating the metal.

The recovery process can be best explained if it is realised that the crystal lattice consists of a regular array of atoms. When the metal is deformed, the atoms in certain planes of the lattice are rearranged. This does not alter the main structure of the lattice, but only the relative positions of atoms in certain adjacent crystallographic planes, the boundaries between these planes being known as dislocations. For each kind of lattice structure there are only certain planes and definite directions along which the plane slip can occur.

When a metal is heated, the application of thermal energy brings about a change in the lattice known as polygonization. This is a recovery mechanism whereby the dislocations are rearranged into different groupings at a lower energy level. When this occurs, the residual stress in the metal is relieved. This is generally accompanied by a large change in electrical resistivity but only a very small change in hardness.

Although polygonization is perhaps the main cause in bringing about stress relief during recovery, it is not the only factor. Stress relief is also brought about by the elimination of the microscopic cracks along the punched edges of the laminations.

During the recovery process there is little change in grain size, in fact there are no observable changes at all in the microstructure.

6.4.3. Recrystallization

In this process, which is both temperature and time dependent, the deformed lattice structure is completely replaced by a new unstrained structure. The new structure, which may have quite a different lattice orientation from that of the original structure, is obtained by a nucleation and growth process. Evidence now shows that the formation of the new structure is closely related to the polygonization mechanism. This is because the energy which is released at the sides of the dislocation is responsible for producing the nuclei of the new crystals.

The rate of formation of nuclei and the rate of their growth are the basic factors determining the rate of recrystallization. Increase in the degree of deformation gives higher strain energy in the lattice and does therefore reduce the time required for recrystallization. A certain degree of deformation must always exist before the recrystallization process can start.

During this process there is an appreciable fall in the hardness of the metal and the overall effect is in the direction of restoring the physical properties of the metal which existed prior to deformation.

6.4.4. Grain growth

If the temperature of a metal is increased beyond that which is required for recrystallization, then the metal will lower its energy further by reducing the total area of the grain surface. This is accomplished by small grains being absorbed into larger grains. The most important factor governing this process is the surface tension of the grain boundaries. At high temperatures, where the atoms are mobile, a grain with fewer sides will tend to

become smaller and, because of the surface tension forces, those with more sides will tend to grow.

Grain growth is influenced by the geometry of the metal and this can be very significant when the metal is in sheet form. When this occurs, the grain size may become comparable with the thickness of lamination. The consequence of this is that the grain boundaries must be normal to the lamination surface and so the growth becomes a two dimensional rather than a three dimensional process.

Beyond the recrystallization temperature, the grain size increases linearly with the logarithm of the time. Size also increases with temperature, but no well defined relationship is readily available.

Note: In metallurgy "grain" and "crystal" are synonymous.

6.5. Metallurgical Analysis

Since the temperature required for annealing is very much a function of the degree of deformation in the metal, it was considered necessary to determine separately the annealing temperature required for each tool clearance. For the two tool clearances used, a detailed study was made of samples of metal taken from the largest lamination.

Each of the laminations used for analysis was cut into eight equal sized sectors, using a slow speed slitting wheel which was supplied with ample coolant. One of the sectors was used to determine the properties of the material in the punched condition, while the properties of the other seven samples were found after being annealed for 6 hours at different temperatures ranging from 400°C to 1000°C. Three types of tests were carried out on each of the samples, these being:-

a) The Vickers micro-hardness test. This was done as near as possible to the deformation area. Because of the practical difficulties of working on a curved surface, especially polishing, the sample was cut as shown in Fig. 18, and the pyramid type impression made at a distance of 0.025 mm. from the punched edge. This was done for both the inner and outer punched surfaces.

b) Bulk grain size. The same section of lamination as used for the micro-hardness test, was used for the grain size measurement. The samples were suitably ground and polished and then etched so as to reveal the grain structure. The image of the sample surface was then projected onto a large screen and the relative grain size measured by means of a linear intercept method.

c) Microscopic examination. This was carried out on each of the samples with magnifications of 100 and 400, to show the nature of the recrystallization taking place at each of the annealing temperatures.

6.6. Micro-Hardness Plots

When stresses are set up in a metal the lattice becomes distorted and its plastic flow capacity decreases. This property is known as Strain Hardening or Work Hardening. Therefore the measurement of hardness is a useful means of determining any change in internal stress of the material. This method of measurement is described by Tweeddale[17].

Hardness plots were taken on several different lamination sizes and thicknesses. The procedure being as follows:

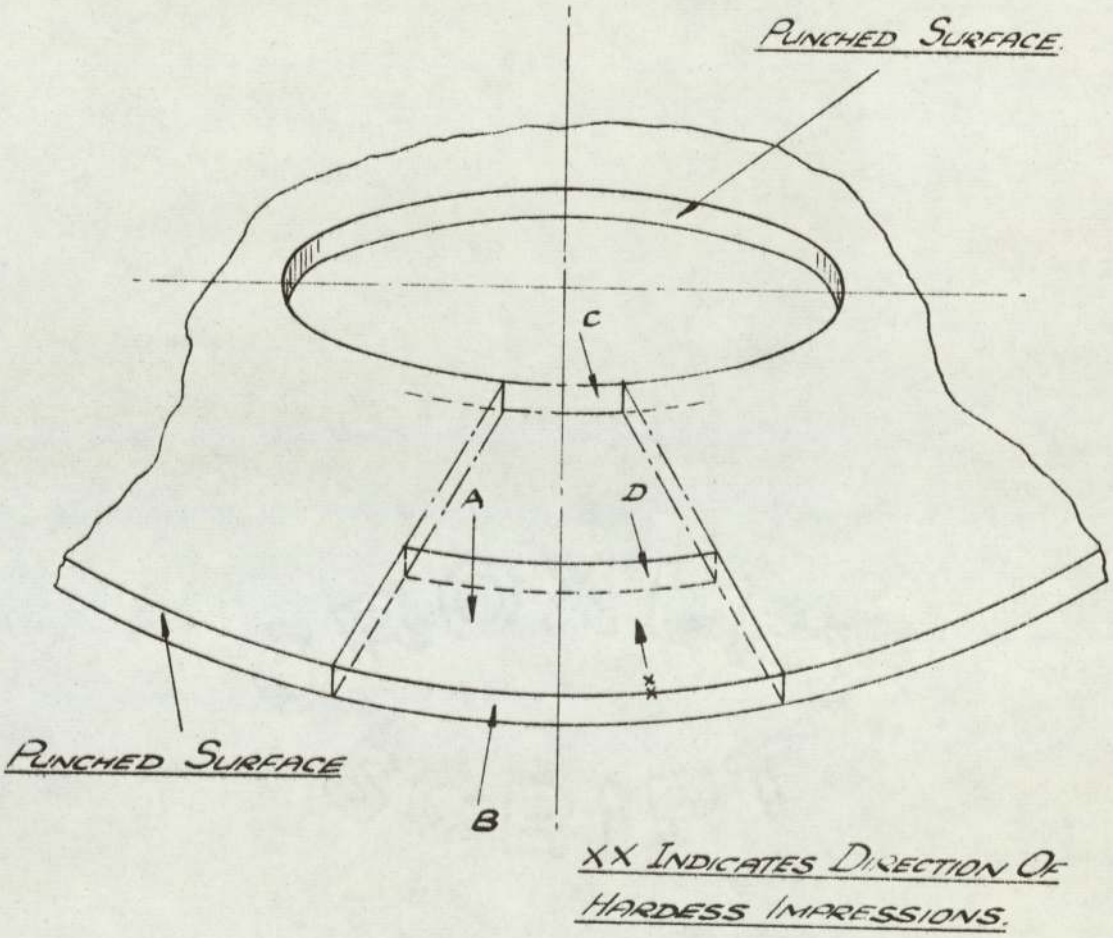

FIG. 18. SECTION OF LAMINATION REMOVED FOR MICRO-HARDNESS TESTS. LETTERS IDENTIFY DIRECTION OF PHOTOGRAPHS SHOWN IN FIGURES

From each punched edge of the lamination, small longitudinal sections were cut as shown in Fig. 18. To avoid any deformations due to the actual cutting operation the sections were removed by means of a slitting wheel which was supplied with ample coolant.

The sections were mounted in 'cold setting' araldite and then wet ground on a series of various grades of silicon papers. After grinding, the specimens were polished on a series of diamond compound impregnated wheels. The grain structure and deformation were then revealed by using an etchant consisting of a 2% solution of nitric acid in alcohol.

The micro-hardness plot was then determined by means of a Leitz micro-hardness tester. This apparatus provides the means of pressing a pyramidal diamond into the surface of a metal. This is done under a fixed load and the resultant indentation measured. From this measurement, the Vickers Pyramid number (V.P.N.) is found as follows:

$$\text{V.P.N.} = \frac{\text{Applied Load}}{\text{Pyramidal area of indentation}}$$

This plot was taken inwards from each punched surface, as shown in Fig. 18, at intervals of 0.025 mm.

Since the hardness of a deformed lattice structure is higher than that of a similar structure having no plastic deformation, it is to be expected that there will be a fall-off in hardness with distance from the punched surface. This will continue until no further change in hardness is detectable.

The variation of the magnetic characteristics with distance from the punched surface was then examined and a possible relationship with the hardness plots investigated. If a correlation can be established between the work hardening around the punched edge of

the laminations and the deterioration in magnetic properties due to punching, then there are two distinct advantages to be gained. These are:-

a) A clear understanding of the factors which cause the work hardening, and effects its magnitude, would inevitably result in useful information concerning the deterioration in magnetic properties.

b) A determination of the extent of the work hardening relative to the total surface area of the material, should give a quantitative indication of the deterioration in magnetic properties.

6.7. Electro-Chemical Etching

Laminations in the required ring form can be obtained by an electro-chemical etching process which does not produce any punching strains in the material. By comparing the magnetization curve for punched material after it has been annealed, the effectiveness of the annealing process in restoring the magnetic properties of the material can be established.

Electro-chemical etching depends on the process of electrolysis, in which a flow of current through an electrolyte results in bydrogen ions being liberated as hydrogen gas and these positively charged ions from the electrolyte are deposited on the cathode. The negatively charged chlorine ions are deposited on the anode in the form of nascent chlorine which causes the anode to be dissolved with the formation of iron chloride. This process continues until the anode is gradually dissolved away.

Prior to etching the lamination squares were prepared by careful cleaning, and an image of the required ring lamination was produced on the lamination material, in an etch resistant lacquer, by a screen printing process. The reverse side of the lamination squares was protected by a stop-off lacquer.

The etching apparatus consisted of a bath containing an electrolyte of diluted hydrochloric acid. This was continuously stirred and kept at a constant temperature of 30°C. The prepared lamination squares were placed in the bath, one at a time, with a suitably sized stainless steel cathode. They were then connected to a constant voltage supply which was controlled so as to give a rate of dissolution of metal from the lamination squares which resulted in a smooth finish on the edges of the ring laminations.

6.8. The Kerr Magneto-Optic Effect

During a visit to the Wolfson Centre for the Technology of Soft Magnetic Materials, at Cardiff University, various measuring apparatus based upon Kerr magneto-optic effect were demonstrated. These demonstrations showed that the Kerr effect might provide an effective means of measuring the magnetic characteristics at a point on the punched surface of the lamination and at subsequent points below the surface.

The Kerr magneto-optic effect, which is explained by Carey and Isaac[18], can be summarized as follows: when a beam of polarized light is reflected from a surface which is magnetized, the reflected beam emerged elliptically polarized. This is because the symmetry is destroyed by the presence of a magnetic field and the field gives rise to a vibrating component called the Kerr component, perpendicular to the incident light vibration. This phenomenon is known as the Kerr magneto-optic effect. There are several ways of

observing this phenomenon, one of which is known as the transverse effect. In this, the magnetic field is not only in the plane of reflection but also occurs in a plane perpendicular to the plane of incidence. This arrangement, which was used in the present investigation, resulted in the intensity of the reflected light varying in proportion to the magnetic flux density.

The general arrangement of the apparatus used by the Wolfson Centre is shown in Fig. 19. This consisted of a source of polarized white light and a variable aperture arranged in such a way as to illuminate a small spot on the surface of the laminations. The light reflected from the surface was monitored by a photo-diode which gave an output proportional to the intensity of the incident light. The lamination was magnetized from a sinusoidal voltage source at 80 Hz with a field strength of 500 A/m. This arrangement gave an output from the photo-diode which was a measure of the magnetic flux density at the point of incidence. This output was carefully calibrated so as to give the relative permeability of the lamination material at a number of points.

In this investigation, the permeability was determined at a point on the punched surface. A layer of material was then removed from the punched surface by a chemical polishing process and the permeability determined again. This procedure was repeated until further change in permeability, with increase in distance from the punched surface became minimal.

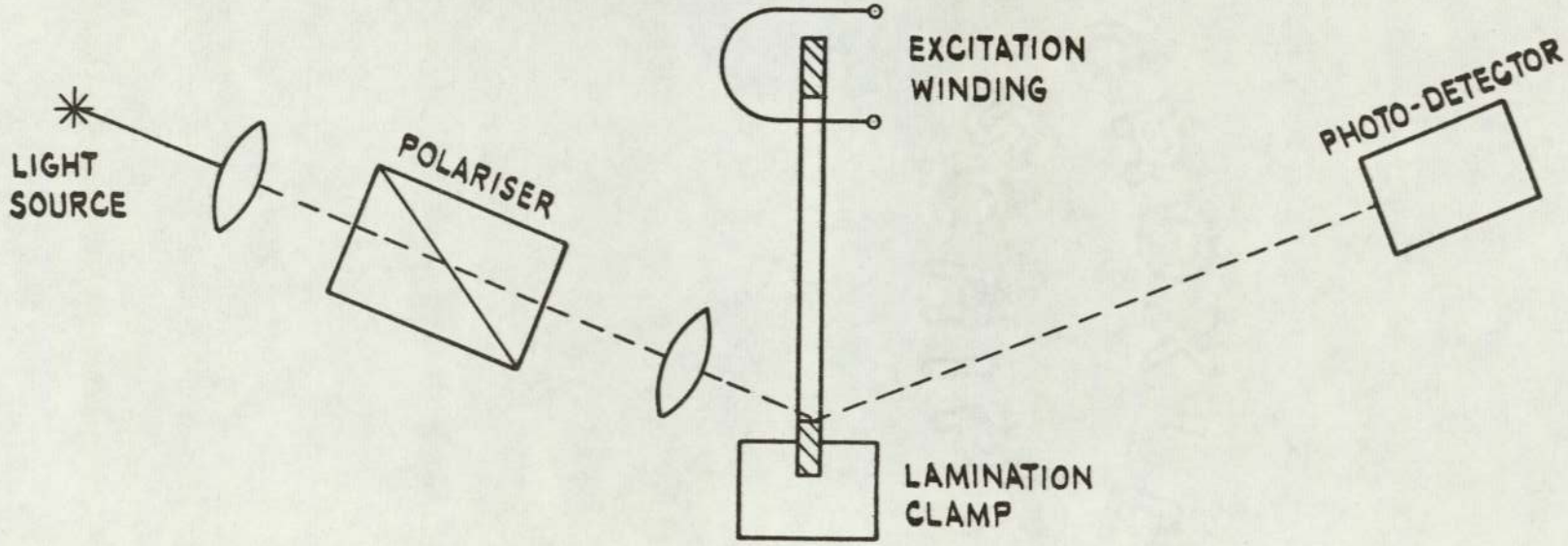

FIG. 19. EXPERIMENTAL ARRANGEMENT FOR MAGNETO-OPTIC EFFECT.

6.9. Microscopic Examination

Besides the microscopic examination already mentioned, in Section 6.5, it was thought necessary to have a general microscopic investigation of the punched surface regions of the laminations. The aim of such an investigation was two-fold. Firstly, to examine any crack propagation and the surface characteristics in the punched region, and secondly, to examine the formation of the oxide layer. This layer was provided so as to form the inter-laminar insulation.

For this investigation, magnifications of up to 2000 were used on the Electron Scanning microscope, and up to 400 on the optical microscope.

SECTION 7

ANALYSIS OF TEST RESULTS

7.1. Dynamic Tests

Readings were taken at a series of constant peak magnetizations, for all the samples tested, and the results plotted as shown in Figs. 20-22 (see Section 6.2). The points were plotted on a linear scale and mean straight line was drawn through the points. The maximum deviation was $\pm$ 6.7%. Although some scatter is present at the higher magnetization values, the results would seem to confirm that a straight line law is acceptable. These results were obtained for the three material thicknesses on four of the ring sizes.

From the curves of loss against dB/dt (Figs. 20-22 and others not included) curves of total energy loss against H were plotted (at 100 dB/dt) and are shown in Figs. 23-26. These curves were plotted for the punched samples before and after annealing. From These curves it would appear that the total iron loss does not seem to increase due to punching. There are two possible explanations for this:

a) It will be seen in Section 7.2 that, for the samples tested, the punching process has a significant effect on the magnetization curve only in the region of the knee of the curve. The static loss is proportional to the area of the hysteresis loop and, even for a hysteresis loop having its maximum co-ordinates in the region of the knee of the curve, the percentage change in static loss due to punching is much

---

Except where otherwise stated all Figures for this section are given on pages 74 to 107 .

smaller than the percentage change in magnetization. In these tests, the change in loss is further diminished since it is only the static loss which is affected by punching (see Section 2.2).

b) The first tool clearance is small and therefore the effect of punching on loss may be expected to be less than with the larger clearances.

In all these curves, the 0.051 cm. thickness always gave a lower loss than the 0.063 cm. and 0.036 cm. thick material. There are two possible reasons for this. Firstly, in these tests the bulk of the total iron loss is the static loss and Littman[10] has shown that there is an optimum thickness for this loss to be a minimum. Secondly, it is probable that different material thicknesses almost certainly would come from different production batches and there is always some variation in properties between batches, which emphasizes that it is the comparison of changes in lamination properties which is important in this work rather than the observation of the actual properties.

Fig. 27 shows a typical relationship between flux density and dB/dt for a range of magnetic field strengths. These curves show that until the material is magnetically saturated there is initially a reduction in flux density as dB/dt increases from zero. This reduction in flux density, which is apparent even in the 0.036 cm. thick material, is caused by the eddy-current reaction. Since the main aim of this work is to investigate the effect of punching, the static magnetization curve was considered to be the most direct and simple way of obtaining the required information on the effect of punching.

Examples of the dynamic hysteresis loop, obtained from the digital X-Y plotter, are shown in Figs. 28 & 29. The increase in loop area with the rate of change of flux can be seen by comparing these loops. Fig. 30 shows a static hysteresis loop and two of its corresponding dynamic loops.

In obtaining this data it was found that at low frequency levels, off set and drift problems in the amplifier control circuit resulted in unreliable readings. For this reason it was found necessary to limit the maximum cycling time around the loop to 100 milliseconds. It was also that sufficient readings could not be obtained for the largest ring size. This was due to the high circuit inductance which caused the circuit impedance to limit the power output from the hysteresigraph.

7.2. Static Tests

Magnetization curves

These curves were obtained, using the method described in Section 4.2, for the majority of the laminations with the first clearance and for the three thicknesses of the smallest ring size with the second tool clearance. The curves are shown in Figs. 31-34. From these curves, the following observations are made:

a) The results show that up to approximately 1.5T, the punched material requires a higher H, for a given flux density, than does the corresponding annealed material.

b) Above 1.5T, the curves for the punched material and the annealed material tend to merge together.

c) For any given value of H, the 0.064 cm. thick material gives the highest flux density and the 0.036 cm. thick material gives the lowest flux density.

d) Above 1.45T, the steel manufacturer's curve shows a higher flux density for a given H than that obtained for any of the annealed material. Below 1.45T some of the annealed material give higher flux density, for a given H, than that shown by the manufacturer's curve (Fig. 35). The steel manufacturers state that their curves relate to average values and that the difference between batches of material may be considerable, due to the small variations in chemical composition and production processes which are likely to occur.

e) The magnetization curve for the chemically etched laminations shows good agreement with the results obtained from the annealed laminations (Fig. 36). This confirms that the annealing process has restored to its original state the B/H characteristics of the material.

f) The magnetization curves, obtained after annealing, for the first and second tool clearances are not identical. This is accounted for by the small variations which are likely to occur in the production processes and chemical composition from one batch to another.

Fig. 37 shows two of the magnetization curves for the annealed material and four of the steel manufacturer's curves for different grades of Ferrosil material. These curves show how close together the B/H characteristics of the four grades are and how far some of the results of the annealed curves depart from these curves. The B/H characteristics of the material is influenced by its small carbon content (approximately 0.05%) and silicon content (1.3% to 2.4%, depending on grade). A slight change in these values has a significant effect on the B/H characteristics.

A chemical analysis of a sample of the annealed test material (Ferrosil 216) gave the following results:

	%
Carbon	0.020
Silicon	1.16
Manganese	0.38
Nickel	0.024
Copper	0.08
Phosphorus	0.006
Sulphur	0.010

This analysis shows the silicon content to be slightly lower than the value quoted by the steel manufacturers for Ferrosil 216 and that the carbon content also seems quite low. A reduction in carbon content generally results in an increase in permeability. These tests show that although the carbon content is low, the annealed material gives a lower flux density, for a given H, than does the steel manufacturer's curve. This would seem to suggest that variations in the cold rolling process may cause structural changes in the material which affects the magnetic properties.

From the magnetization curves, data was obtained to produce curves showing the increase in H required, due to punching, against flux density (Figs. 38-41). From these curves the following observations are made:

1) The increase in required H, rises with increasing flux density up to a maximum value corresponding to the knee of the magnetization curve. Beyond this point, the required H falls rapidly with increasing flux density.

2) For each set of laminations tested, the maximum required increase in H occurs at practically the same flux density level.

3) The required increase in H due to punching, is dependant on the punching factor (equation 3.4).

4) Comparing the results of the first tool clearance with the limited results on the second tool clearance (Fig. 41), it would seem that the influence of increasing the tool clearance is considerable.

The position of maximum increase in required H corresponds to a condition where the ratio of the magnetic field strength ordinates of the unannealed curve to that of the annealed curve is equal to the ratio of the slopes of these two curves (see Appendix C).

Static loops

For the first clearance, tests were taken on all the samples of the smallest ring size and on the ring size of external diameter = 16.3 cm., internal diameter = 13.0 cm. and thickness = 0.036 cm. The tests were taken before and after annealing. From the results of the tests (Figs. 42 & 43) the following observations were made:

a) The 0.036 cm. thick material gives the highest static hysteresis loss and the 0.051 cm. thick material gives the lowest loss. This confirms the findings of the Dynamic Tests (see Section 7.1). Total iron loss at 100 dB/dt and the static loss results are shown in Fig. 44.

b) Although an increase in static hysteresis loss is incurred on the first tool clearance, with a punching factor of 0.5, the increase is regarded as small. Details of these losses are shown in Table 2.

c) Good correlation is obtained between the results of the Static Loss Tests (Figs. 42 & 43) and those of the Dynamic Tests at dB/dt = 0 obtained by extrapolation (Figs. 20-22). This suggests that, over the range of flux density and dB/dt being tested, no anomaly factor was required.

TABLE 2

STATIC HYSTERESIS LOSS TEST RESULTS

	FLUX DENSITY TESLAS	0.2	0.4	0.6	0.8	1.0	1.2	1.4	1.5
0.063 cm. Thickness	(1) UNANNEALED Joules/cycle/m^3	31	62	102	158	237	347	495	585
	(2) ANNEALED Joules/cycle/m^3	11	34	72	127	202	300	423	495
	$\frac{(1)-(2)}{(2)} \times 100$	180	83	42	25	17	16	17	18
0.051 cm. Thickness	(1) UNANNEALED Joules/cycle/m^3	27	55	91	141	212	311	444	513
	(2) ANNEALED Joules/cycle/m^3	12	36	74	126	193	275	371	425
	$\frac{(1)-(2)}{(2)} \times 100$	125	53	23	12	10	13	20	21
0.036 cm. Thickness	(1) UNANNEALED Joules/cycle/m^3	46	79	114	173	275	441	690	
	(2) ANNEALED Joules/cycle/m^3	45	79	114	173	261	398	597	
	$\frac{(1)-(2)}{(2)} \times 100$	0	0	0	0	5	11	16	

It would seem that the effect of punching upon the static hysteresis loss is much smaller than its effect upon the magnetization curve. The reason for this is explained in Section 7.1.

From the results obtained from the static hysteresis loop tests, attempts were made to express the loss in terms of Steinmetz's equation. It was found however, that the exponent of the flux density in the equation was a variable and could be as high as 3.0 at a flux density of 1.5T.

Correlation of the test results was obtained by using a computer regression program and then expressing the results in a form of a 3rd order polynomial.

$$W = a + b.B + c.B^2 + d.B^3 \qquad (8.1)$$

where W = static hysteresis loss, W.

B = magnetic flux density, T.

a,b,c & d = constants.

The constants obtained from the six samples of the smallest ring size (Fig. 42) are shown in Table 3. These results show that there is a significant difference in the constants of each curve. It will also be seen that the linear and cubic terms all increase in the same direction, while the square term increases in the opposite direction. The reason for constant 'a' not being zero in curve Nos. 1,2 and 6 is due to small experimental errors in obtaining the test results.

The results do show that the 3rd order polynomial is a convenient form of equation for expressing the static hysteresis loss.

TABLE 3

THE CALCULATION OF STATIC HYSTERESIS LOSS CONSTANTS USING A 3RD ORDER POLYNOMIAL EQUATION

CURVE NO. IN FIG.42	CONSTANTS OF EQUATION (8.1)			
	a	b	c	d
1	-3.6	320.1	-461.2	418.6
2	-2.2	288.7	-337.7	312.3
3	0.0	163.8	-84.3	157.0
5	0.0	144.6	-69.7	137.8
4	0.0	29.6	116.6	55.6
6	3.0	8.6	181.6	0.0

Curve No.1. 0.036 cm. thick material before annealing.
Curve No.2. 0.036 cm. thick material after annealing.
Curve No.3. 0.064 cm. thick material before annealing. } as in Fig.42
Curve No.4. 0.064 cm. thick material after annealing.
Curve No.5. 0.051 cm. thick material before annealing.
Curve No.6. 0.051 cm. thick material after annealing.

7.3. Annealing Tests

The method of analysis is described in Section 6.5.

The results of the Vickers microhardness tests are shown in Fig. 45. The results were obtained with 100 gram applied load and each Vickers pyramid number was calculated from the average of four impressions. The results show that minimum microhardness occurs in the material in a temperature region of 800°C to 900°C. Smallman[16] explains that minimum hardness is associated with minimum internal strain in the material.

The relative grain sizes at the various temperatures are shown in Table 4. A magnification of 100 was used.

TABLE 4

GRAIN SIZE OF LAMINATION MATERIAL AT VARIOUS TEMPERATURES

1st Tool Clearance

Temp. °C.	Amp	400	500	600	700	800	900	1000
Grain Size mm.	0.17	0.15	0.16	0.17	0.15	0.15	0.14	0.12

2nd Tool Clearance

Temp. °C	Amp	400	500	600	700	800	900	1000
Grain Size mm.	0.14	0.11	0.11	0.14	0.15	0.17	0.15	0.11

The reason why the grain size was measured in the bulk of the material, and not in the area of deformation, was because the purpose of this particular test was to ensure that the grain size in the bulk of the material was not any greater than it was in the material as received from the manufacturers.

Some of the results of the microscopic examination of the annealed samples are shown in Fig. 46 & 47. The examination shows that, at each of the temperatures, there is a close similarity of results between the samples of the first and second clearances.

The samples clearly show recrystallization around the punched edges at 500°C. At this temperature however, the extent of re-crystallization is small and does not extend more than 0.010 mm. inward, from the surface. At 600°C the recrystallization extends as far as 0.025 mm. inwards from the surface. At 900°C the recrystallization has reached a distance of at least 0.6 mm. from

the punched edge. At 900°C also, recrystallization is beginning to take place in a plane at right angles to the direction of the punched surface. At 1000°C there is considerable growth of the new crystals, which have formed along all the lamination edges, and these can be seen growing out towards the centre of the lamination. It can be seen (Fig. 46) that the growth of the new crystals has the effect of dividing the crystals which are present in the centre area of the lamination. Despite the fact that the samples were annealed in an inert gas, above 800°C a considerable oxide layer can be seen.

The following conclusions are drawn from the results.

a) Recovery takes place over the temperature range of ambient to approximately 400°C. There is little change in hardness over this range.

b) Recrystallization in the areas of plastic deformation commences at a temperature somewhere between 400°C and 500°C.

c) There is a temperature lag of approximately 500°C between the start of recrystallization in the deformed areas and that in the main area of the lamination material.

d) Beyond 800°C, the growth of the new crystals is in such a direction to produce a material structure which is different from the material as received from the manufacturers. It also had the effect of dividing the crystals and thereby reducing their size.

These tests clearly indicate that the correct temperature for annealing the first and second clearance laminations was 800°C and hence annealing was carried out at this temperature.

7.4. Micro-Hardness Plots

The results of the plots taken on each of the three thicknesses on the first clearance, using the method described in Section 6.6, are shown in Figs. 48-50. From these results the following observations are made:

a) Up to a given distance from the punched surface, there is a reduction in hardness as the distance from the surface is increased. This is as anticipated since the hardness of a material is highest where the deformation is a maximum.

b) On all three thicknesses the micro-hardness tends to level out to a constant value at a depth of less than0.30 mm. below the surface. This therefore is the depth to which the punching process hardens the material.

c) There is no real difference in the hardness pattern for the three thicknesses.

d) For a given lamination, the hardness beyond the deformation region is not the same for the inner punched surface as for the outer punched surface. This is essentially due to the heterogeneity in the material.

7.5. The Kerr Magneto-Optic Effect

The deterioration in magnetic properties of lamination material was investigated at the Wolfson Centre using this method of analysis (see Section 6.8). The Centre was supplied with samples of the 1st clearance, punched lamination material before it was annealed.

The results of these tests are shown plotted in Fig. 51. Correlation of these results was obtained by means of a computer regression program. The curve was drawn in the form of a 2nd

order polynomial. Higher order equations did not explain away any significant increase of the total variation between the points and so were not used.

From these results the following observations are made:

a) Permeability increases with distance from the punched surface. This trend continues to a depth of at least 1 mm. from the surface.

b) The curve obtained is a direct indication of the effect of punching strains upon the magnetic properties of the material. At any given depth below the surface, the magnitude of the permeability, relative to that pertaining in the bulk of the material, could be an indication of the degree of strain at that point.

c) Comparing Fig. 51 with Figs. 48-50 it will be seen that the micro-hardness levels to a constant value at a much smaller distance from the surface than does the permeability. This suggests that there appears to be no direct relationship between the change in hardness and the deterioration in magnetic properties.

The intention of this investigation was to repeat the tests on the laminations after they had been annealed. From these tests the improvements in magnetic properties, due to annealing, would have been observed. Unfortunately, the Wolfson Centre experienced difficulties in preparing the surfaces of the annealed material and their time schedule did not allow the large amount of time required to complete this work.

Tests were first tried out on a single lamination but problems were experienced due to the low signal to noise ratio at the punched surface. This resulted from a reduction in the signal level due to the corners of the punched edge being rounded during chemical polishing and a significant noise level due to the magnetostrictive vibration of the lamination. This difficulty was overcome by using several laminations clamped together.

7.6. Microscopic Examination

The punched surfaces of each of the three lamination thicknesses, for the first and second clearances, were examined using an Electron Scanning Microscope. Some of the results are shown in Figs. 52 & 53. The extensive crack formation, which is evident in these photographs, was found to be only in the oxide layer. There was no evidence of cracks in the punched surface of the metal.

Fig. 4 (Page no. 20) shows the oxide coating which forms the inter-laminar insulation. The average thickness of this coating is 0.009 mm. There is a variation in the appearance of the oxide film on the laminations, but the results of the Dynamic Tests have shown the film to be effective.

The microscopic examination of the chemically etched surface of the annealed samples show the size of the individual grains to be large compared to the thickness of the material. This is particularly so for the 0.036 cms. thick material and would therefore explain why this thickness gives the highest static hysteresis loss. The reason being as given by Littman[10] who states that high magnetostatic loss is associated with thin material and large grain size.

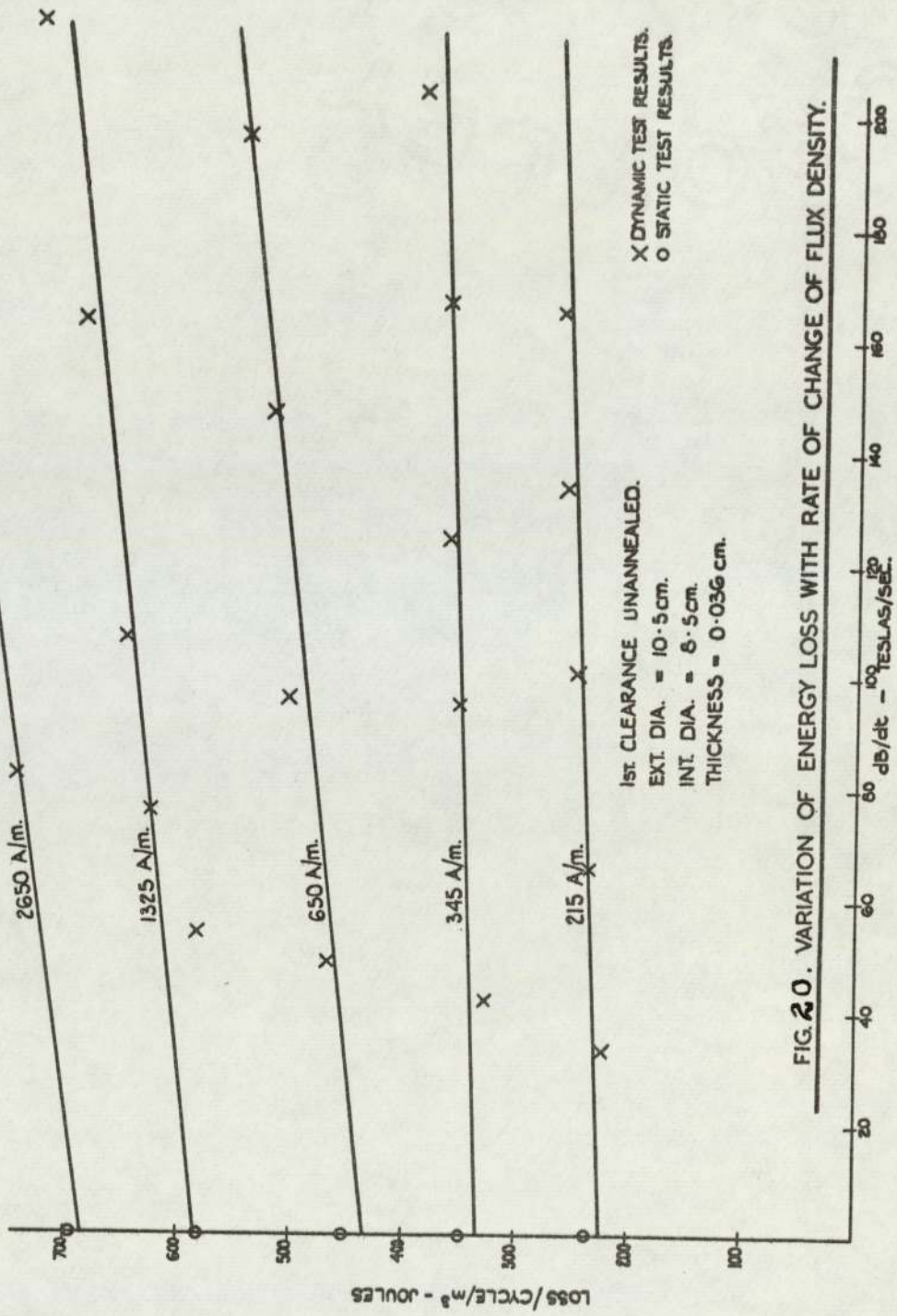

FIG. 20. VARIATION OF ENERGY LOSS WITH RATE OF CHANGE OF FLUX DENSITY.

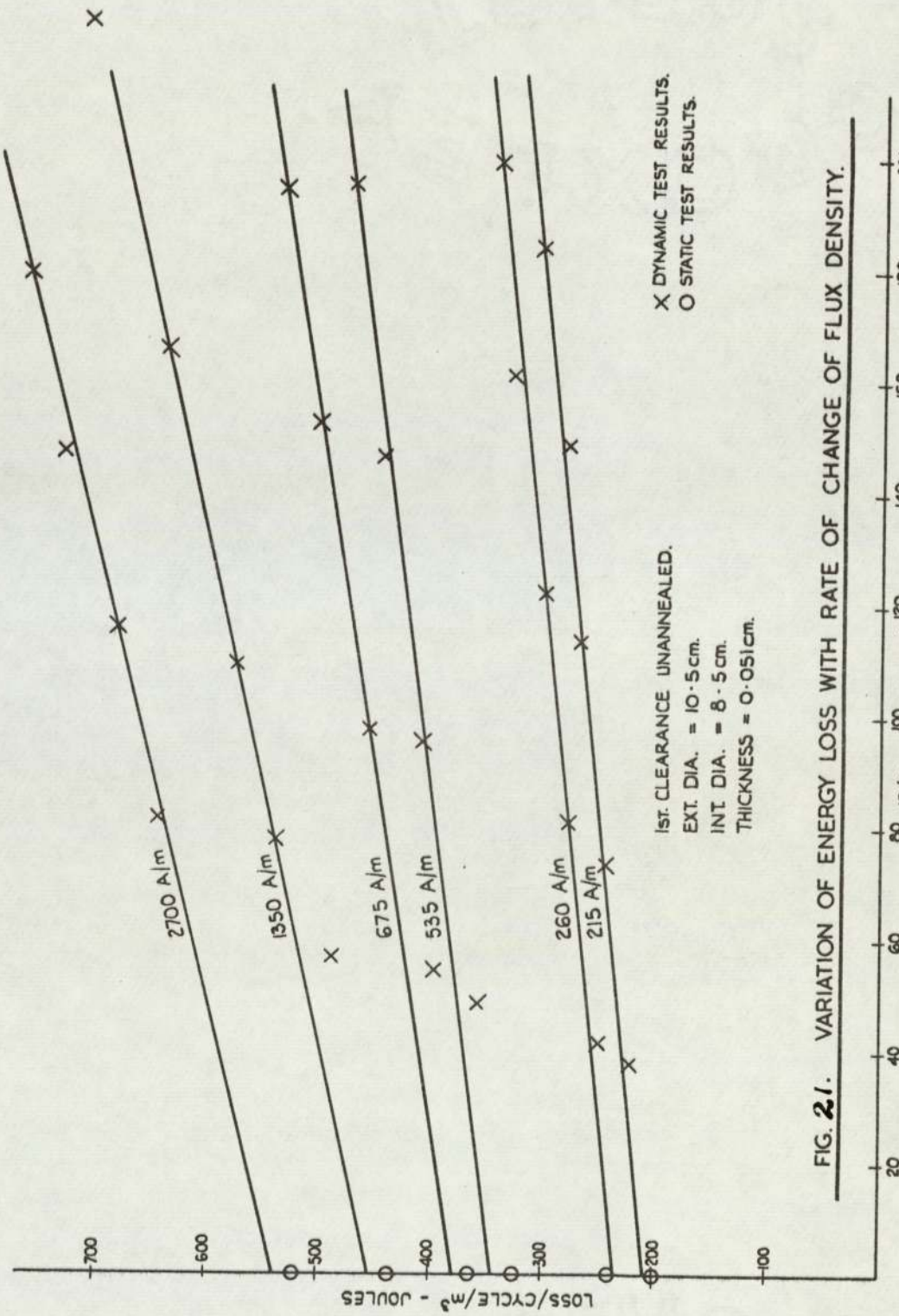

FIG. 21. VARIATION OF ENERGY LOSS WITH RATE OF CHANGE OF FLUX DENSITY.

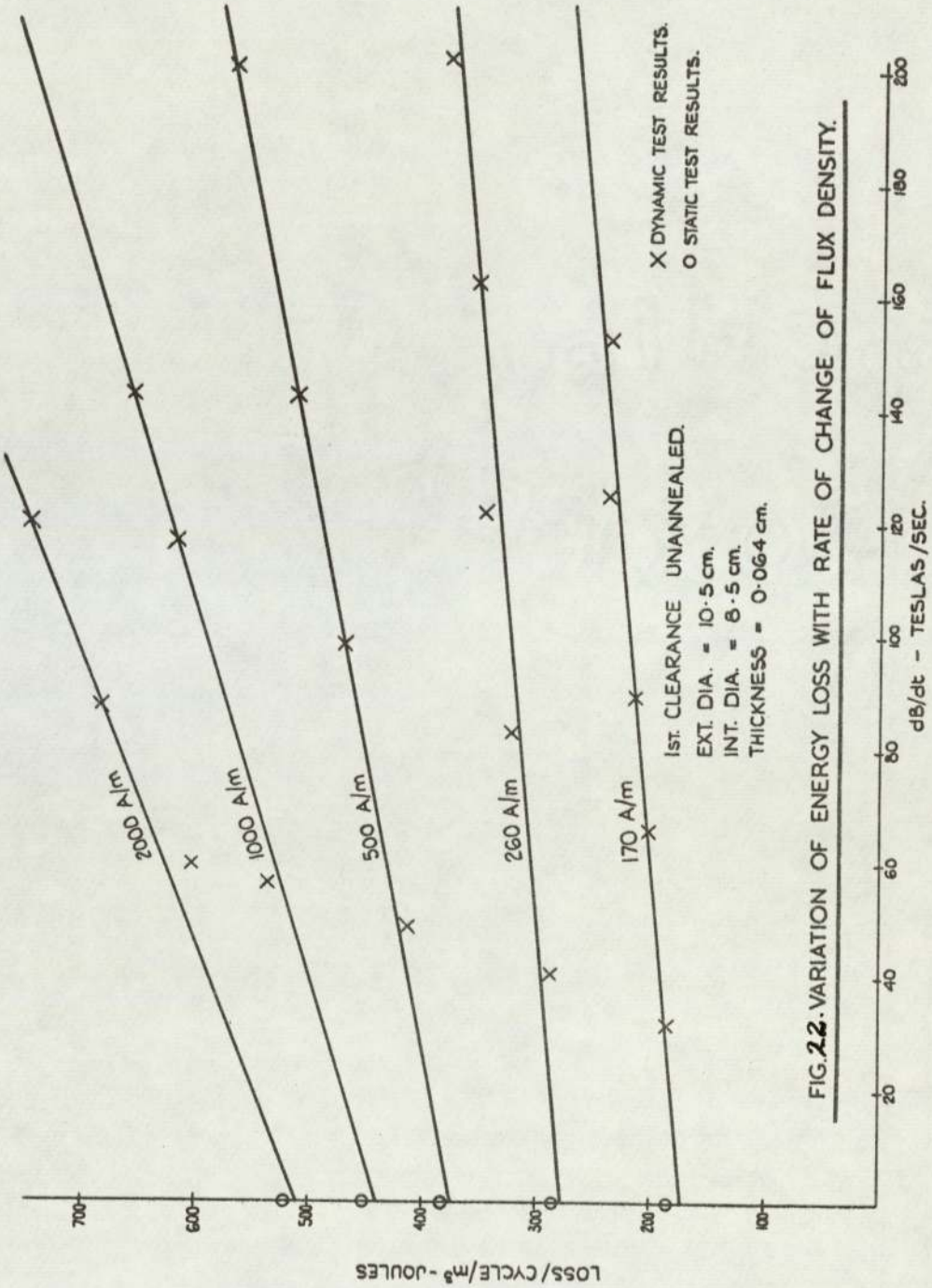

FIG. 22. VARIATION OF ENERGY LOSS WITH RATE OF CHANGE OF FLUX DENSITY.

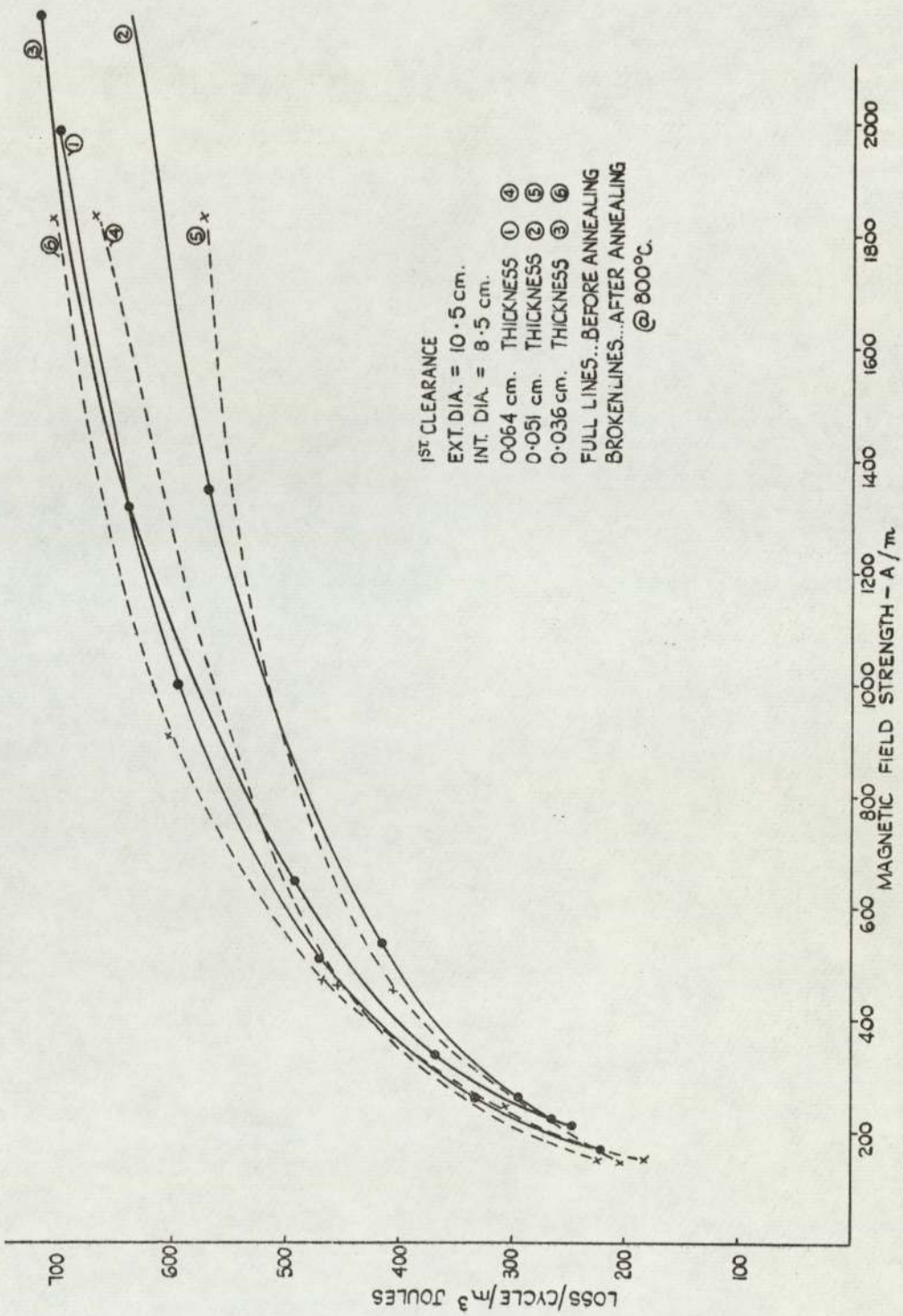

FIG.23 VARIATION OF TOTAL IRON LOSS @ 100 dB/dt WITH MAGNETIC FIELD STRENGTH.

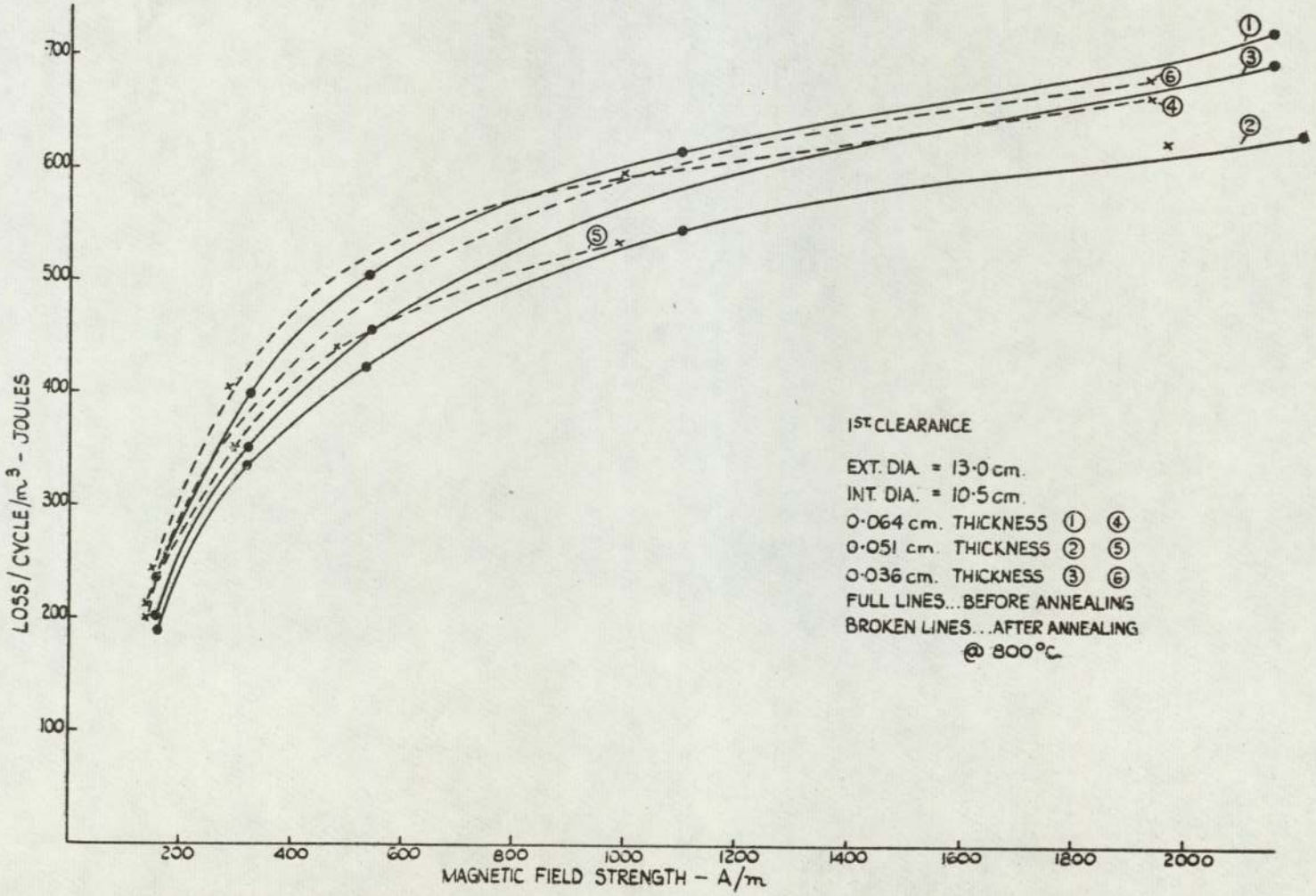

FIG24 VARIATION OF TOTAL IRON LOSS @ 100 dB/dt WITH MAGNETIC FIELD STRENGTH.

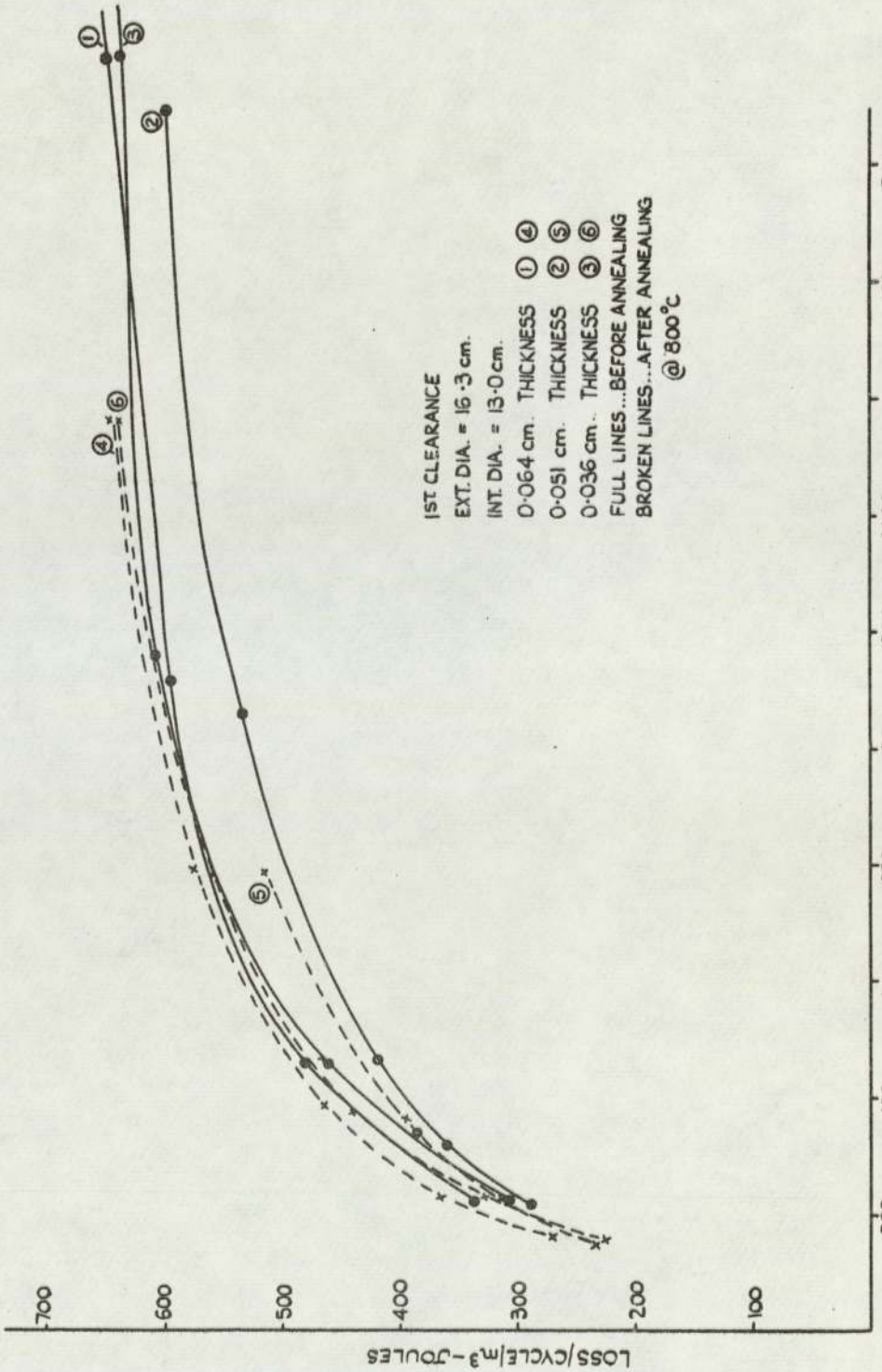

FIG25. VARIATION OF TOTAL IRON LOSS @ 100 dB/dt WITH MAGNETIC FIELD STRENGTH.

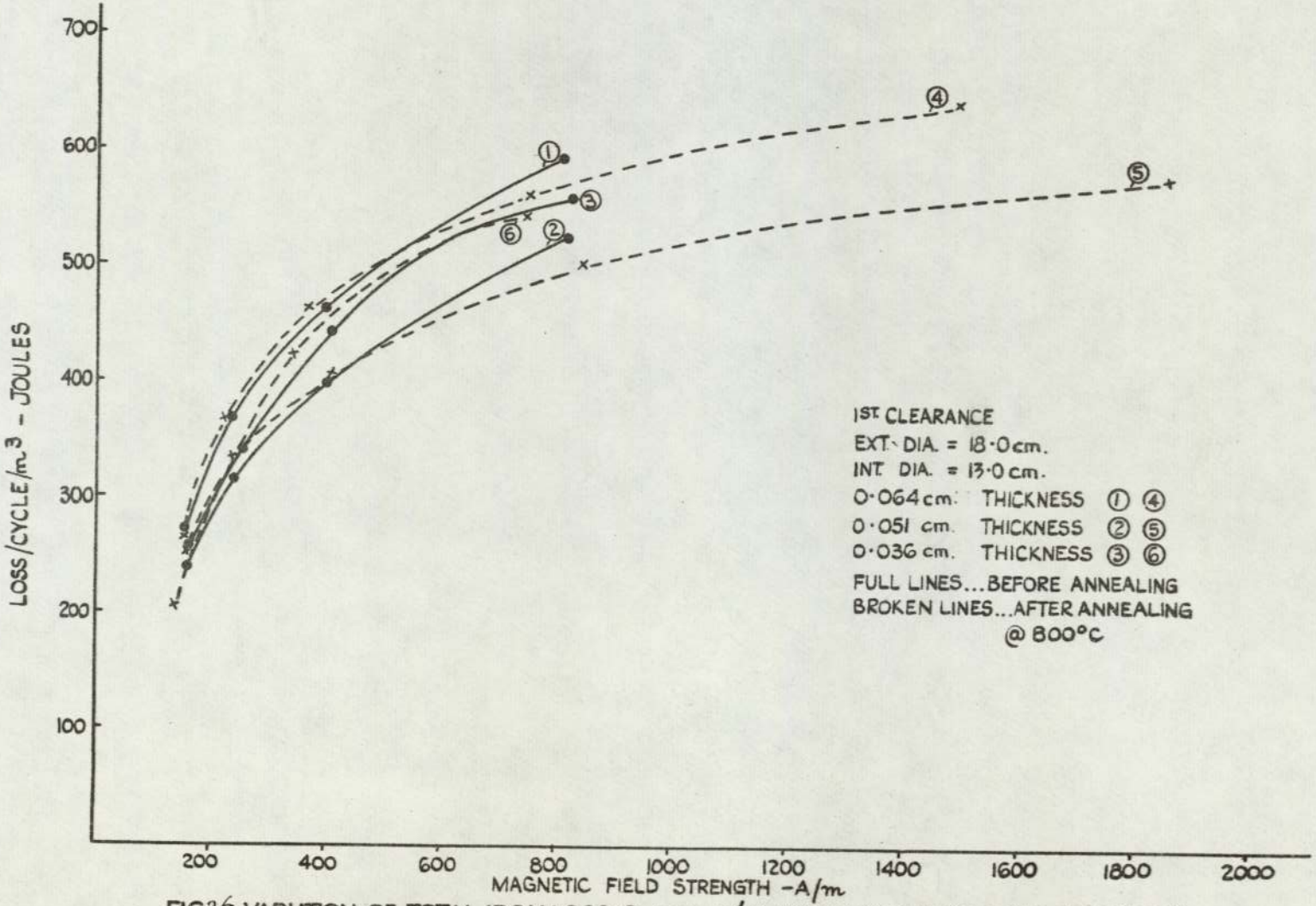

FIG 26. VARIATION OF TOTAL IRON LOSS @ 100 dB/dt WITH MAGNETIC FIELD STRENGTH.

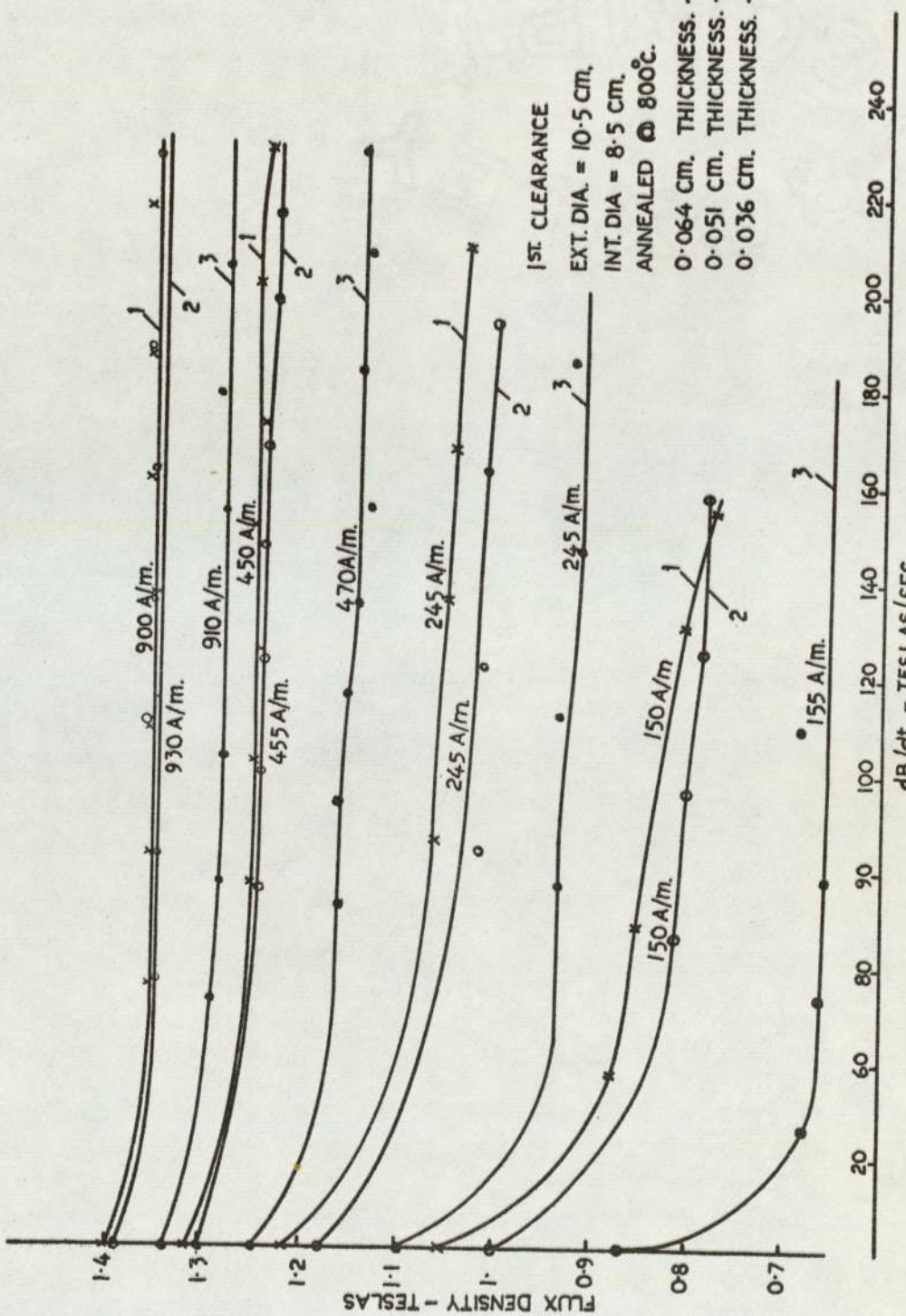

FIG. 27. FLUX DENSITY AGAINST dB/dt

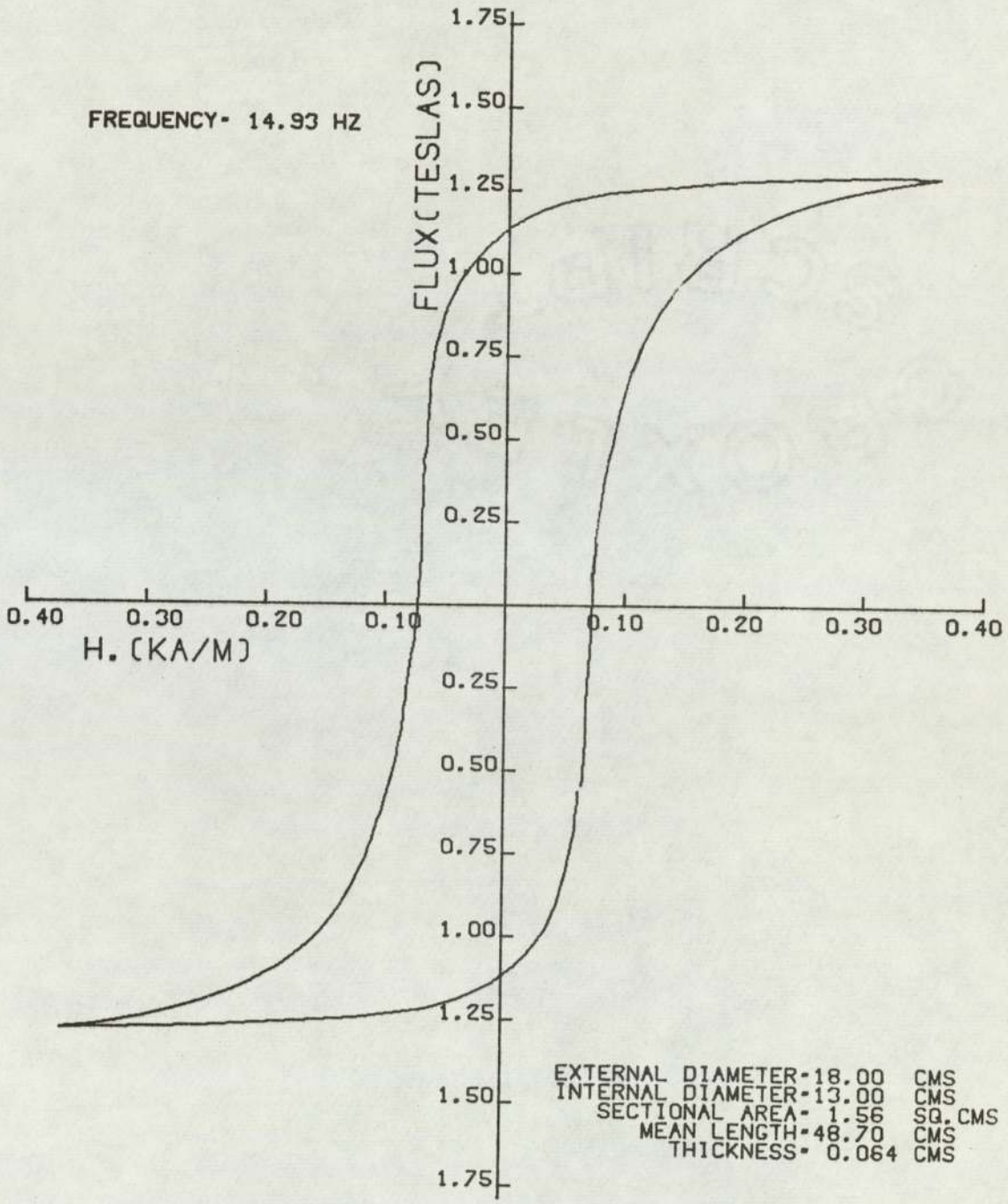

FIG.28. TYPICAL PRINT OUT FROM X-Y PLOTTER

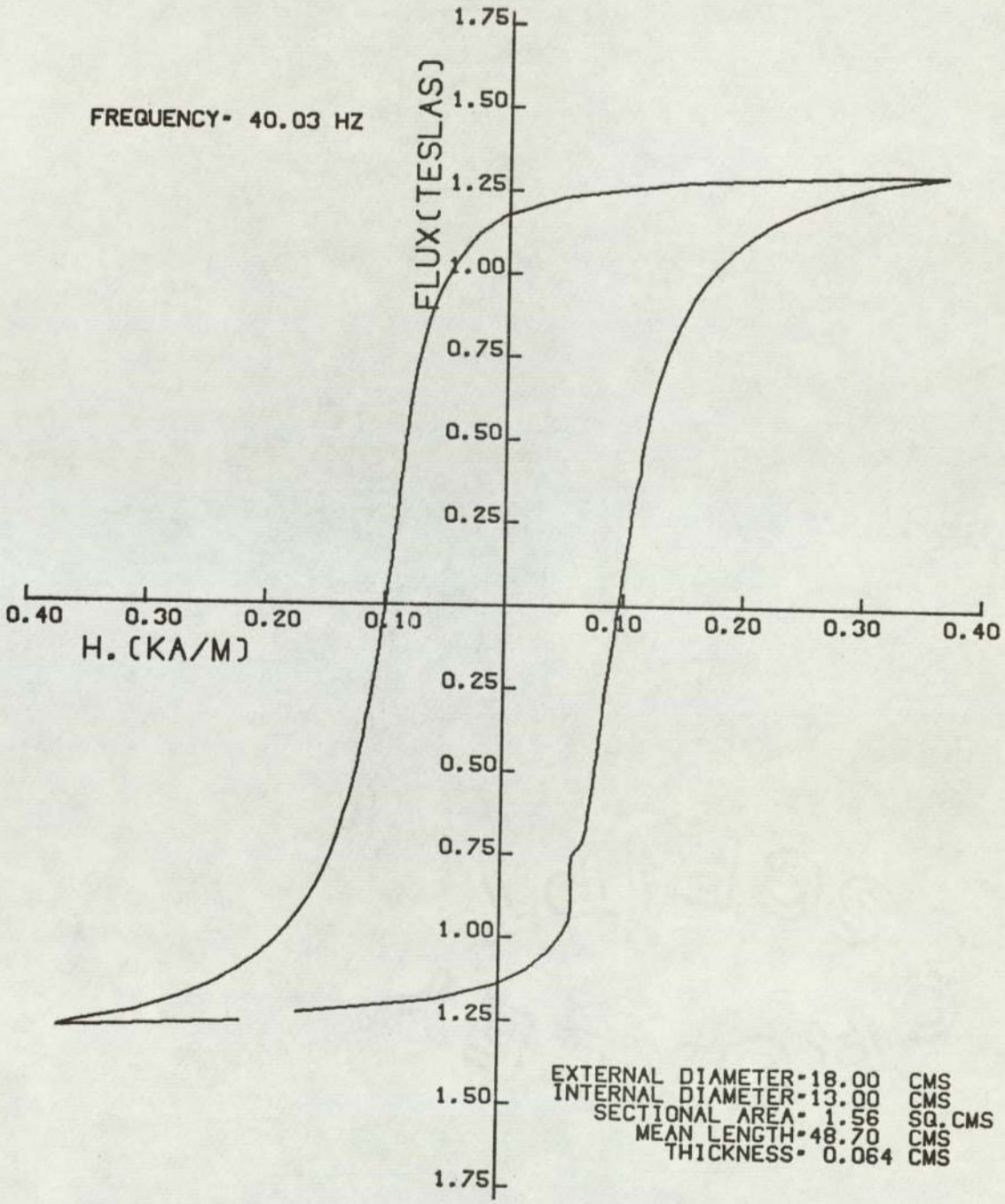

FIG.29. PRINT OUT FROM X-Y PLOTTER

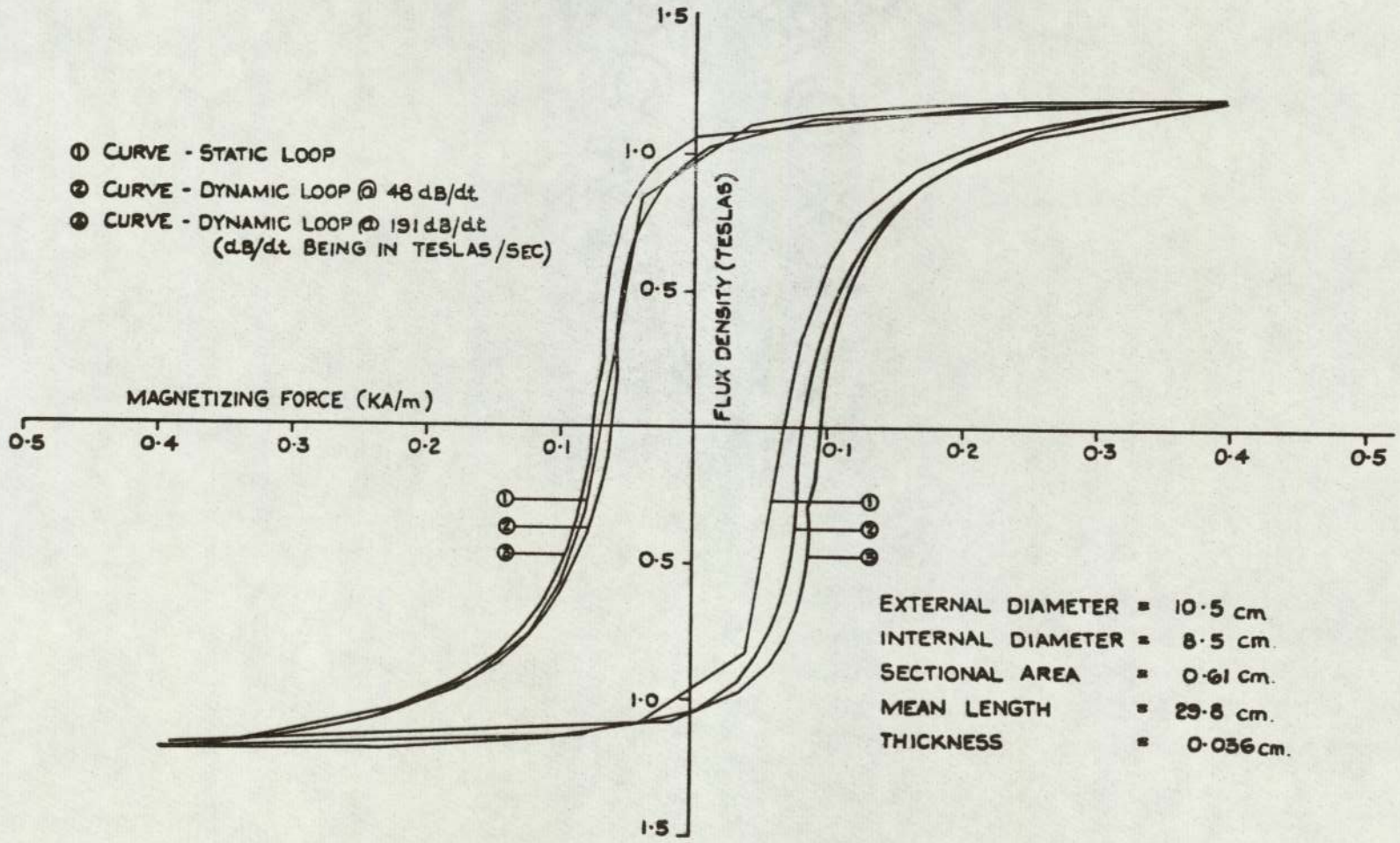

FIG.30. STATIC AND DYNAMIC HYSTERESIS LOOPS

1ST. CLEARANCE-ANNEALED @ 800°C.

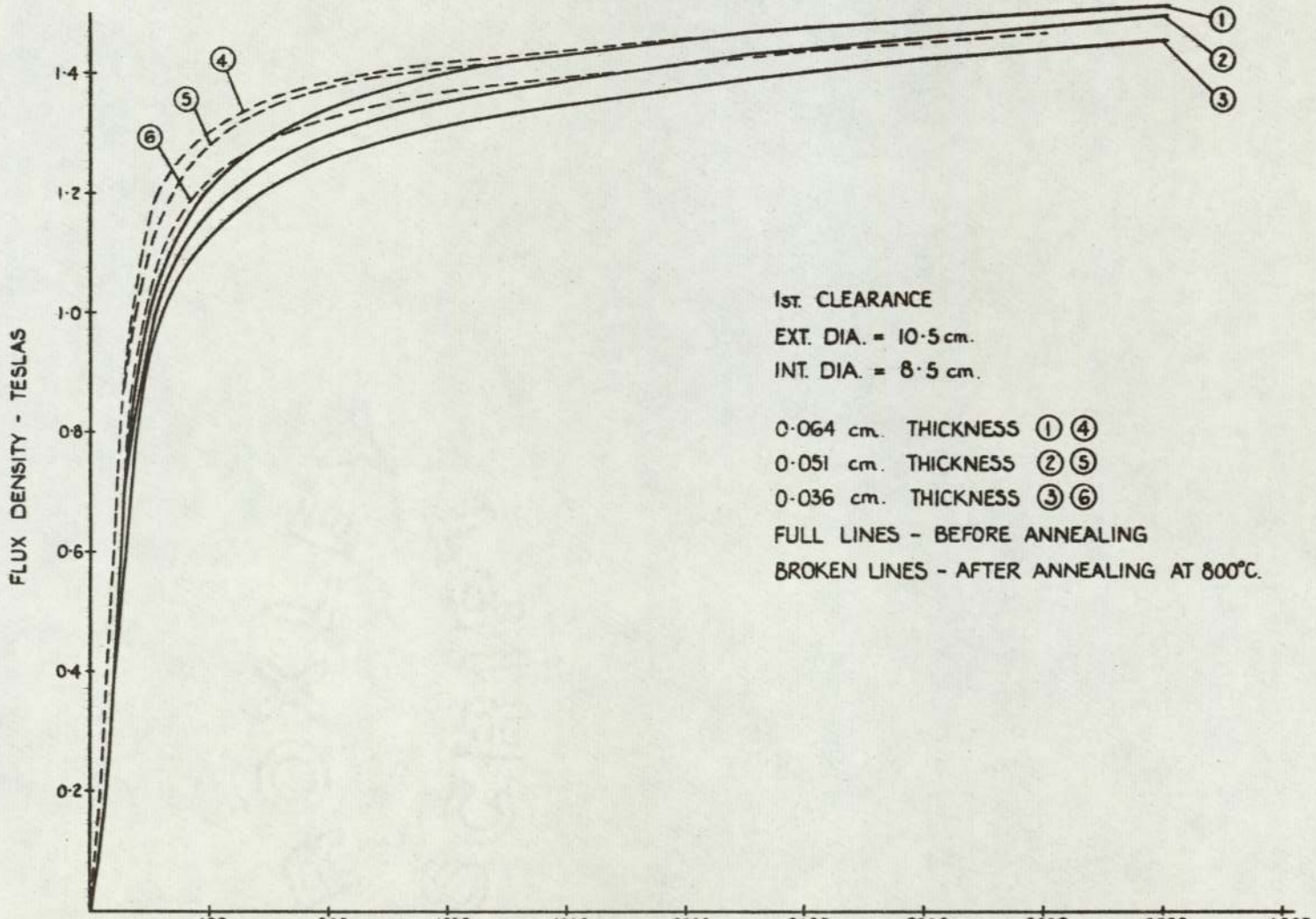

FIG.31 MAGNETIZATION CURVES.

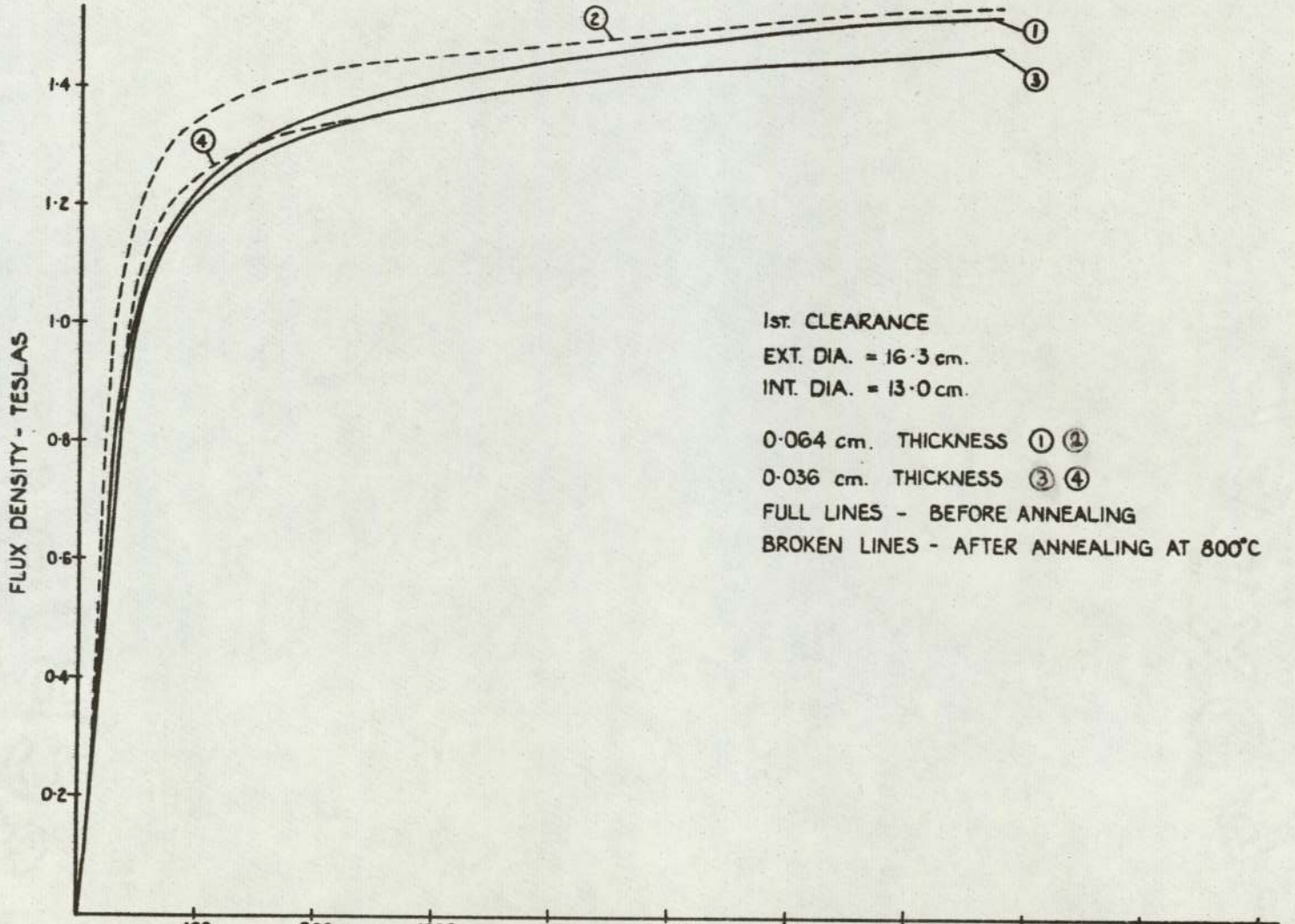

FIG. 32. MAGNETIZATION CURVE.

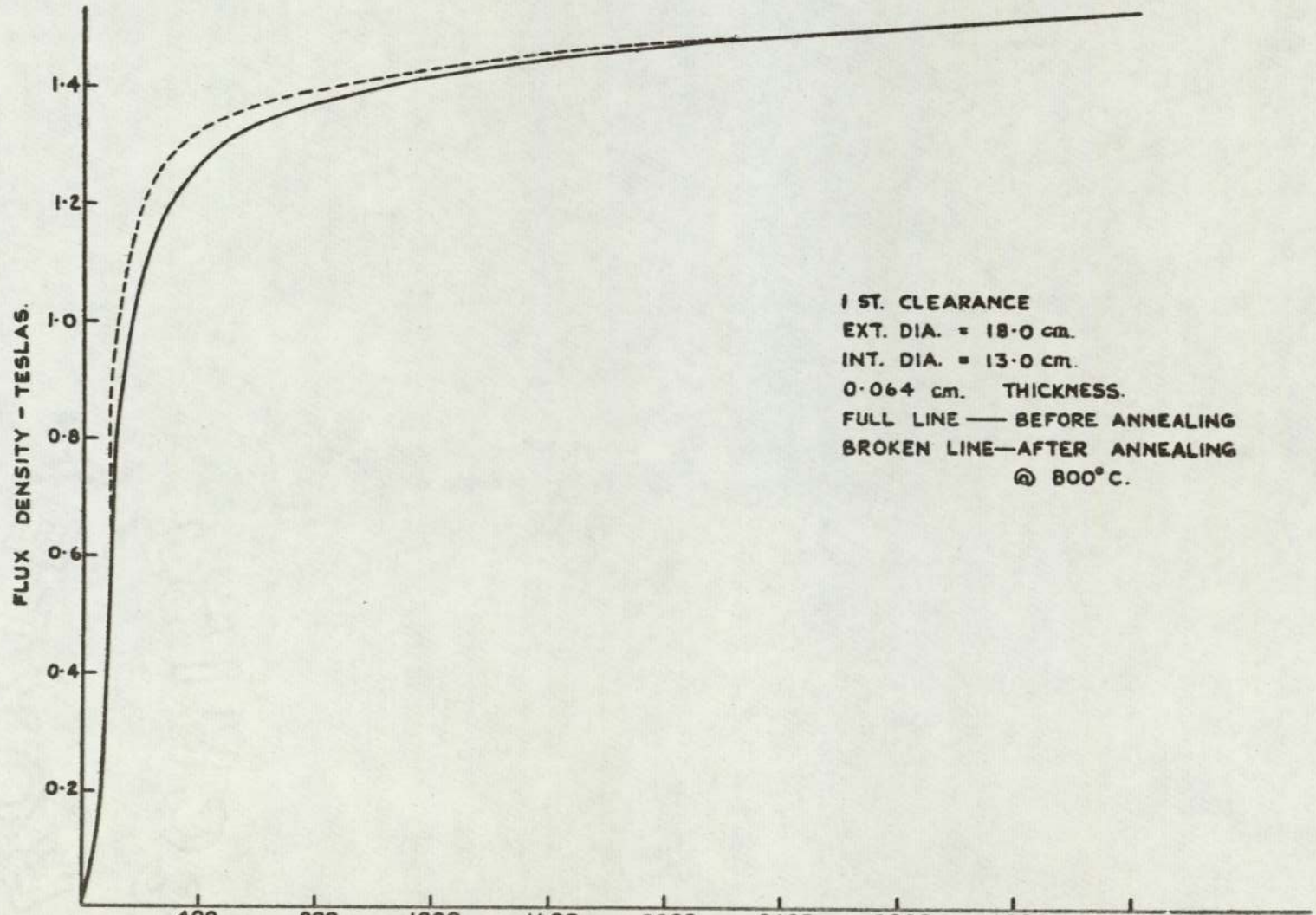

FIG. 33. MAGNETIZATION CURVE

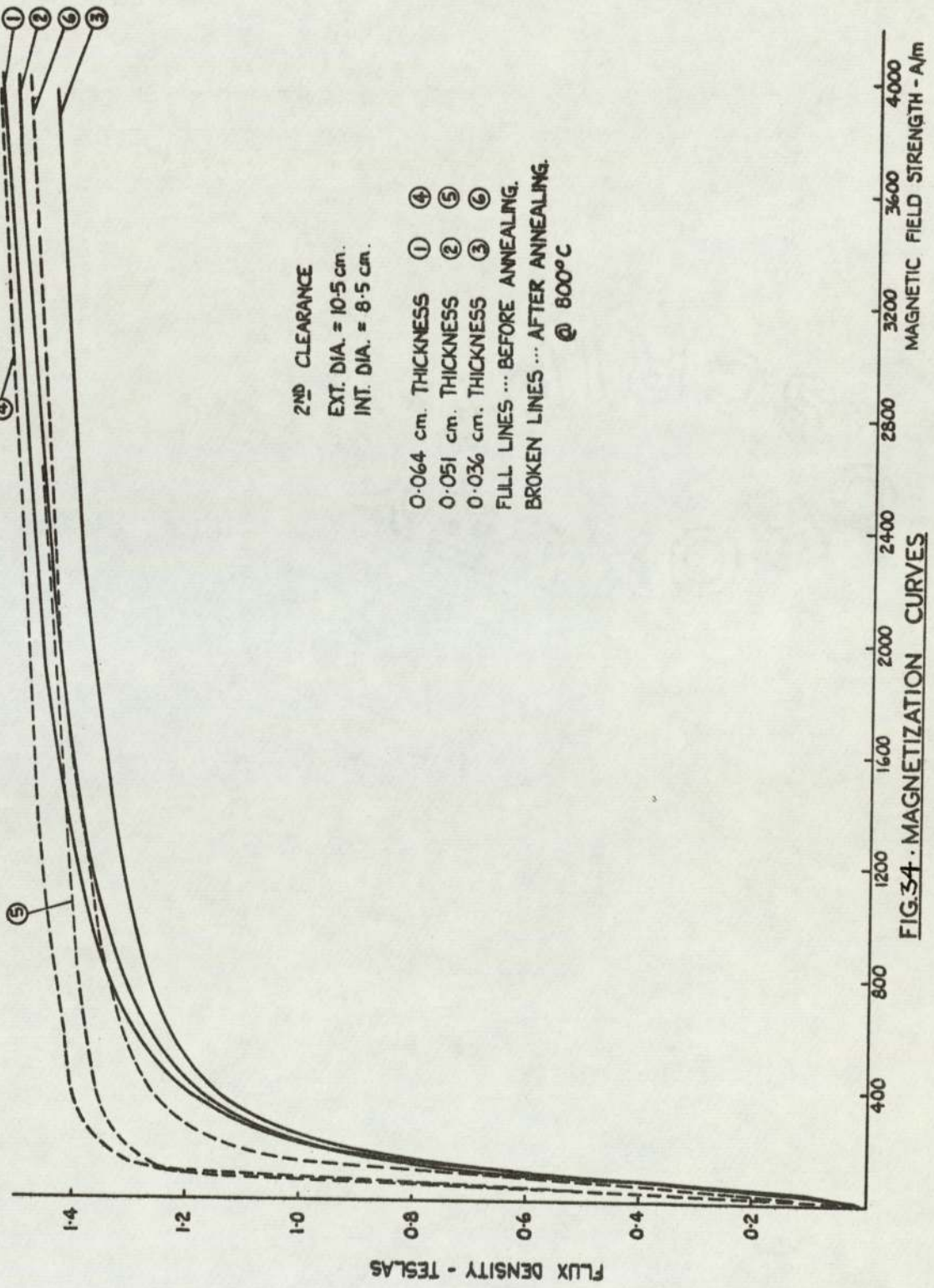

FIG.34. MAGNETIZATION CURVES

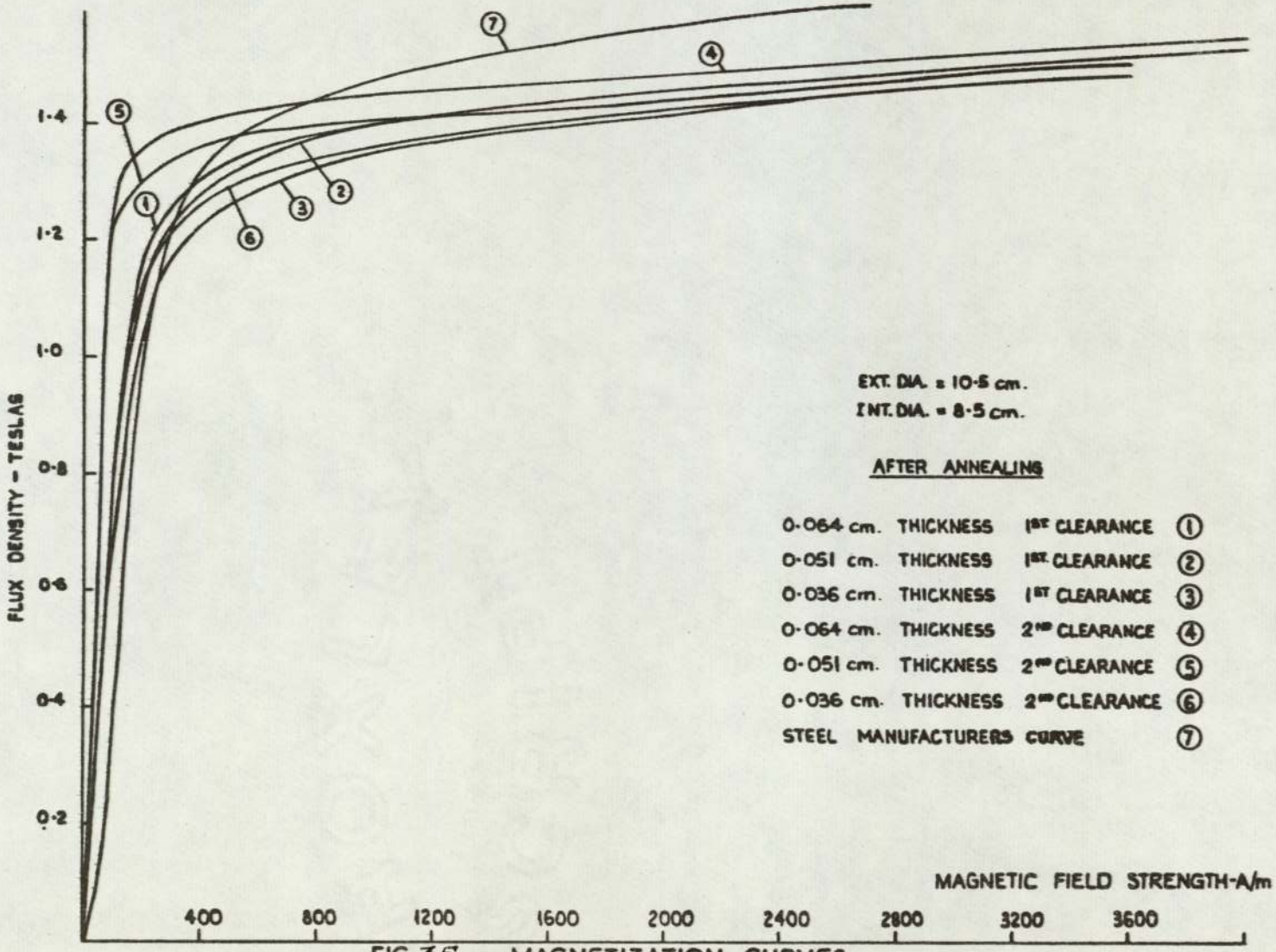

FIG. 35. MAGNETIZATION CURVES.

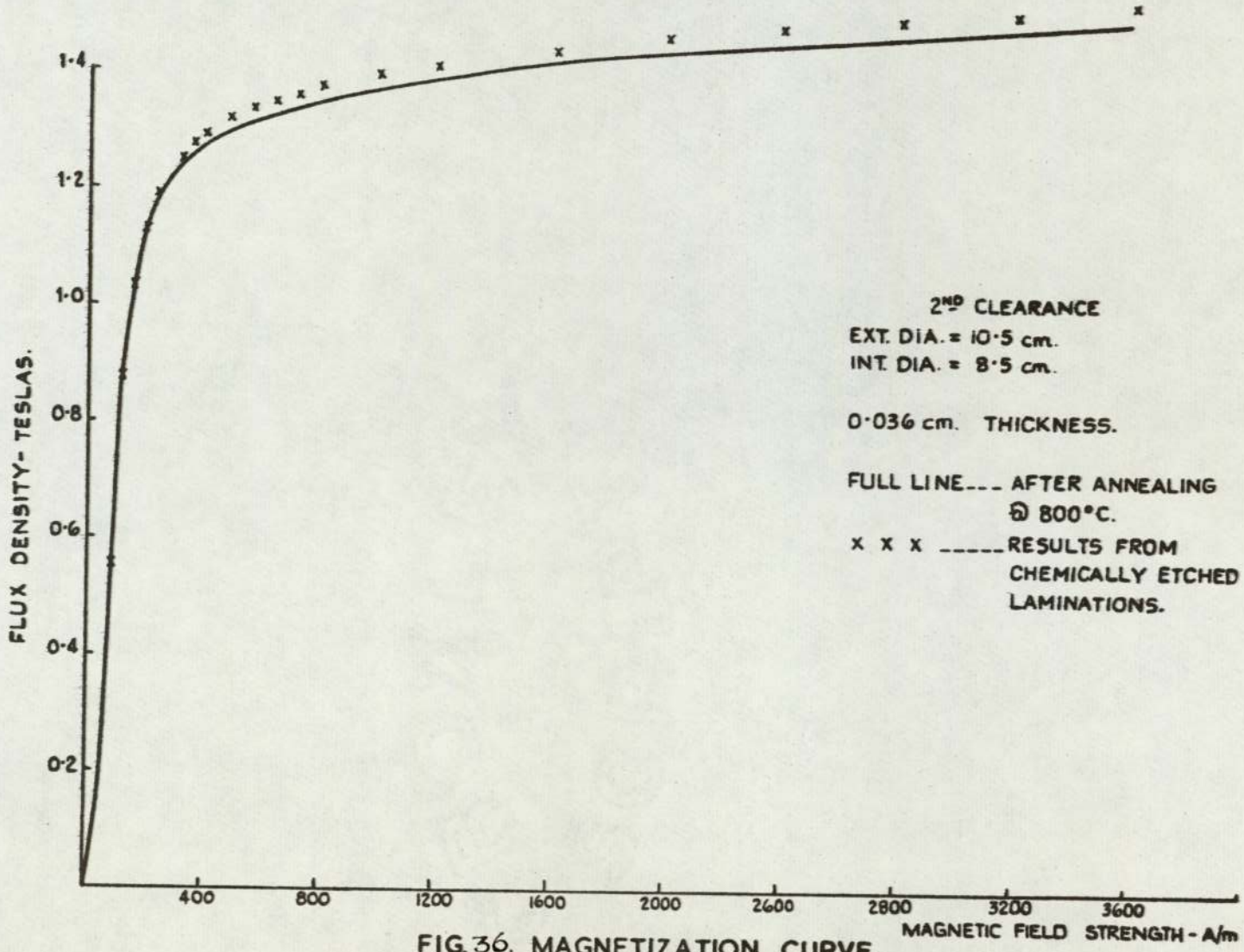

FIG. 36. MAGNETIZATION CURVE.

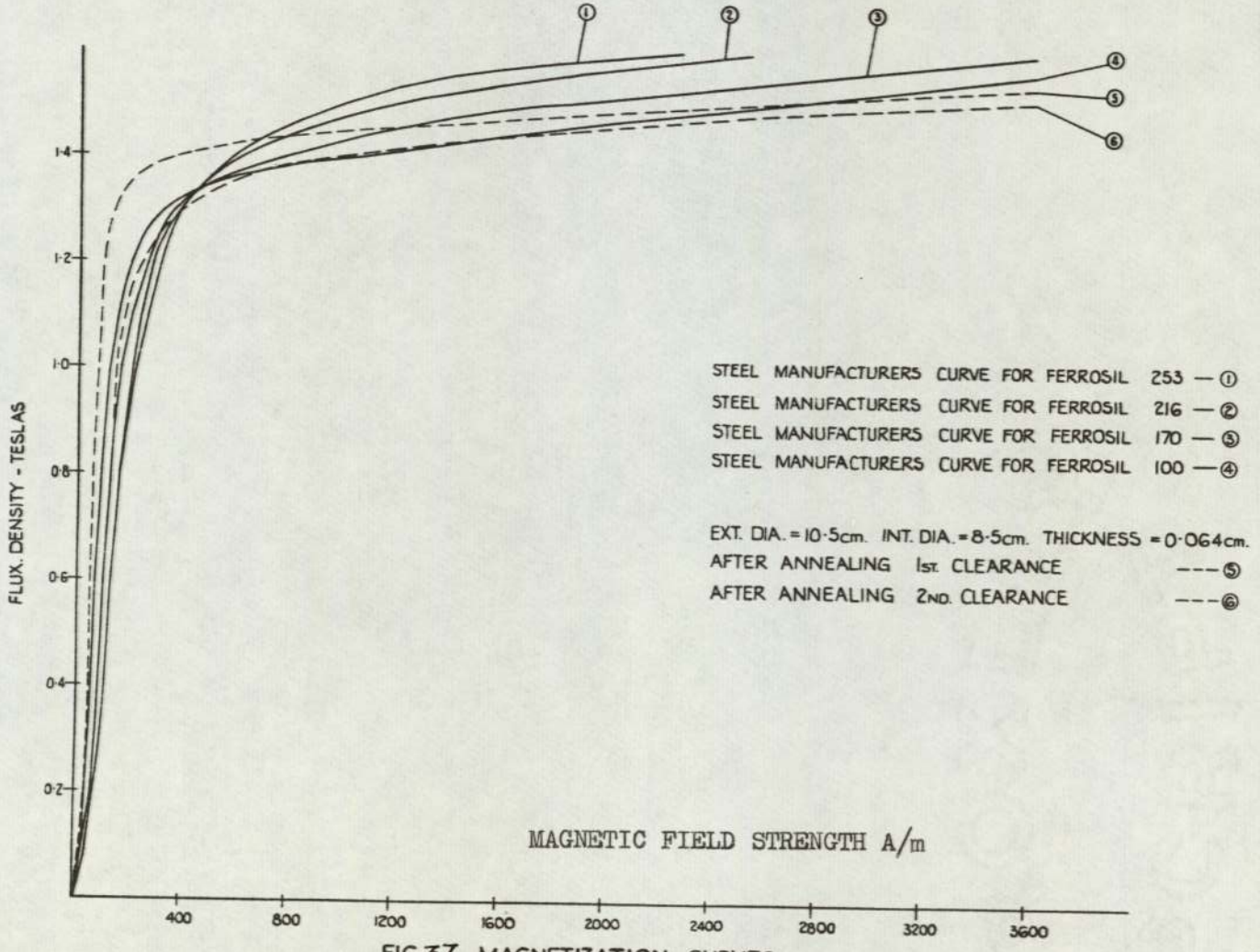

FIG 37. MAGNETIZATION CURVES

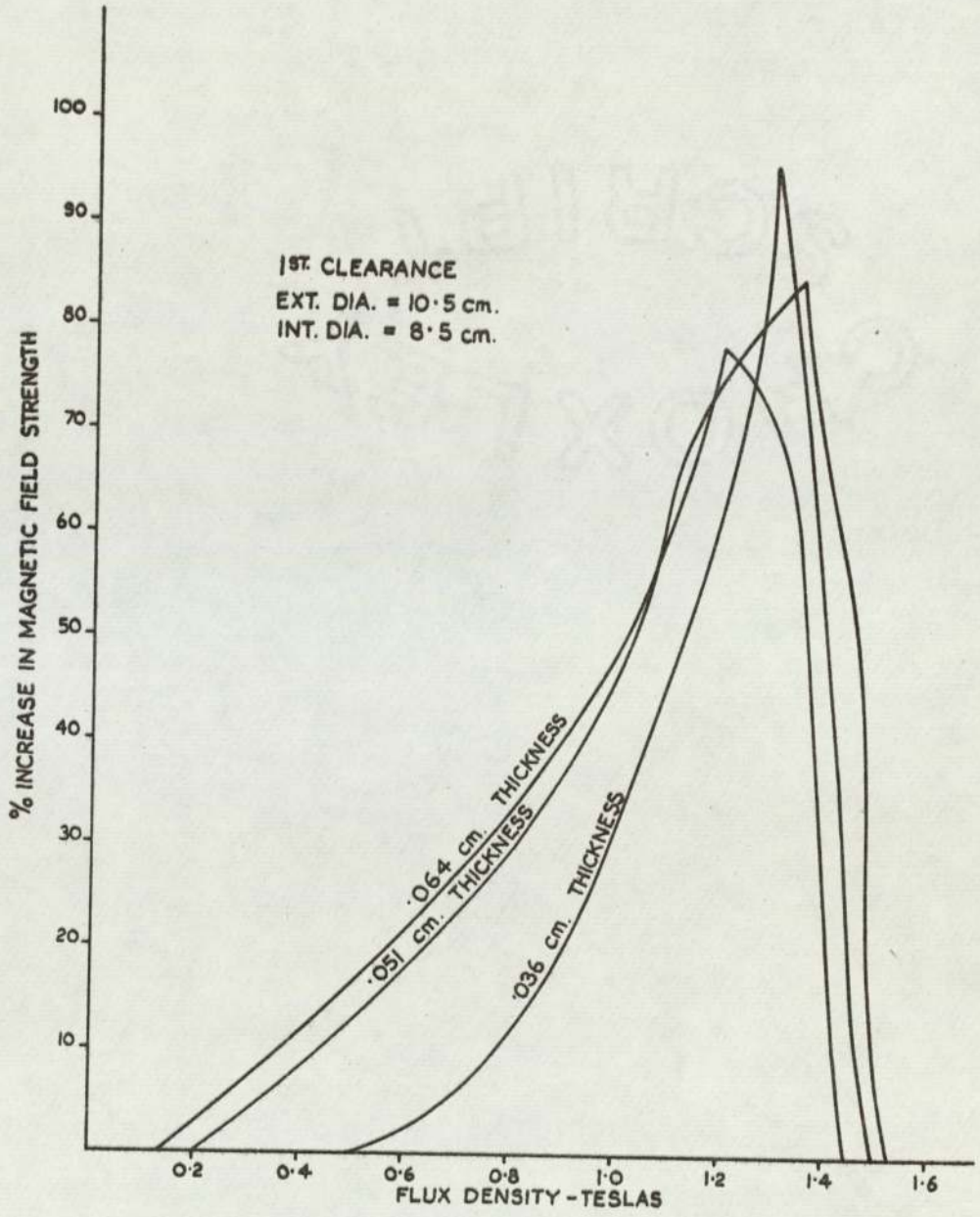

FIG. 38. % INCREASE IN MAGNETIC FIELD STRENGTH DUE TO PUNCHING, RELATED TO FLUX DENSITY.

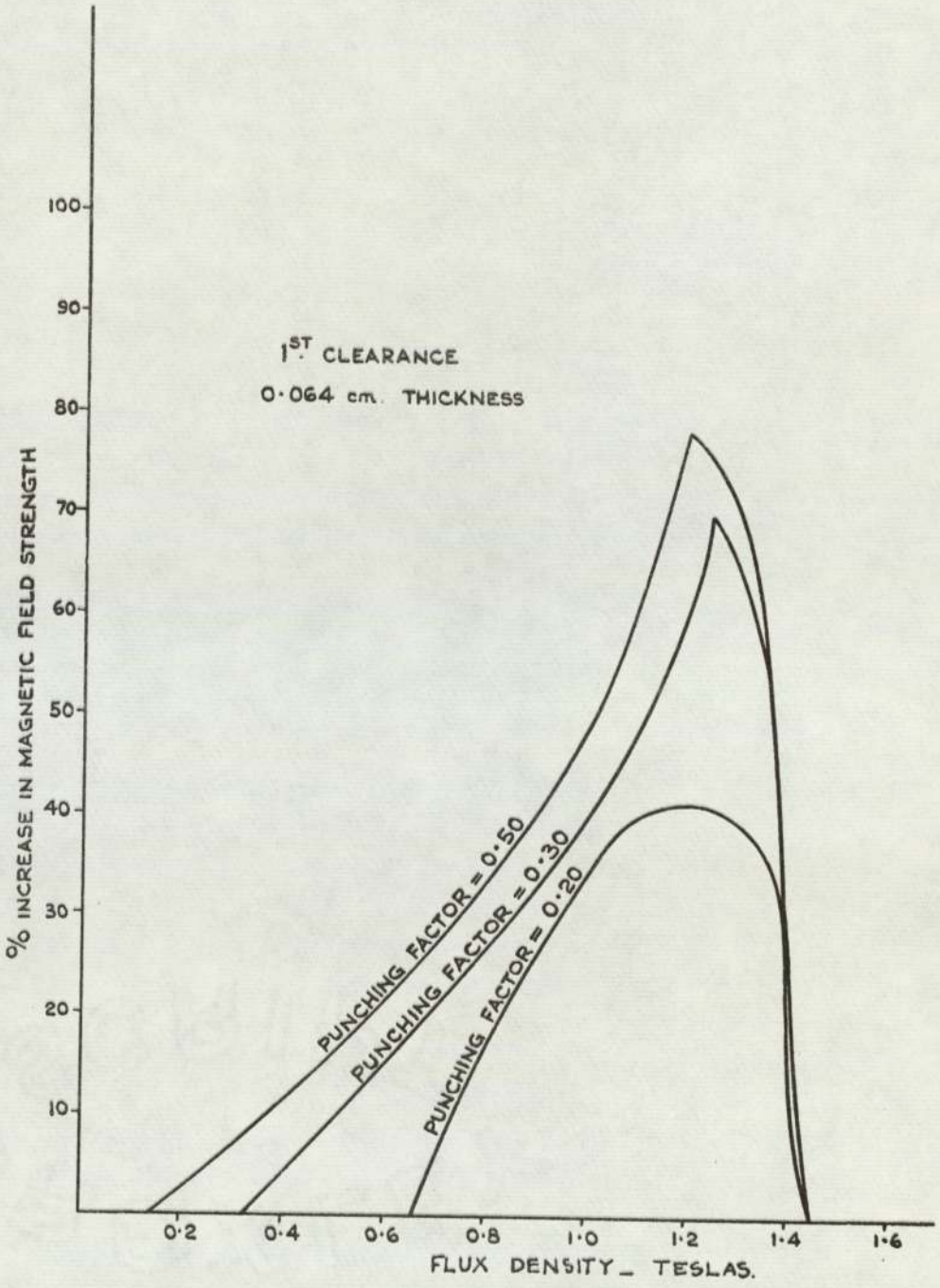

FIG.39. % INCREASE IN MAGNETIC FIELD STRENGTH DUE TO PUNCHING, RELATED TO FLUX DENSITY.

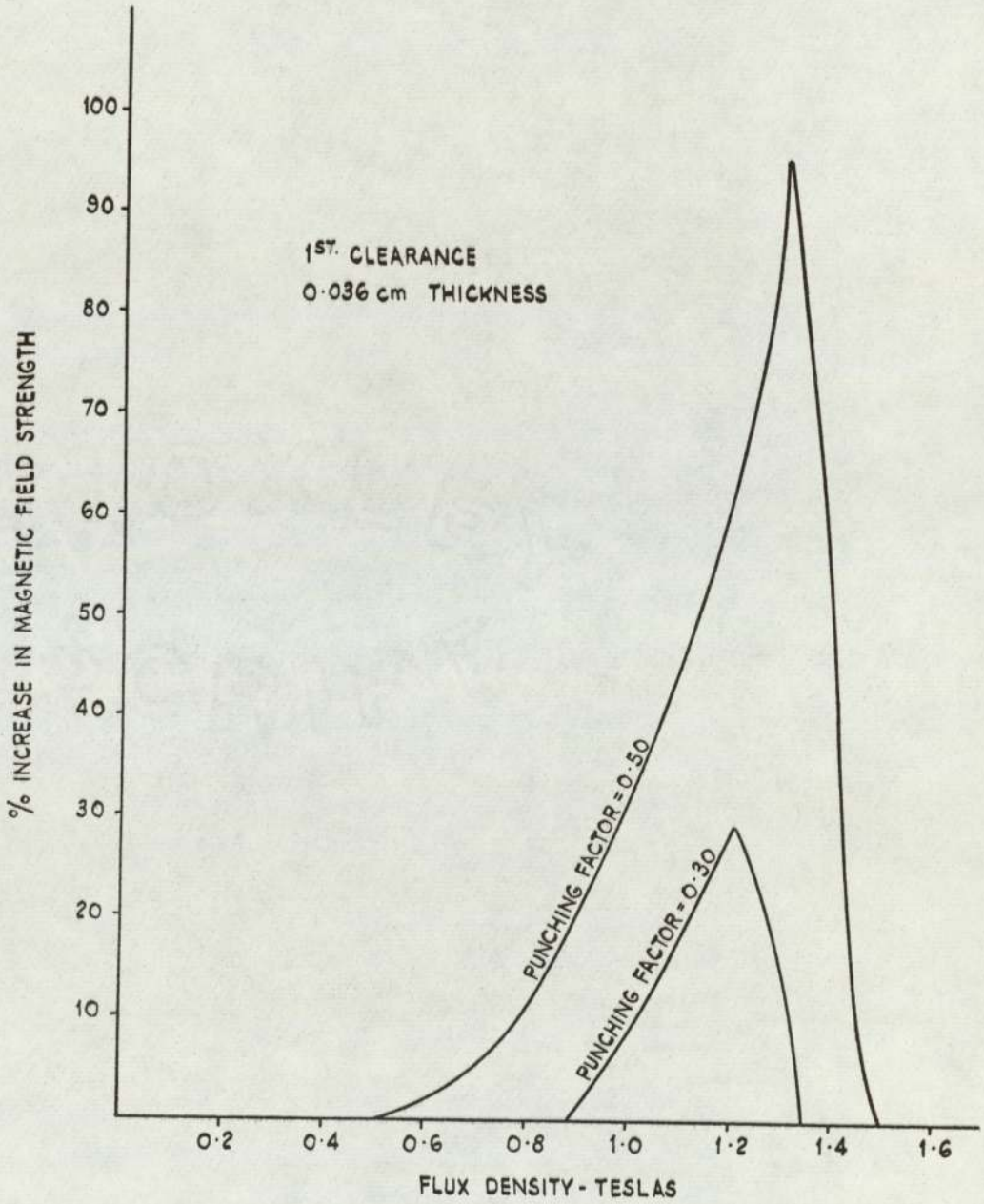

FIG.40. % INCREASE IN MAGNETIC FIELD STRENGTH DUE TO PUNCHING, RELATED TO FLUX DENSITY.

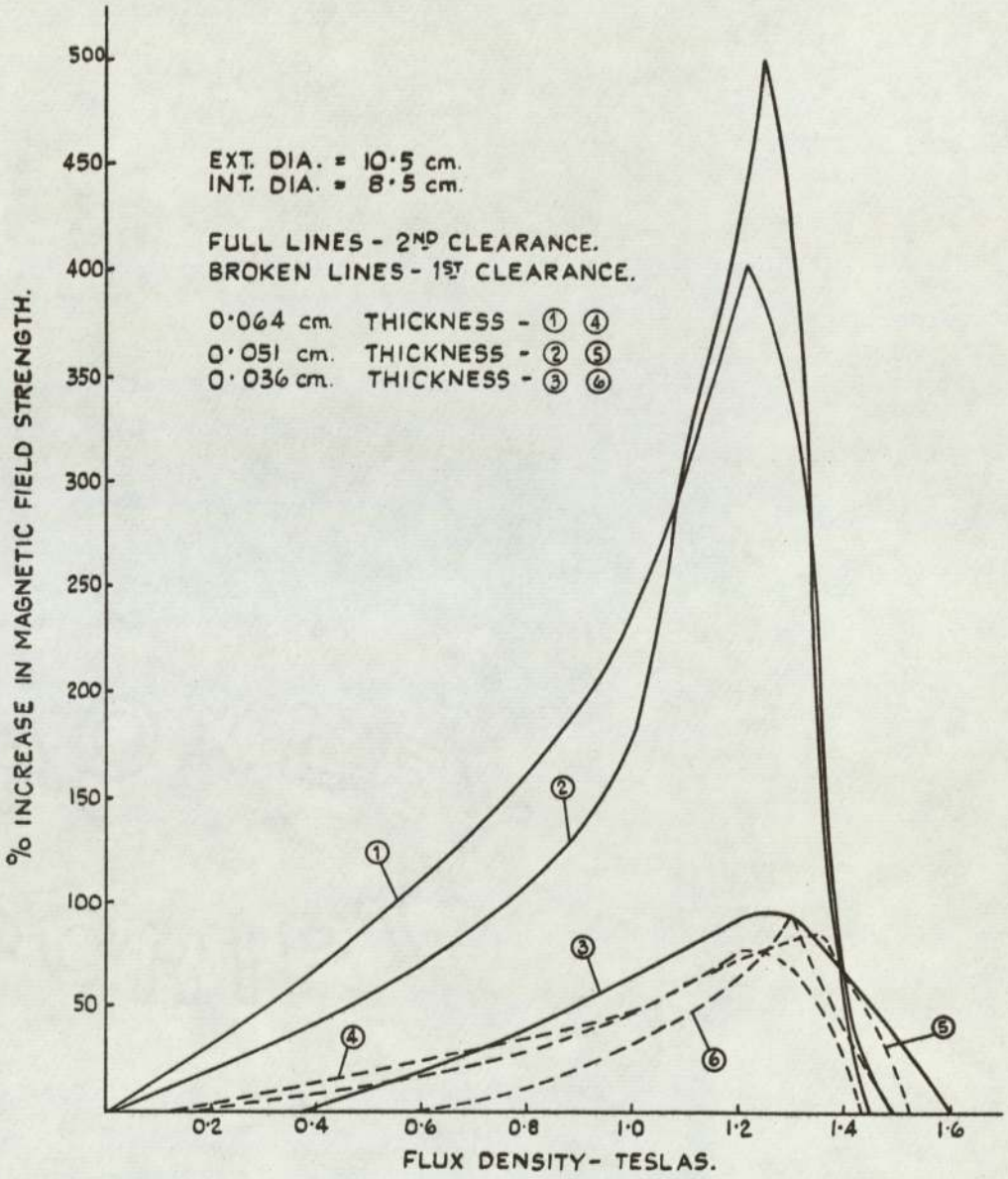

FIG.41. % INCREASE IN MAGNETIC FIELD STRENGTH DUE TO PUNCHING, RELATED TO FLUX DENSITY.

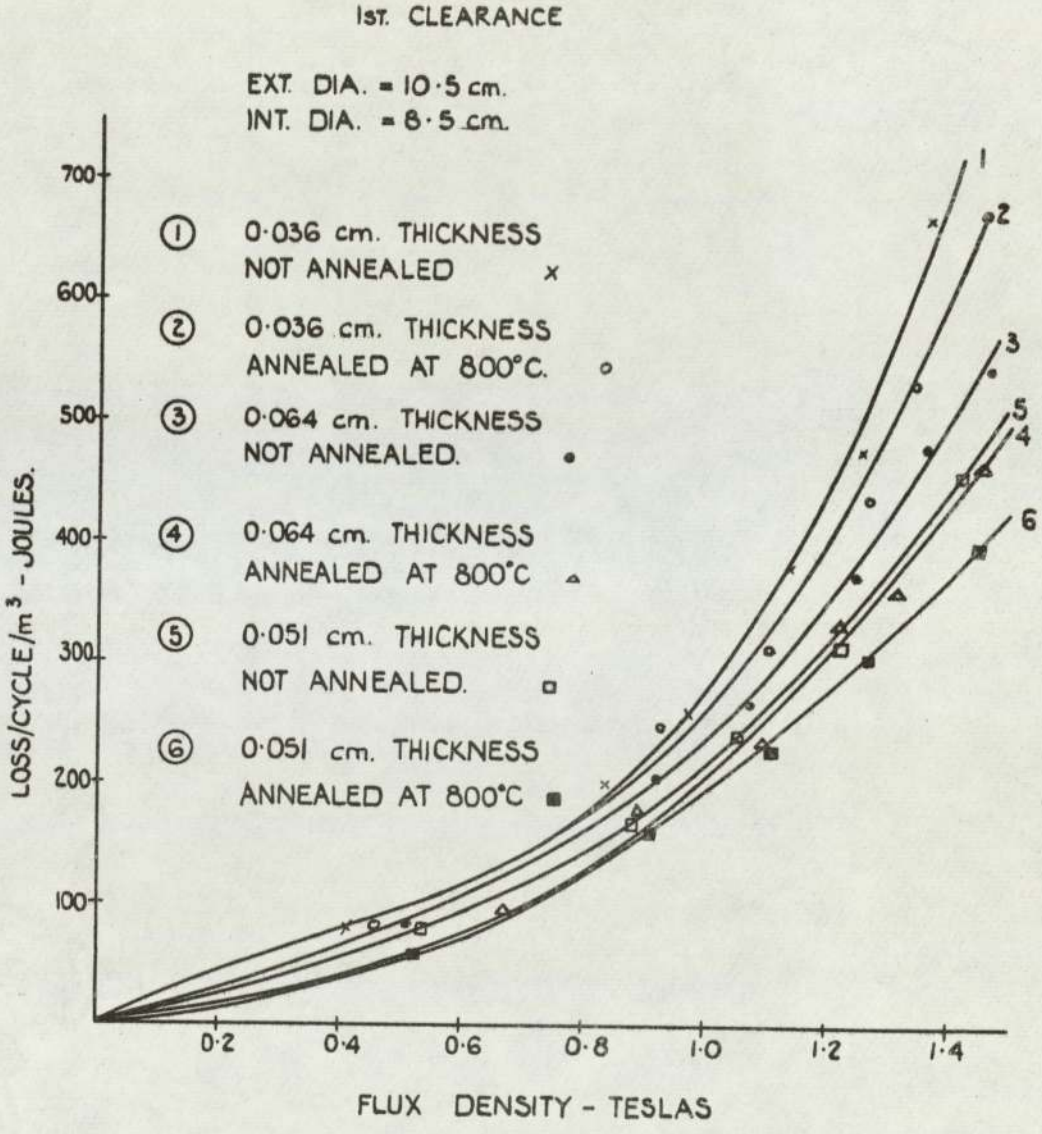

FIG. 42. VARIATION IN STATIC HYSTERESIS LOSS WITH FLUX DENSITY.

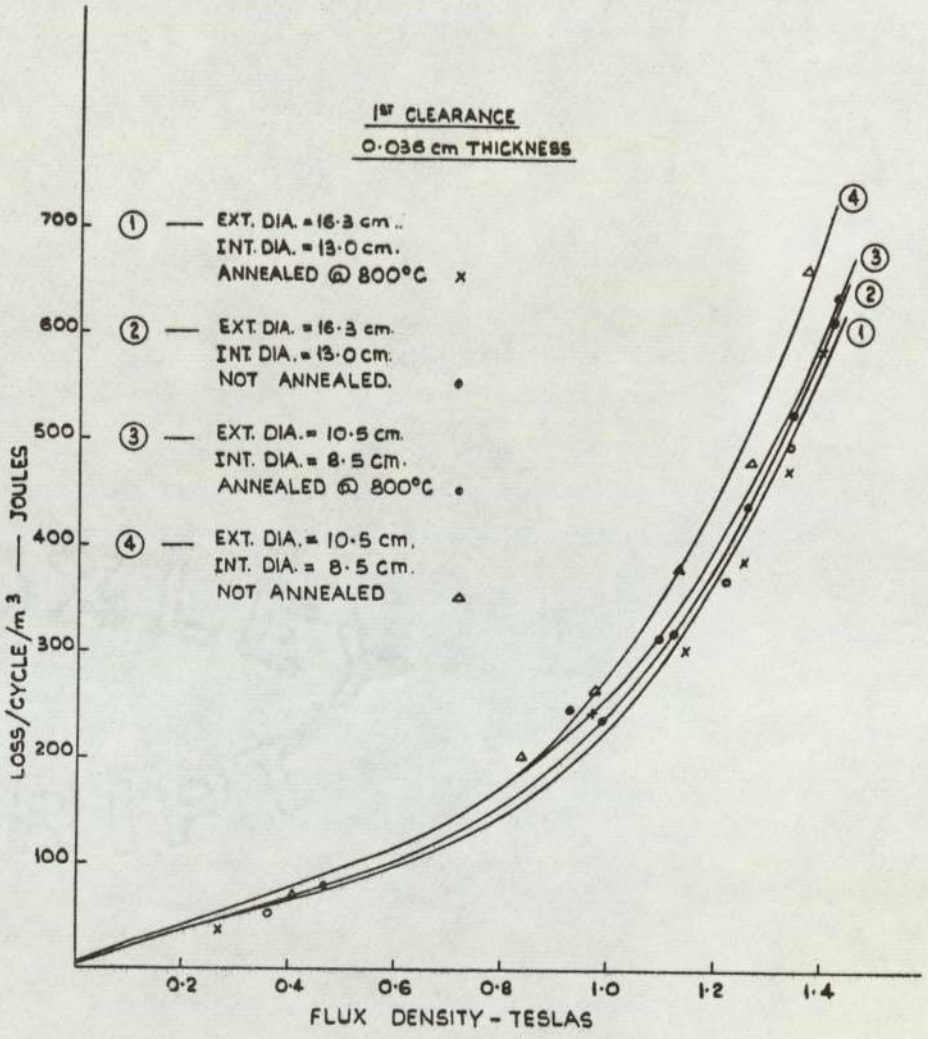

FIG. 43. VARIATION IN STATIC HYSTERESIS LOSS WITH FLUX DENSITY.

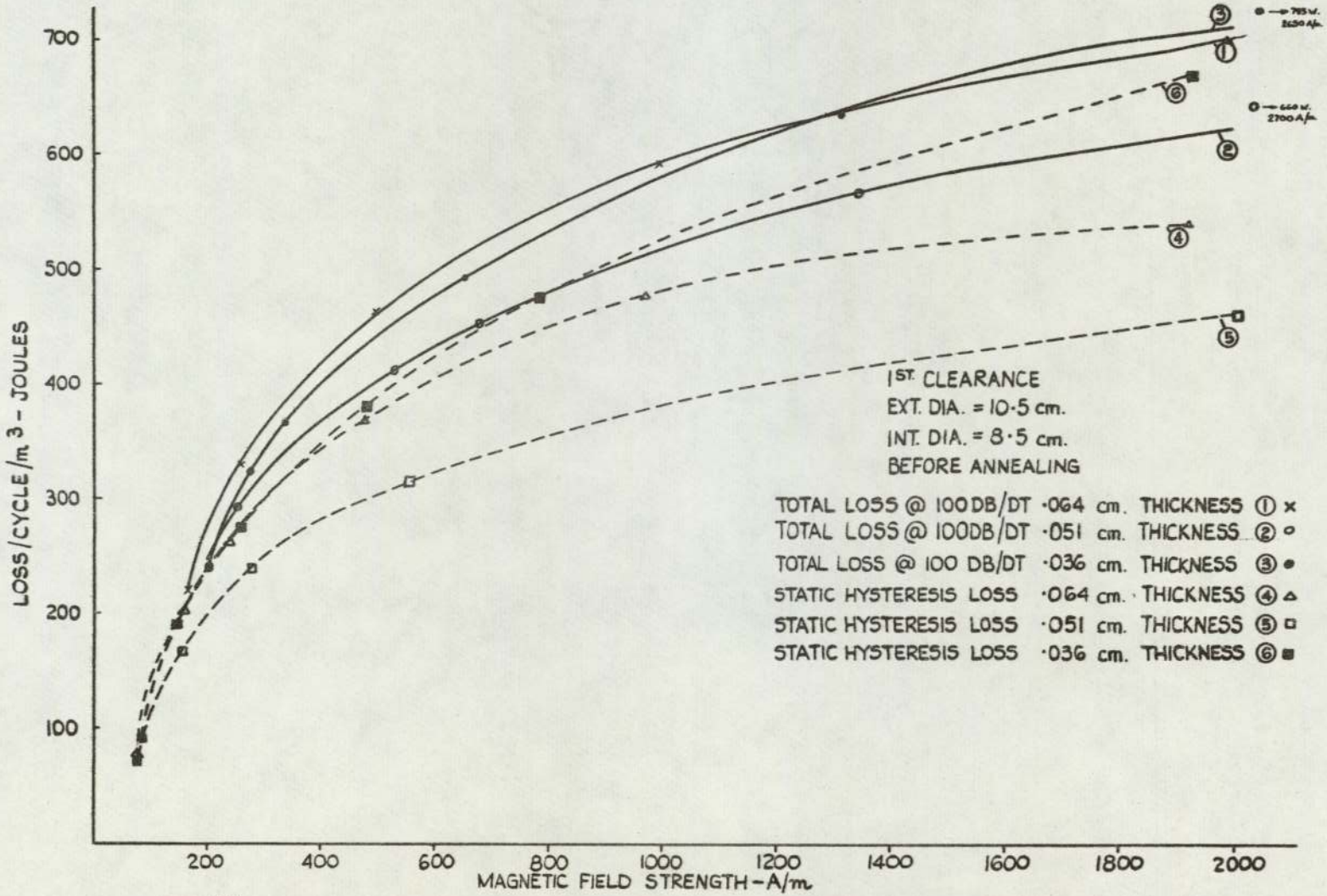

FIG.44 · VARIATION OF IRON LOSS WITH MAGNETIC FIELD STRENGTH.

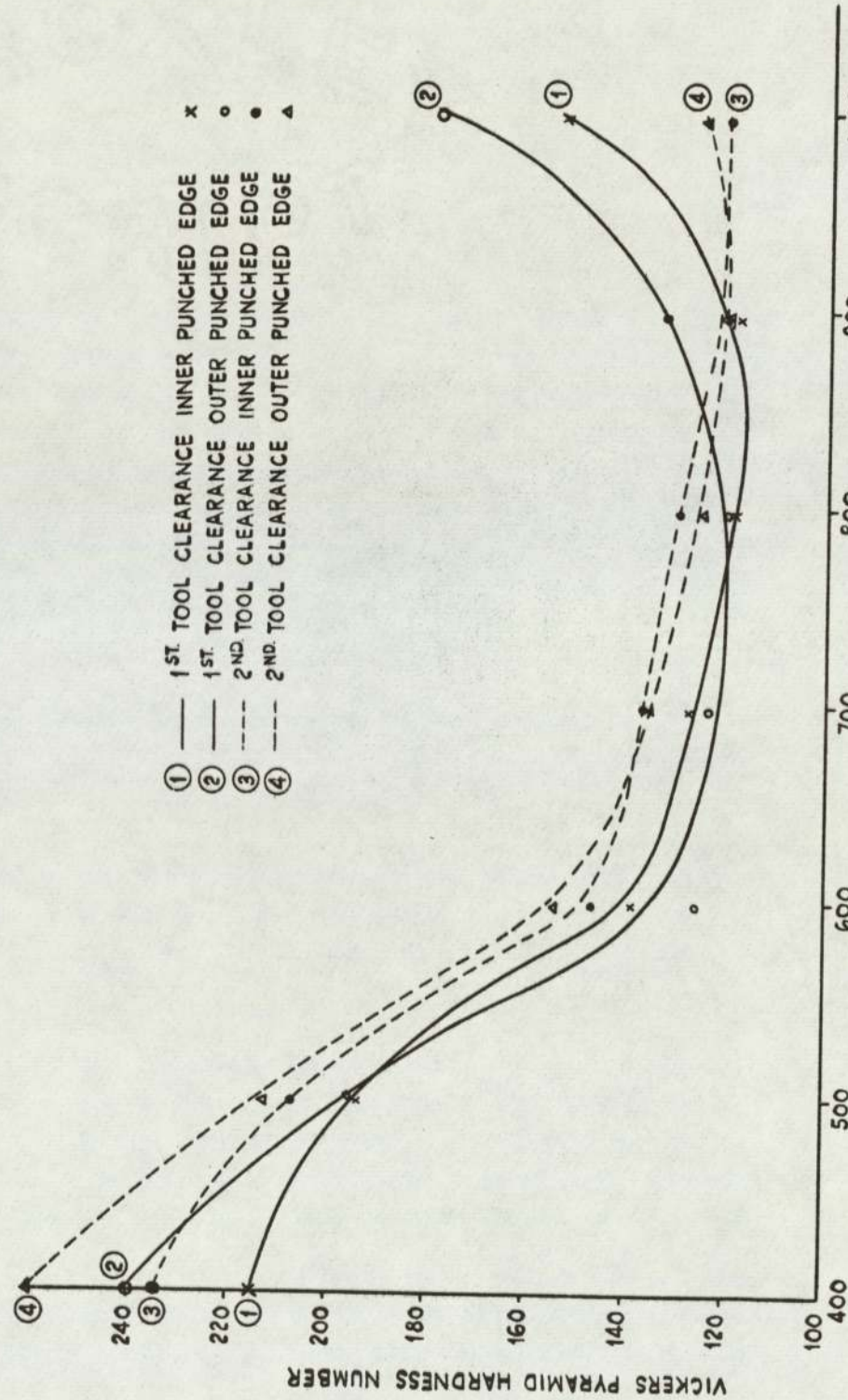

FIG. 45. VARIATION OF MICROHARDNESS WITH ANNEALING TEMPERATURE.

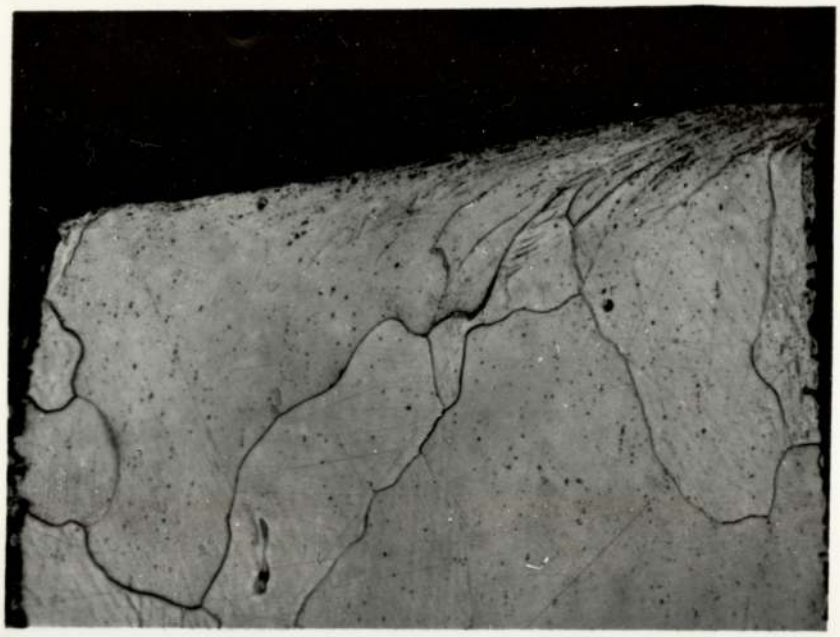

Ambient Temperature

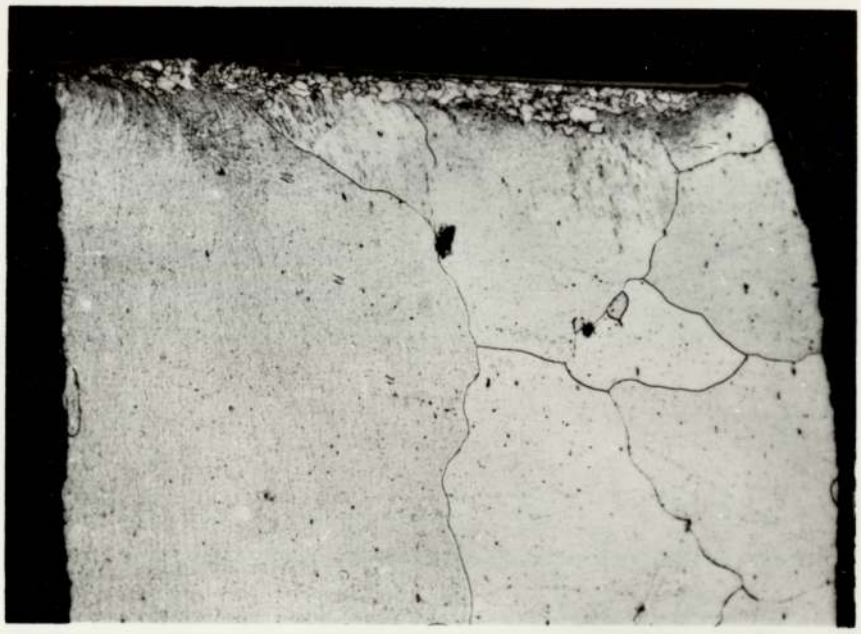

Annealed for 6 Hours @ 500°C

Magnification = 200

Ext. Dia. = 18.0 cms Int. Dia. = 8.5 cms

0.51 cms Thickness 1st Clearance

FIG.46. THE CRYSTAL STRUCTURE OF A LAMINATION IMMEDIATELY BELOW THE PUNCHED EDGE

Annealed for 6 Hours @ 800°C

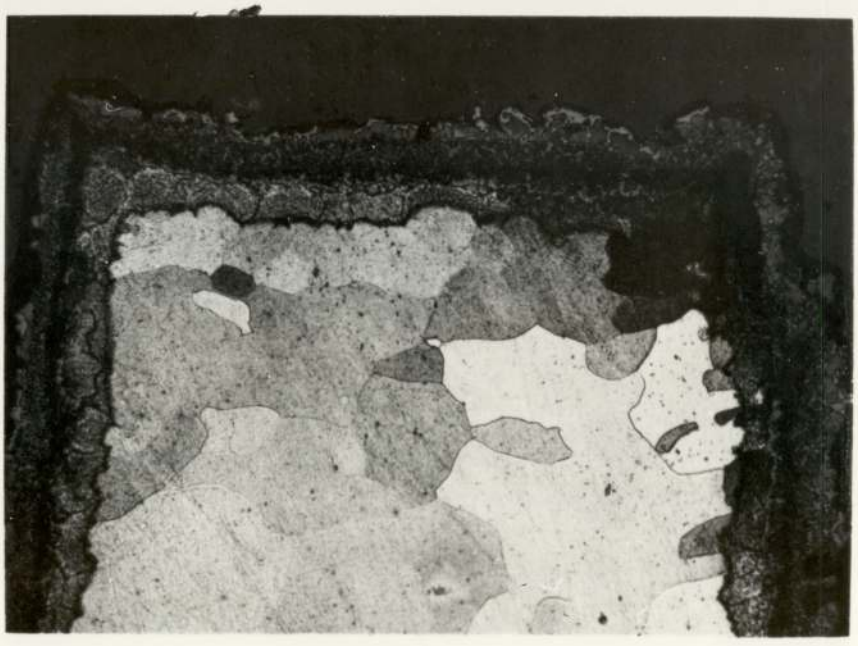

Annealed for 6 Hours @ 1000°C

Magnification = 200

Ext. Dia. = 18.0 cms Int. Dia. = 8.5 cms

0.051 cms Thickness 1st Clearance

FIG 47. THE CRYSTAL STRUCTURE OF A LAMINATION IMMEDIATELY BELOW THE PUNCHED EDGE

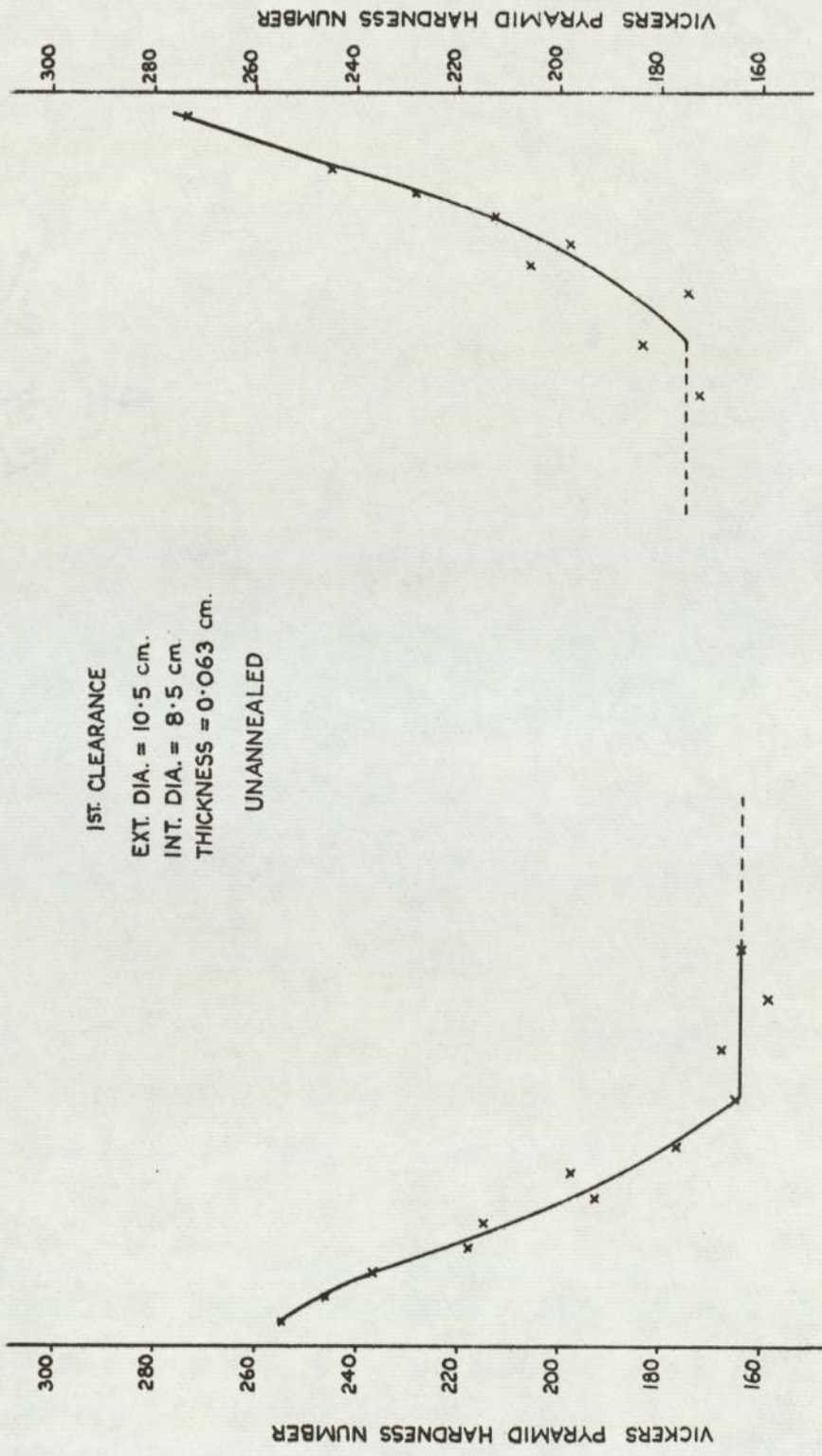

FIG.48. VARIATION OF MICROHARDNESS WITH DISTANCE BELOW PUNCHED SURFACE

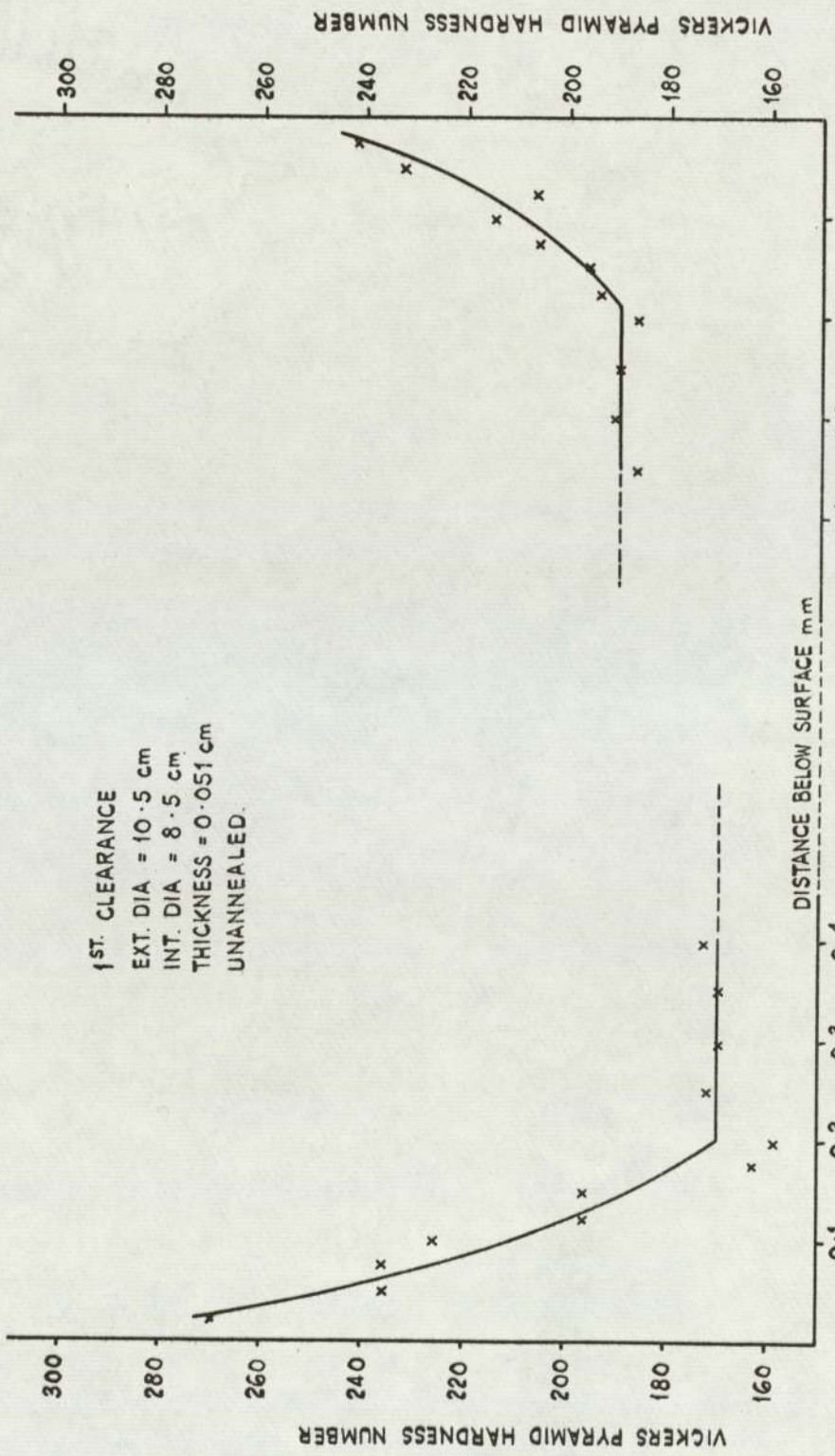

FIG.49. VARIATION OF MICROHARDNESS WITH DISTANCE BELOW PUNCHED SURFACE.

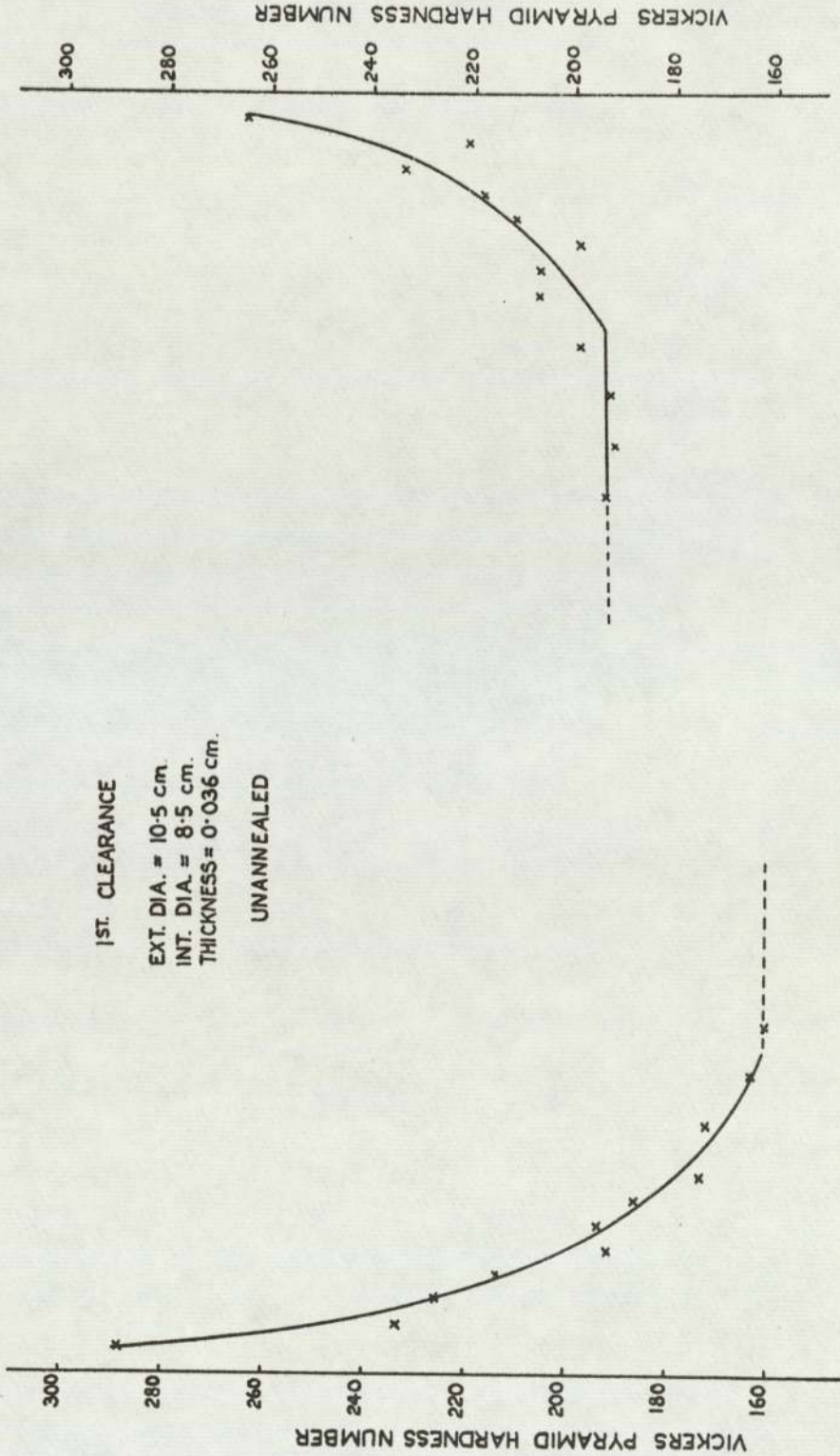

FIG.50. VARIATION OF MICROHARDNESS WITH DISTANCE BELOW PUNCHED SURFACE

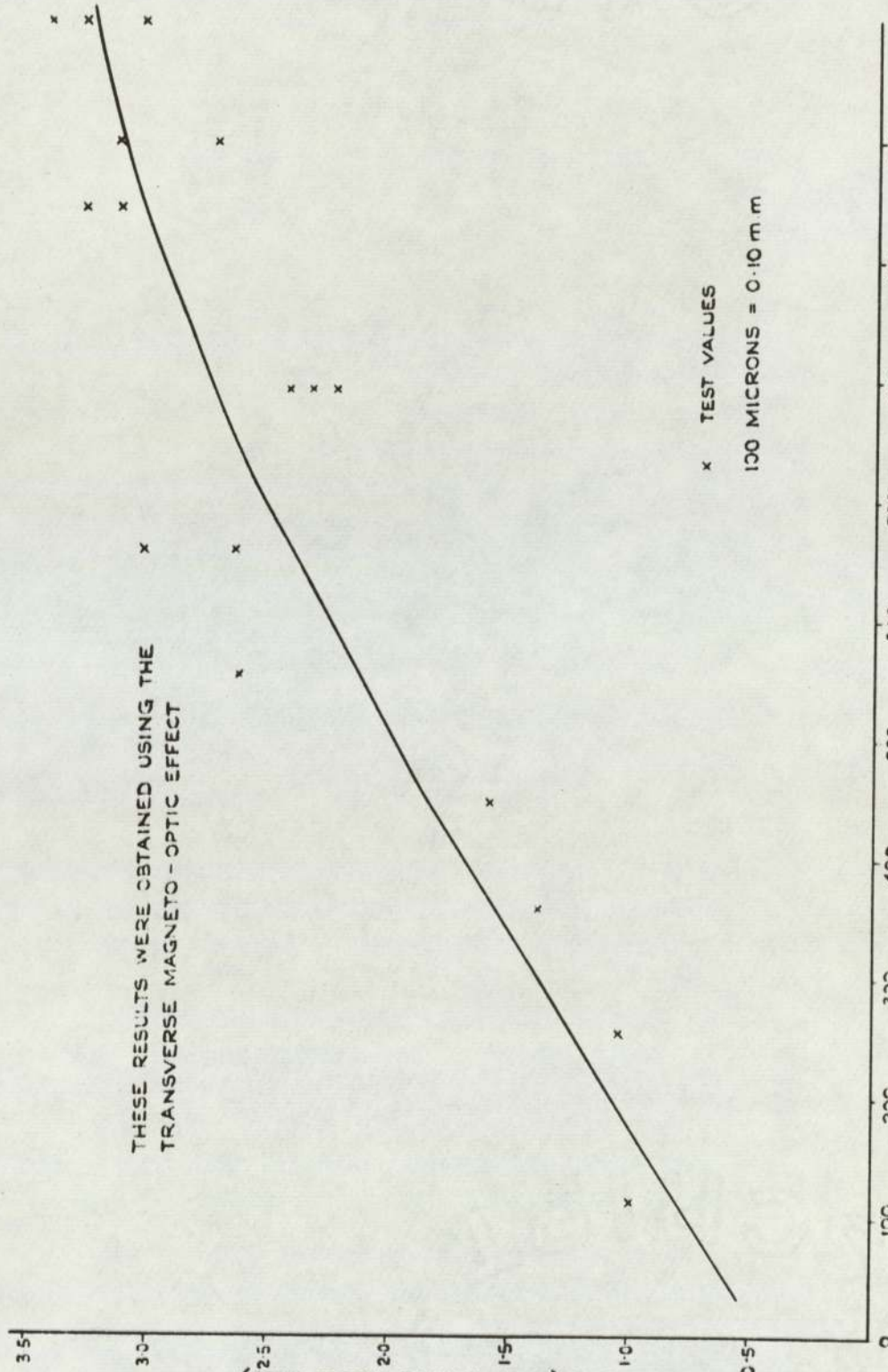

FIG 51. PERMEABILITY MEASURED AT A POINT PLOTTED AGAINST DISTANCE FROM PUNCHED SURFACE.

B

A

Magnification = 1960

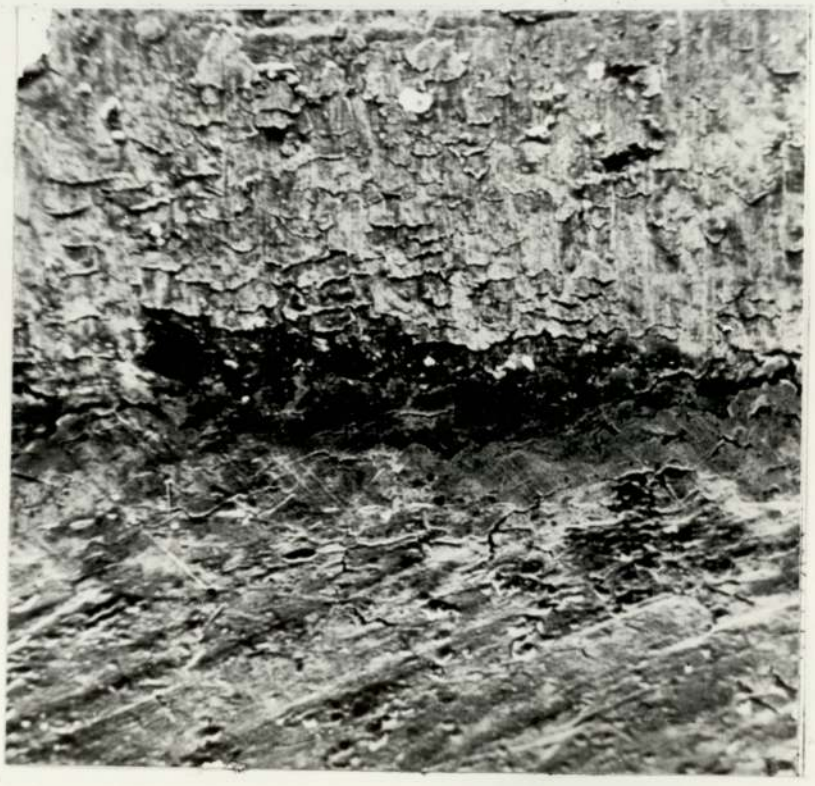

B

A

Magnification = 390

Ext. Dia. = 10.5 cms Int. Dia = 8.5 cms

0.036 cms Thickness 2nd Clearance

Letters A & B indicate direction of photograph - See Fig. 18.

FIG. 52. MICROSCOPIC EXAMINATION OF LAMINATION SURFACE

D

A

Magnification = 1720

Ext. Dia. = 10.5 cms Int. Dia. = 8.5 cms

0.036 cms Thickness 2nd Clearance

Letter A & D indicate direction of photograph - See Fig.18.

FIG.53. MICROSCOPIC EXAMINATION OF LAMINATION SURFACE

SECTION 8

CONCLUSIONS

In investigating the effect of the punching process upon one grade of cold reduced non-oriented silicon steel, the following conclusions were reached:

1. The punching effect causes deterioration in the magnetic properties of lamination material. This deterioration, which is caused by the plastic deformation of the material, is most evident in the shape of the magnetization curves as can be seen in Figs. 31-34 (pages 85-88). The deviation of the punched material curve, from the curve of the unstrained material, can be appreciable. This is seen in Figs. 38-41 (pages 92-95) and in Table 5.

TABLE 5

INCREASE IN MAGNETIC FIELD STRENGTH, FOR A GIVEN FLUX DENSITY, DUE TO PUNCHING

EXT. DIA. = 10.5 cm. INT. DIA. = 8.5 cm. THICKNESS = 0.051 cm.

FLUX DENSITY TESLAS	% INCREASE IN H	
	1st Test	2nd Test
0.6	20	78
0.8	29	118
1.0	47	175
1.1	65	310
1.2	75	430
1.3	84	410
1.4	69	58
1.5	8	0

1st Test 0.025 mm. diametral clearance between punch and die.

2nd Test 0.050 mm. diametral clearance between punch and die.

On all the lamination samples tested, the maximum increase in H occurs at approximately 1.3T. For the punching factors and clearances investigated so far, the two curves always merge together at approximately 1.5T. Beyond this flux level there seems to be no difference in the two magnetization curves.

2. The deterioration of the magnetization curve is dependent upon the ratio of punched area to total surface area of the lamination. The degree of deterioration can be seen from Fig. 39 (page 93). The evidence of the tests so far completed indicate that it is also dependent on the clearance distance of the punching tool (Table 5).

3. For the first tool clearance (0.025 mm. diametral) the effect of the punching upon the static hysteresis loss is small. Even for the sample with the largest increase in hysteresis loss, the increase only exceeded 25% at flux densities below 0.8T (Table 2). For a machine operating at a flux density above 1.0T, at a moderate speed, the total iron loss would be such that the increase in hysteresis loss, due to punching, would be negligible.

4. The variations in the magnetization curves of the lamination material in the unstrained state (annealed)is appreciable. For the first and second tool clearances, the extent of this variation is comparable with the magnitude of the change in the magnetization curve due to punching. This is seen by comparing the difference between the curves shown in Figs. 31 & 35 (pages 85&89).

5. Beyond 1.4T, all the Ferrosil 216 material tested in the unstrained state, required a higher magnetic field strength, for a given flux density, than that shown by the steel manufacturer's curve. Since the magnitude of H required for the same value of flux density on two different curves in the saturated region can differ considerably, the consequences of using the wrong curve can be serious. For example, at 1.5T the manufacturer's curve shows an H of 1210 A/m and the curve for the 0.064 cm. thick annealed material, with the 1st tool clearance, shows an H of 3200 A/m.

6. The results of the static hysteresis loss tests gave reasonably good correlation with the results obtained from the dynamic hysteresis loss tests (Fig. 20-22, pages 74-76). This confirms that, over its working range, the method employed for measuring the dynamic iron loss in this project affords a satisfactory and convenient means of determining the total iron loss in ring form laminations. The dynamic loss tests also provide a means of measuring and recording the flux densities occurring in the material under dynamic conditions. If means of extending the frequency range of the electronic hysteresigraph can be found, then the equipment used in this project will have a wide application in the routine testing of material used in the manufacture of electrical machines.

The results of this investigation show, for the grade of magnetic material being considered, that if an electrical machine is designed on the basis of the steel manufacturer's magnetization curve, then even if the material is annealed after punching,

the performance of the machine may be lower than predicted at the design stage. Should the machine be operating at flux levels below 1.4T and the laminations being annealed, then the performance of the machine could be reduced still further.

If the correct magnetization curve is known for the unstrained lamination material, and knowing also the flux level at which the machine is working, the punching factor (defined in Section 3.3) and the punching tool clearance, then on the basis of data obtained in this investigation it is possible to make the necessary modification to the value of H obtained from the magnetization curve.

SECTION 9

RECOMMENDATIONS

The following recommendations are made as a result of the findings of the present investigation.

1. Magnetization curves which are supplied by the steel manufacturer for each of their grade of magnetic material, should only be used as a guide to probable typical values. Design information should be obtained from regular tests taken to determine the magnetization curve of each grade and thickness of magnetic material used.

2. Further information should be obtained concerning the effects of the punching process upon the magnetic properties of lamination material. This should be done for the present grade of material with larger punching tool clearances and also for different grades of material. The results of the present work has indicated that the effect of punching may be considerable on larger tool clearances. Since punching tools are sometimes used with upto 0.4 mm. diametrical clearances, before being replaced, it is important to obtain sufficient information to find the complete pattern of change in the magnetic properties of the material over the full clearance range that exists in the life of a punching tool.

3. The test rig, which was designed and built for the present project, and the electronic hysteresigraph should be considered as a standard piece of test equipment. This would involve using the equipment for a more general application and would require making certain modifications

to the electronic circuit. When used in conjunction with an on-line computer, this equipment would prove to be of great value.

REFERENCES

1. COLE, G.H. : "Effect of punching strains on the magnetic properties of electrical sheet steel", The Electric Journal, February 1924, Vol.XX1, No.2, pp. 55-61.

2. SEEGER, D. : "The increase of iron losses of dynamo sheets due to various preparation processes involved in the construction of electrical machines", E.T.Z-A, 1963, Vol.84, No.19, pp. 622-627.

3. OBERRETL, K. : "The more exact calculation of the magnetizing current of three-phase asynchronous machines", Bulletin Oerlikon, 1959, No.335, pp. 66-84.

4. "Blanking and piercing - A metallographic study of the mechanism of constrained shear", Production Engineering Research Association, Report No.93, December 1961.

5. RISCH, R. : "Separation of the eddy current losses by means of the eddy current ellipse", Scientia Electrica, Vol.6 (2), pp. 75-79.

6. MASTERO-GIURCANEANU, S. : "Contribution to the predetermination of losses in ferromagnetic packs", Docteur en Sciences Appliqueers Thesis, Polytechnical Faculty of Mons, 1967, pp. 89-107.

7. STEINMETZ. C.P. : "On the law of hysteresis" AIEE Transactions, 1892, Vol.9, pp. 3-51.

8. WEBB, C.E. : "The power losses in magnetic sheet material at high flux densities", I.E.E. Journal, April 1926, Vol.64, No.352, pp. 409-435.

9. RICHARDSON, F.R. and FALKOWSKI, E.C. : "Relation of AC losses to hysteresis losses in electric sheet steels", IEEE Transactions on Power Apparatus and Systems, September 1967, Vol.PAS-86, No.9, pp. 1072-1076.

10. LITTMANN, M.F. : "Iron and Silicon-Iron Alloys", IEEE Transactions on Magnetics, March 1971, Vol.MAG-7, No.1, pp. 48-60.

11. RANDALL, W.F. and SCHOLEFIELD, H.H. : "Some metallurgical and structural factors affecting properties of soft magnetic material", I.E.E. Proceedings, April 1950, Vol.97, Part 2, pp. 133-140.

12. GOLDING, E.W. : "Electrical measurements and measuring instruments", Sir Isaac Pitman & Sons Ltd., Third edition revised, 1948.

13. MAZZETTI, P. and SOARDO, P. : "Electronic hysteresigraph holds dB/dt constant", The Review of Scientific Instruments, May 1966, Vol.37, No.5, pp. 548-552.

14. HAMMOND, P. : "Leakage flux and surface polarity in iron ring stampings", I.E.E. Monograph, January 1955, No.116, pp. 138-147.

15. WALKER, J.H., ROGERS, G. J. and JACKSON, R.L. : "Pressings and clamping laminated cores", I.E.E. Proceedings, March 1964, Vol. 111, No. 3, pp. 565-577.

16. SMALLMAN, R.E. : "Modern physical metallurgy", Butterworth & Co. (Publishers) Ltd., 1962.

17. TWEEDDALE, J.G. : "Mechanical properties of metals", George Allen & Unwin Ltd., 1964.

18. CAREY, R. and ISAAC, E.D. : "Magnetic domains and techniques for their observation", The English Universities Press Ltd., 1966.

APPENDIX A

THE ELECTRONIC HYSTERESIGRAPH

The electronic hysteresigraph (Fig. 54) is based upon the principles used in the system developed by Mazzetti and Soardo[13]. In this system the rate of charge of flux (dB/dt) is monitored via a search coil wound on the lamination pack. This search coil voltage is amplified by two stages of gain in amplifiers A_1 and A_2. The circuit used for the test programme required an overall gain of 100 in these two stages and this was achieved by the choice of the values of R_1, R_3, R_4 and R_6 which fix the gain of the integrated circuit amplifiers A_1 and A_2. It was convenient to separate this overall gain into two stages in order to provide a suitable signal level to the analogue to digital converter from the output of A_1.

The amplified dB/dt signal is compared with a d.c. reference voltage at the input of a high gain integrating comparator formed by amplifier A_3, its input resistors R_7 and R_8, and the feedback capacitor 6_1.

The output of this comparator drives a power amplifier identical to that developed by Mazzetti and Soardo. This amplifier supplies current to the excitation coil wound round the lamination pack, and thereby provides a feedback system via the magnetic flux and search coil. This feedback loop maintains the dB/dt at the level equivalent to the reference voltage on the input of A_3 as the excitation current rises.

Excitation current is measured by a series resistor and the voltage developed across this is amplified by A_4. This signal is compared with a fixed reference which is derived from the resistor

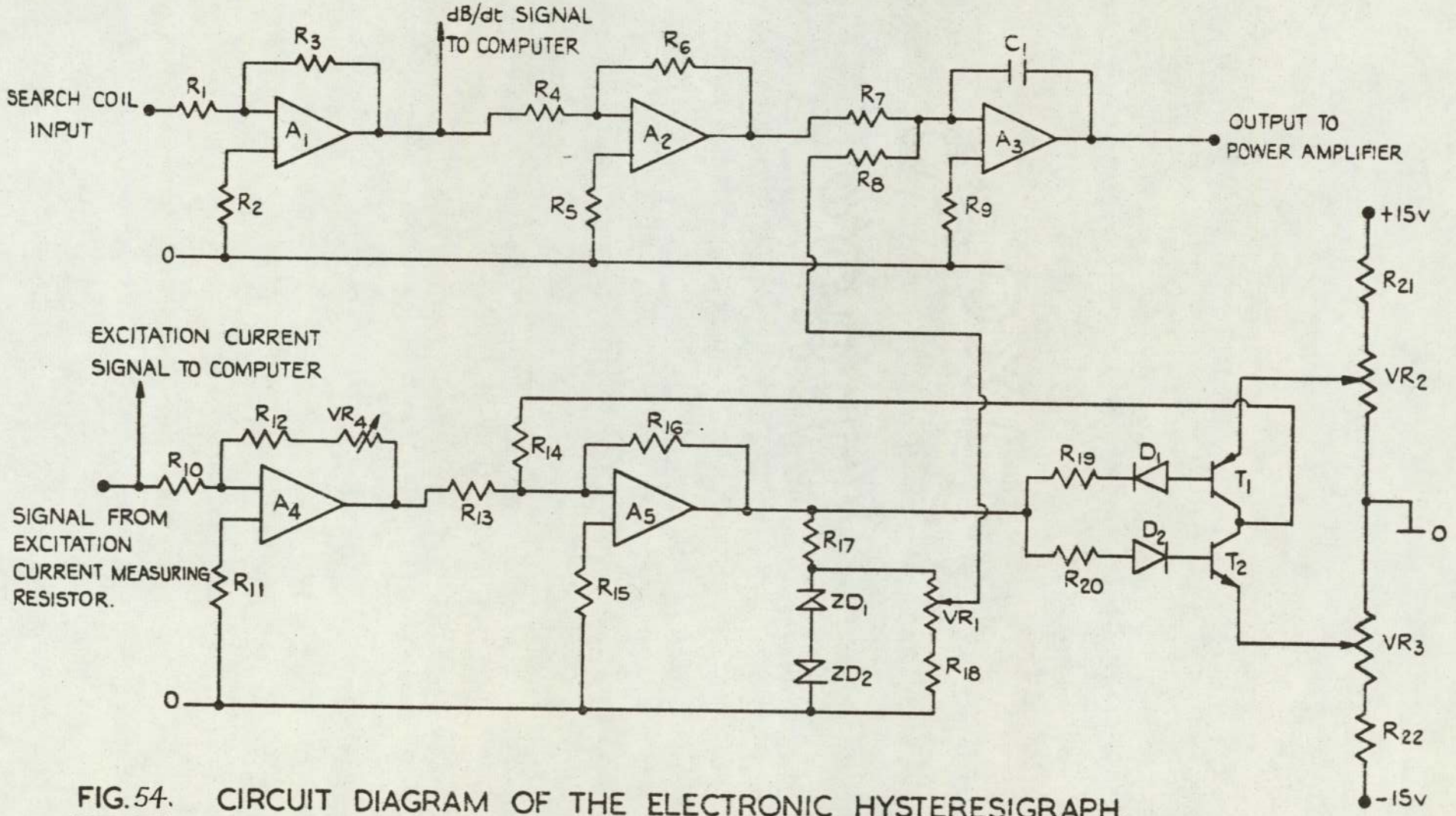

FIG. 54. CIRCUIT DIAGRAM OF THE ELECTRONIC HYSTERESIGRAPH.

chain R_{21} - R_{22}. A_5 is a high gain comparator which is driven into saturation when the current signal exceeds the reference. This causes the polarity of both the current and dB/dt reference levels to reverse. The reversal of the dB/dt reference is detected by A_3 which drives the power amplifier in the opposite direction in order to cause the flux in the magnetic circuit to decay. Adjustment of the gain of A_4, by varying VR_4, provides control of the current level at which reversal takes place, i.e. VR_4 sets the peak excitation current, hence peak flux. Separate control of the valve of dB/dt is provided by adjustment of VR_1 which varies the reference level supplied to A_3. VR_1 and VR_4 are 10 turn potentiometers with calibrated dials which facilitate easy control and logging of the two variables of peak current and dB/dt.

CIRCUIT COMPONENTS FOR FIG. 54

R_1 - 1K2	R_{15} - 1K5	T_2 - BC107
R_2 - 1K2	R_{16} - 6M8	ZD_1, ZD_2 - BZY88C10
R_3 - 12K	R_{17} - 1K5	D_1, D_2 - ec401
R_4 - 1K2	R_{18} - 680R	A_1 - A_5 - SN741P
R_5 - 1K2	R_{19} - 10K	
R_6 - 12K	R_{20} - 10K	
R_7 - 100K	R_{21} - 220R	
R_8 - 100K	R_{22} - 220R	
R_9 - 100K	VR_1 - 50K linear	
R_{10} - 1K2	VR_2 - 250R linear	
R_{11} - 1K2	VR_3 - 250R linear	
R_{12} - 1K2	VR_4 - 50K linear	
R_{13} - 2K2	C_1 - 3300 pF	
R_{14} - 10K	T_1 - BCY71	

APPENDIX B

COMPUTER PROGRAM DATA

Computer Program for Dynamic Hysteresis Loop.

Flow Diagram for the Program.

Typical Computer Print Out.

PAGE 0001

```
C     FORTRAN PROGRAM FOR DYNAMIC HYSTERESIS LOOP
C     -------------------------------------------
C
C
      INTEGER II(2000),X(1000),Y(1000)
      COMMON II,AB
      WRITE (2,109)
      READ (1,106) R,S,A,L,T
      WRITE (2,107) R,S,A,L,T
1     READ (1,100) N1,NP,NT
      READ (1,104) C1,C2,C3
      N=N1+1
      IF (NP.NE.0) WRITE (2,103)
      CALL PERME(N,PER)
      TM=PER/FLOAT(NT-1)
      NT2=2*NT
      CALL ADSEQ (N1,II(1),2,TM,PER,NT2,IND,K)
      IF (IND.EQ.0) GO TO 3
      PAUSE 1
      GO TO 1
3     BM=0
60    DO 2 J=1,K
      JJ=J*2
      B(J)=FLOAT(II(JJ))
2     BM=BM+B(J)
      RK=K
      BM=BM*0.5/RK
      DO 4 J=1,K
4     B(J)=B(J)-BM
      FLUX(1)=0.0
      LOSS=0.0
      MMF1=FLOAT(II(1))*C1/204.8
      ICNT=1
      KK=2
      DO 25 J=2,K
      J7=J-1
25    DB(J)=(B(J)+B(J7))*0.5*C2/204.8
      AB(J)=DB(J)*TM*1.0E-3
26    FLUX(J)=FLUX(J7)+AB(J)
      SUM=0
      DO 99 J=1,K
99    SUM=FLUX(J)+SUM
      E=SUM/FLOAT(NT)
      FLUX(1)=-E
      IF(NP.NE.0)WRITE(2,101)ICNT,MMF,FLUX(1)
```

PAGE 0002

```
      DO 20 J=2,K
      J2=J*2-1
      DB(J)=FLOAT(II(J2))*C1/204.8
      FLUX(J)=FLUX(J)-E
      DE=DB(J)*AB(J)*C3
      LOSS=LOSS+DE
      IF(FLUX(J).GT.FLXMX)FLXMX=FLUX(J)
      IF(DB(J).GT.HMAX)HMAX=DB(J)
      IF (KK.EQ.NP) GO TO 5
      KK=KK+1
      GO TO 20
5     WRITE (2,101) J,DB(J),FLUX(J),PQ
      KK=1
20    CONTINUE
      WRITE(2,113)HMAX,FLXMX
      ENERGY=LOSS*A*L*1.0E-6
      LOSS=ENERGY*1000.0/PER
      WRITE (2,105) PER,FREQ
      WRITE(2,108)ENERGY,PR
      WRITE (2,102) LOSS
      GO TO 1
113   FORMAT (//8H  MAX.H=,F11.3,22X,6HMAX.B=,F10.2)
100   FORMAT (2I3,I5)
101   FORMAT (I4,2F12.3,F16.2)
102   FORMAT (6H LOSS=,F13.3,6H WATTS/)
103   FORMAT (4H NO,7X,3H H ,9X,4HFLUX,11X,5HDB/DT/11X,4HKA/KM,
     1         8X,5HTESLA,8X,10HTESLAS/SEC//)
104   FORMAT (F10.4)
105   FORMAT (//8H PERIOD=,F9.1,9H MILL-SEC,15X,9HFREQUENCY,
     1         F6.2,3H HZ)
106   FORMAT (4F6.2,F7.3)
107   FORMAT (22H    EXTERNAL DIAMETER=,F5.2,5H  CMS/
     1         22H    INTERNAL DIAMETER=,F5.2,5H  CMS/
     2         22H       SECTIONAL AREA=,F5.2,8H  SQ.CMS/
     3         22H          MEAN LENGTH=,F5.2,5H  CMS/
     4         22H            THICKNESS=,F6.3,4H CMS/)
108   FORMAT(/8H ENERGY=,F12.4,7H JOULES,14X,6HDB/DT=,F8.3/)
109   FORMAT (8H    DATE,2X,10H..........,15X,13HNOT ANNEALED/)
      END
```

PAGE 0001

```
C     FORTRAN PROGRAM FOR X-Y PLOT OF DYNAMIC HYSTERESIS LOOP
C     ------------------------------------------------------
C
C
      INTEGER X(1000),Y(1000),C,FN
      REAL L
      DIMENSION FILE N(2)
      DATA FILE N(1), FILE N(2)/5HEXPNO, 4H1LAW/
  123 WRITE (2,100)
        READ(1,101)A
        CALL INSERT(A,FILE N(2))
      CALL SEEK(6,FILE N)
      READ(6)X
      READ(6)Y
      READ(6) R,S,A,L,T
        READ(6)C1,C2,NT,FREQ
        C1=1.75
        IF(C2.EQ.80.0)C2=5.0
        IF(C2.EQ.100.0)C2=4.0
        IF(C2.EQ.500.0)C2=0.8
        IF(C2.EQ.1000.0)C2=0.4
        IF(C2.EQ.2000.0)C2=0.2
      CALL CLOSE(6)
      CALL PLOT(0,-425,-550)
        CALL PLOT(5,-400,0)
        CALL PLOT(4,400,0)
        CALL PLOT(5,0,-500)
        CALL PLOT(4,0,500)
      DO 11 J=2,NT
        I=-X(J)
        IF(IABS(I).GT.425)GOTO 11
      IF(J.EQ.2)CALL PLOT(5,I,Y(J))
      CALL PLOT(4,I,Y(J))
   11 CONTINUE
      CALL PLOT(3,0,0)
      CALL CONTRO(5,0,3,0)
      CALL CONTRO(5,1,1000,0)
      CALL CONTRO(5,2,-60,250)
      WRITE(5,20)
      CALL CONTRO(5,0,2,0)
      CALL CONTRO(5,1,0,1000)
      DO 33 I=1,7
      F=FLOAT (I)/7.0*C1
      FN=70.0*FLOAT(I)
        CALL PLOT(5,0,FN)
        CALL PLOT(4,10,FN)
      CALL CONTRO(5,2,-50,FN)
   33 WRITE(5,30)F
        CALL CONTRO(5,2,-350,400)
        WRITE(5,110)FREQ
      DO 44 I=1,7
```

PAGE 0002

```
      F=-FLOAT (I)/7.0*C1
      FN=-70.0*FLOAT(I)
        CALL PLOT(5,0,FN)
        CALL PLOT(4,10,FN)
      CALL CONTRO(5,2,-50,FN)
   44 WRITE(5,30)F
      CALL CONTRO(5,0,3,0)
      CALL CONTRO(5,2,-350,-50)
      WRITE(5,50)
      CALL CONTRO(5,0,2,0)
      DO 66 I=1,4
        B=-FLOAT(I)/4.0*C2
      C=-100.0*FLOAT(I)
        CALL PLOT(5,C,0)
        CALL PLOT(4,C,10)
        C=C-15
      CALL CONTRO(5,2,C,-20)
   66 WRITE(5,60)B
      DO 77 I=1,4
      B=FLOAT (I)/4.0*C2
      C=100.0*FLOAT(I)
        CALL PLOT(5,C,0)
        CALL PLOT(4,C,10)
        C=C-30
      CALL CONTRO(5,2,C,-20)
   77 WRITE(5,60)B
    9 CALL CONTRO(5,0,2,0)
      CALL CONTRO(5,1,0,1000)
      CALL CONTRO(5,2,0,-400)
      WRITE(5,90)R,S,A,L,T
      PAUSE
      GO TO 123
   20 FORMAT(13H FLUX(TESLAS))
   30 FORMAT(F5.2)
   50 FORMAT(9H H.(KA/M))
   60 FORMAT(F5.2)
   90 FORMAT(23H      EXTERNAL DIAMETER=,F5.2,5H  CMS/
     1       23H      INTERNAL DIAMETER=,F5.2,5H  CMS/
     2       23H         SECTIONAL AREA=,F5.2,8H  SQ.CMS/
     3       23H            MEAN LENGTH=,F5.2,5H  CMS/
     4       23H              THICKNESS=,F6.3,4H CMS)
  100   FORMAT(8H RUN NO.)
  101   FORMAT(1A1)
  110   FORMAT(11H FREQUENCY=,F6.2,3H HZ)
      END
```

FORTRAN PROGRAM FOR DYNAMIC HYSTERESIS LOOP

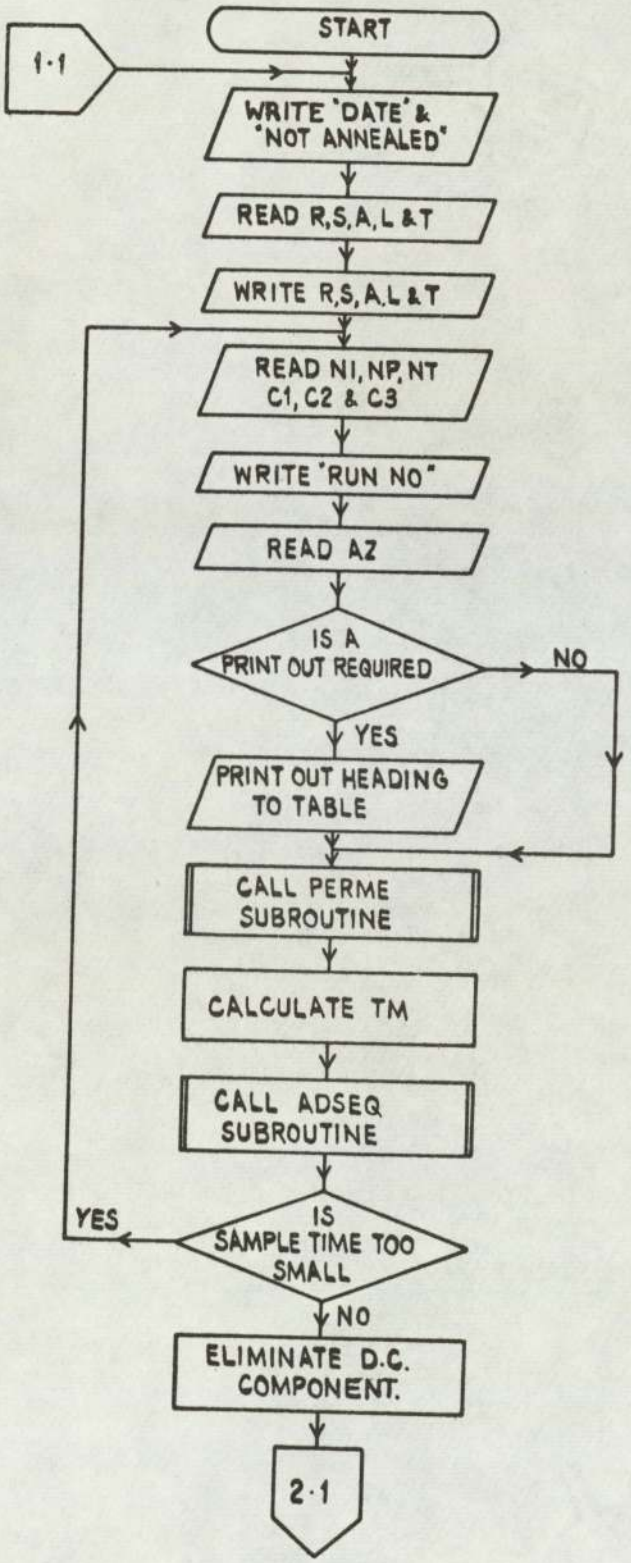

R = EXTERNAL DIAMETER
S = INTERNAL DIAMETER
A = SECTIONAL AREA
L = MEAN PATH LENGTH
T = LAMINATION THICKNESS
NI = TERMINAL NUMBER
NP = No. OF SAMPLES BETWEEN PRINT OUTS
NT = TOTAL No. OF SAMPLES ON EACH CHANNEL
C1 = MMF CONSTANT
C2 = FLUX CONSTANT
C3 = LOSS CONSTANT
AZ = RUN No.
PERME = SUBROUTINE FOR PERIOD
IND = TOTAL SAMPLING TIME
TM = TIME BETWEEN SAMPLES
ADSEQ = SUBROUTINE TO ENABLE No. OF SIGNALS TO BE DEALT WITH IN SEQUENCE
MMF = MAGNETO-MOTIVE FORCE
AB = CHANGE IN FLUX BETWEEN SAMPLES
B = FLUX
DB = RATE OF CHANGE OF FLUX.

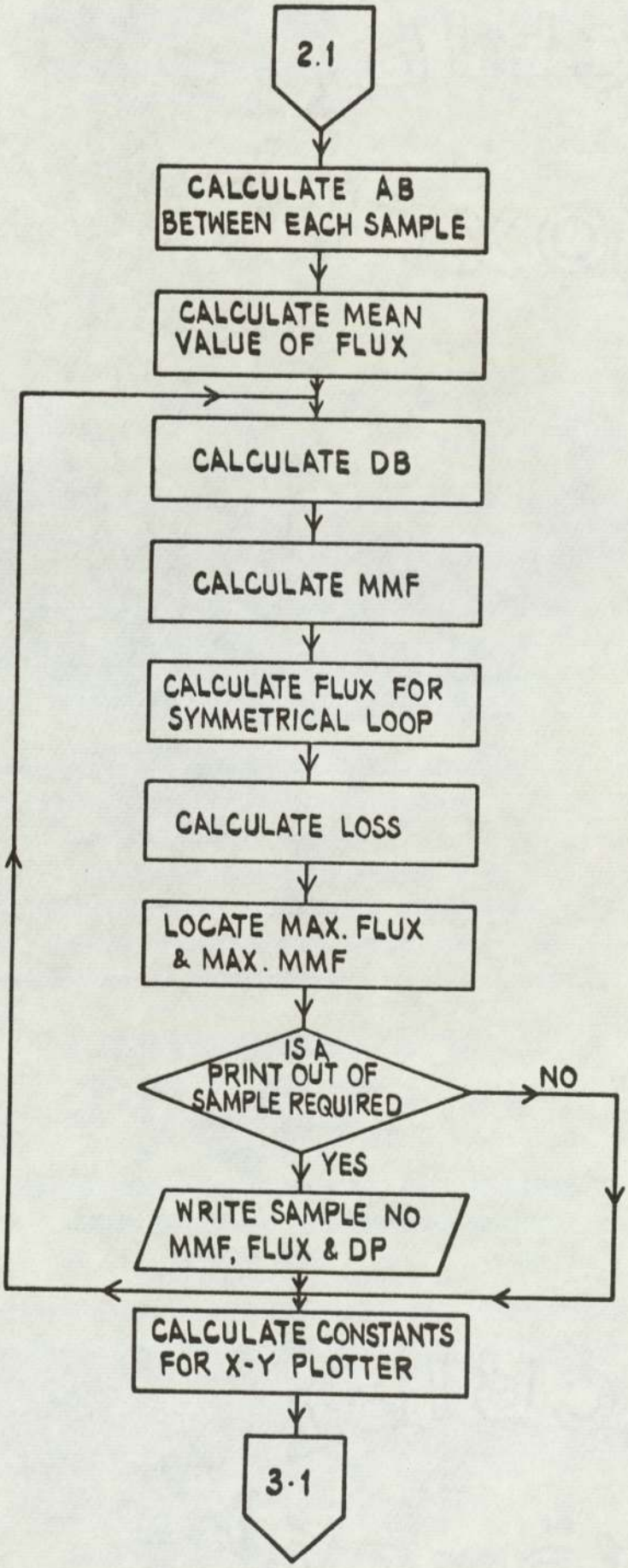
2.1
CALCULATE AB BETWEEN EACH SAMPLE
CALCULATE MEAN VALUE OF FLUX
CALCULATE DB
CALCULATE MMF
CALCULATE FLUX FOR SYMMETRICAL LOOP
CALCULATE LOSS
LOCATE MAX. FLUX & MAX. MMF
IS A PRINT OUT OF SAMPLE REQUIRED
NO
YES
WRITE SAMPLE NO MMF, FLUX & DP
CALCULATE CONSTANTS FOR X-Y PLOTTER
3·1

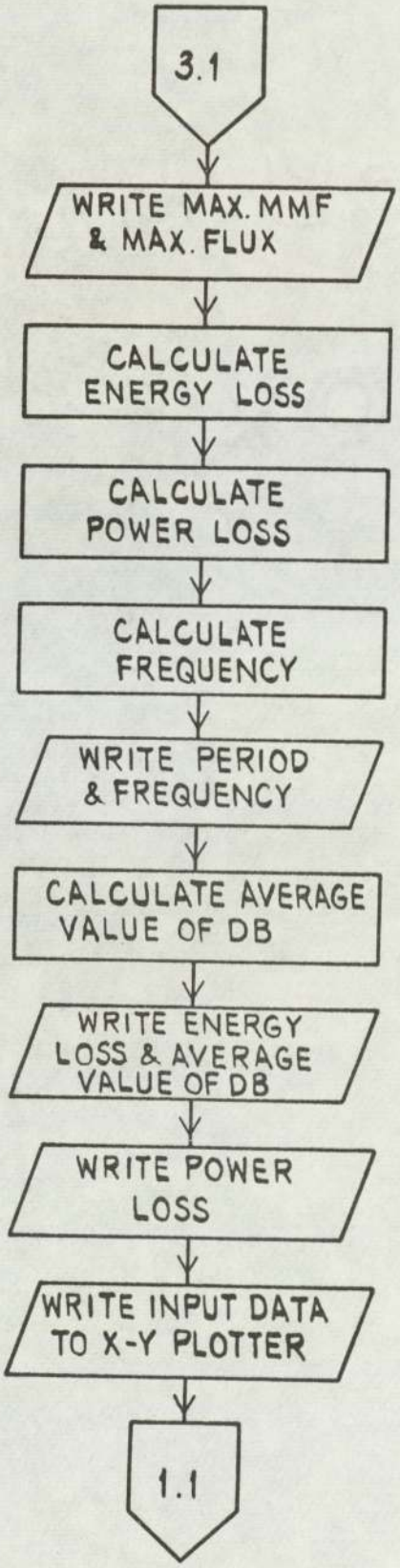
3.1
WRITE MAX. MMF & MAX. FLUX
CALCULATE ENERGY LOSS
CALCULATE POWER LOSS
CALCULATE FREQUENCY
WRITE PERIOD & FREQUENCY
CALCULATE AVERAGE VALUE OF DB
WRITE ENERGY LOSS & AVERAGE VALUE OF DB
WRITE POWER LOSS
WRITE INPUT DATA TO X-Y PLOTTER
1.1

TS

DATE 3:11:71... NOT ANNEALLED @ 500°C.

```
  13.0  10.5  0.78  36.9  0.051
   EXTERNAL DIAMETER=13.00  CMS
   INTERNAL DIAMETER=10.50  CMS
      SECTIONAL AREA= 0.78  SQ.CMS
         MEAN LENGTH=36.90  CMS
           THICKNESS= 0.051 CMS

  1  2  120
0.0577
45.9
-1000.0
RUN NO.
E
```

NO	H KA/M	FLUX TESLA	DB/DT TESLAS/SEC
1	0.000	1.231	
2	-0.225	1.195	-174.60
4	-0.030	1.089	-241.06
6	0.009	1.003	-205.53
8	0.036	0.916	-205.42
10	0.054	0.830	-204.52
12	0.066	0.745	-204.19
14	0.074	0.659	-204.19
16	0.081	0.573	-204.19
18	0.086	0.487	-204.19
20	0.089	0.402	-203.85
22	0.092	0.316	-203.74
24	0.094	0.231	-203.96
26	0.095	0.145	-204.64
28	0.097	0.059	-205.20
30	0.098	-0.028	-206.43
32	0.101	-0.114	-205.87
34	0.104	-0.201	-205.98
36	0.108	-0.287	-206.43
38	0.112	-0.374	-206.09
40	0.117	-0.460	-205.76
42	0.124	-0.547	-205.42
44	0.132	-0.633	-205.08
46	0.142	-0.719	-204.75
48	0.156	-0.805	-204.52
50	0.174	-0.891	-204.30
52	0.198	-0.977	-204.86
54	0.234	-1.063	-205.64
56	0.288	-1.149	-205.87
58	0.380	-1.234	-198.36
60	0.476	-1.283	-52.79
62	0.115	-1.202	250.78
64	0.032	-1.103	214.36
66	-0.002	-1.015	208.08
68	-0.023	-0.929	205.95
70	-0.038	-0.842	206.29
72	-0.048	-0.756	206.40
74	-0.055	-0.669	206.96
76	-0.060	-0.582	207.41
78	-0.066	-0.495	207.52
80	-0.067	-0.407	207.64
82	-0.069	-0.320	207.86
84	-0.072	-0.233	207.64
86	-0.074	-0.146	208.31
88	-0.076	-0.058	207.75
90	-0.078	0.029	208.31
92	-0.081	0.117	208.08
94	-0.084	0.204	208.87
96	-0.087	0.292	208.76
98	-0.092	0.379	208.98
100	-0.097	0.467	209.20
102	-0.104	0.555	208.53
104	-0.112	0.643	208.53
106	-0.124	0.730	208.20
108	-0.140	0.817	207.52
110	-0.161	0.904	207.19
112	-0.190	0.991	207.41
114	-0.232	1.079	208.31
116	-0.300	1.166	205.95
118	-0.419	1.248	193.18
120	-0.356	1.247	-88.65

MAX.H= 0.476 MAX.B= 1.27

PERIOD= 25.0 MILL-SEC FREQUENCY 40.03 HZ

ENERGY= 0.0148 JOULES DB/DT= 202.657

LOSS= 0.593 WATTS

A TYPICAL COMPUTER PRINT-OUT

APPENDIX C

CONDITION FOR MAXIMUM INCREASE IN H DUE TO PUNCHING

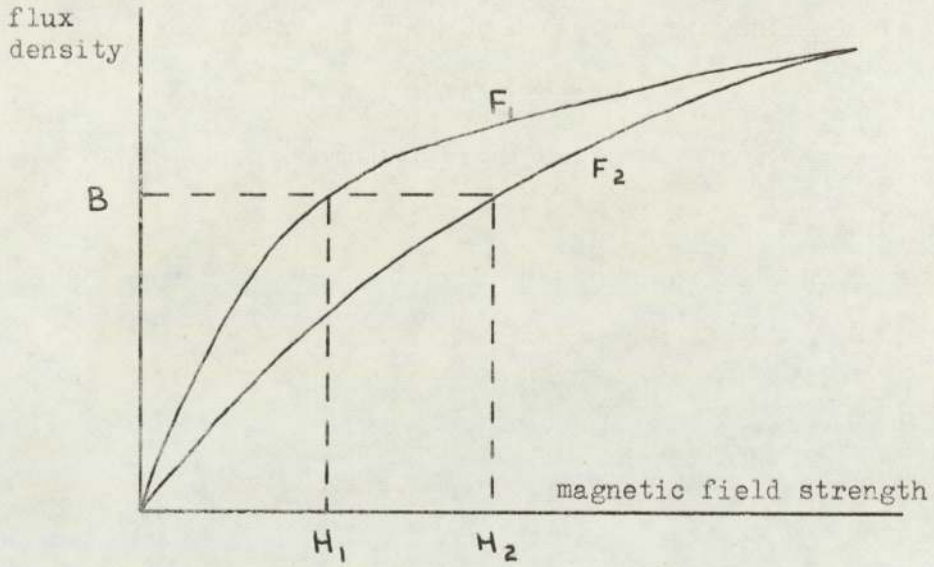

Magnetization Curve

$H_2 = F_2(B)$ is a function representing the magnetization curve of the punched material before annealing.

$H_1 = F_1(B)$ is a function representing the magnetization curve of the punched material after annealing.

Each value of B will have a corresponding value of H_1 and H_2.

Considering the behaviour of $\frac{H_2 - H_1}{H_1}$,

this can be written as $y = \frac{H_2 - H_1}{H_1}$

$$\frac{dy}{dB} = \frac{F_1(B)\,[\,F_2{}^1(B) - F_1{}^1(B)\,] - F_1{}^1(B)\,[\,F_2(B) - F_1(B)\,]}{[\,F_1(B)\,]^2}$$

Equating $\frac{dy}{dB}$ to zero to find the turning point,

$$F_1(B).F_2{}^1(B) - F_1(B).F_1{}^1(B) = F_1{}^1(B).F_2(B) - F_1(B).F_1{}^1(B)$$

$$\frac{F_1(B)}{F_2(B)} = \frac{F_1{}^1(B)}{F_2{}^1(B)}$$

Since $H_2 - H_1$ is always positive, the above equation must always relate to the maximum condition.